ZIKA VIRUS-INDUCED PREGNANCY LOSS: LESSONS FROM THE MOUSE EMBRYO

By

Jennifer Leticia Watts

A DISSERTATION

Submitted to
Michigan State University
in partial fulfillment of the requirements
for the degree of

Physiology – Doctor of Philosophy

2021

ABSTRACT

ZIKA VIRUS-INDUCED PREGNANCY LOSS: LESSONS FROM THE MOUSE EMBRYO

By

Jennifer Leticia Watts

Adults contracting Zika virus (ZIKV) exhibit mild cold-like symptoms, whereas newborn babies exhibit fetal defects ranging from mild growth retardation to miscarriage. Aside from transmission via mosquito, ZIKV is also sexually transmitted, which introduces the possibility that ZIKV infection could occur shortly after conception. However, the mechanisms underlying ZIKV-induced birth defects in early development are not understood. I hypothesize that sexually transmitted ZIKA virus infects embryos around the time of conception, leading to the most severe congenital defects. Consistent with this hypothesis, I have discovered that candidate proviral factors are present in mouse embryo-derived stem cell lines and preimplantation development. However, embryo-derived stem cell lines exhibited low viral infection and replication. Nevertheless, Puerto Rican ($ZIKV^{PR}$) and the Ugandan ($ZIKV^{UG}$) strains of ZIKV caused two-cell embryos to undergo developmental arrest. Moreover, infected blastocyst exhibited reduced SOX2 expression, an epiblast cell marker, CDX2 a trophectoderm cell marker, and SOX17, a primitive endoderm marker. Therefore, my results suggest that preimplantation ZIKV infection causes embryonic demise or embryonic cell fate defects depending on the time of infection. My studies are significant to human health because they will further our knowledge of viral infection in early pregnancy and the outcomes.

ACKNOWLEDGEMENTS

First and foremost, I want to thank my thesis advisor, Dr. Amy Ralston, for your outstanding mentorship and guidance throughout these last five years. I learned so much from you as a junior researcher and as a person. One of the biggest lessons that I will take from you is the importance of advocacy for mentees and myself. You have been one of my biggest advocators, instilling confidence in my lab work and personal life. You have been the best mentor in my academic career. It has been a great pleasure to work with you on this project where we were both learning. I appreciate you for molding me into a well-rounded scientist.

I want to thank my guidance committee, Dr. Hua Xiao, Dr. Kathleen Gallo, Dr. Narayanan Parameswaran, Dr. Zhiyong Xi, and Dr. Ripla Arora, for your thoughtful discussions during my committee meetings. Your diverse skillsets have improved the way I think about science and experimental design. I cannot thank you enough for you all believing in me. A special thank you to you, Dr. Zhiyong Xi, and your lab for the Zika virus training and for sharing your materials. This work would not be what it is today without you and your teams expertise. Additionally, I would like to thank the Reproductive and Developmental Science Training Program (NIH T32 HD087166) and the directors, Dr. Keith Latham and Dr. Asgi Fazleabas, for fine-tuning my training in developmental biology and the ample opportunities to share my work and network with other scientists in my field.

Thank you to my labmates, past and present, for your continuous support throughout my doctoral journey in the lab. Dr. Anthony Parenti, Dr. Tristan Frum, and Dr. Alyson Lokken-Greene thank you for helping me jumpstart my research and become comfortable with developmental biology techniques. Miranda McMillian, Daniel OHagan, and Barbara Makela, thank you for running the lab smoothly and mitigating reagent crises. You all were and are the heart of the lab. I would also like to thank Alex Moauro, Tayler Murphy, Robin Kruger, Robert Fidis, and Dr. Shannon Walsh for being great lab mates and late night/early morning partners. Your input and suggestions in my scientific work have stuck with me, and I am grateful.

I want to thank the groups I have been involved in for their support academically and professionally: Alliance for Graduate Education and the Professoriate, Black Graduate Student Associate, Summer Research Opportunities Program, Physiology Graduate Student Council, and Mid-Michigan Graduate Women in Science. In addition, Steven Thomas has been a fantastic mentor by putting me in leadership positions and providing mentorship opportunities. Along the way, you have become a great friend.

I then want to thank my colleagues and friends. You all have been an inspiration to me in your work. We have been through a lot together, and I hope we can remain in contact. I especially want to thank Christián Henry and Dr. Alshae Logan-Jackson for being shoulders to cry on and serving as my family while I lived away from home. You both inspired me to keep going and finish when I did not believe in myself. Thank you for the hikes and sharing your families with me. I want to thank Felecia and Gazelle for picking up the phone whenever I call, making sure I was taking care of myself, and being good friends since grade school. I couldn't ask for better group people in my chosen family. I really appreciate you.

Last but certainly not least, I want to thank my family for their support throughout my life and academic career. Words cannot describe how much you all mean to me. At times, it was hard to explain my goals, but you guys have stuck beside me in this process. I hope I have made you all proud. Judy Watts (Mom), Nevaeh, and Brownie and Coco (the dogs), thank you for moving across the country to support me in my dreams. You guys have kept me grounded and allowed me to vent when tired and frustrated. Those three years you lived in Lansing helped me get through the most strenuous part of my doctoral training. The Watts crew: Baron Sr (Dad), Baron Jr. and Robert (brothers), and my niece, Olivia, you have been my lifelines throughout all the hardships. Im happy that you all could witness me FINALLY finishing school! You all have been instrumental in my success, and I cannot thank you enough for the emotional, academic, and professional support.

TABLE OF CONTENTS

LIST OF TABLES

LIST OF FIGURES

CHAPTER 1

INTRODUCTION

1.1 ZIKV infection: A window into the 2015 epidemic

1.1.1 ZIKV epidemiology

Zika virus (ZIKV) was first discovered in 1947 in Uganda in non-human primates [1] (Figure 1.1). ZIKV is under the flavivirus classification, which includes West Nile, yellow fever, and dengue viruses based on the genome, structure, and transmission. ZIKV is transmitted by *Aedes* mosquitos which typically reside in tropical and subtropical climates. ZIKV garnered attention after a sizeable human outbreak that occurred decades later in French Polynesia in 2013 [1, 2]. Adults contracting the virus were often asymptomatic or experience cold or flu-like symptoms [3]. More severe effects include Guillain Barré syndrome, an autoimmune disorder of the nerves, causing mild limb weakness to temporary paralysis [1, 4]. Nevertheless, Guillain-Barré is treatable, and no ZIKV-associated Guillain Barré disease-related deaths were reported [5].

Upon increased frequency of ZIKV infection in 2013, infection-associated birth defects also emerged [2]. Clinically, pregnant women were tested for ZIKV infection and found that babies had developed microcephaly [6, 7, 8]. Microcephaly, the malformation of the head, is exhibited in approximately 6% of newborns from ZIKV-infected pregnant mothers in the US [9, 10]. The decreased head size is characterized by at least two standard deviations below the average head size and is primarily concentrated in the occipitofrontal region of the brain [11]. Other microcephaly-associated defects include ocular malformations, intrauterine growth restriction, and other neurological conditions [12, 13]. ZIKV epidemiological and regional case studies have shown a spectrum of effects in fetuses: no effect, microcephaly, and fetal demise [6, 14]. Additionally, infected babies can postnatally develop neurological defects such as visual impairment and epileptic seizures [15]. Most devastatingly, congenital ZIKV infection can also result in fetal loss, accounting

for up to 5% of American infected pregnant population [16, 17, 18]. However, it is still unknown how the timing of infection could contribute to the severity of ZIKV fetal effects.

In 2015 and 2016, ZIKV-induced microcephaly became a public health concern with the outbreak in South America [19, 20]. This alarming birth defect caught the world's attention, especially with the Rio Olympic Games occurring in the 2015 [21, 22]. At the same time sexually transmitted route ZIKV infection was widely recognized due to the rise and spread of cases in more northern geographical regions such as Mexico and the US [23]. As a result, the Centers of Disease Control and Prevention (CDC) recommended that men and women not conceive for up to 2 months from time of possible ZIKV contact regardless of ZIKV testing results to lower risks of adverse pregnancy outcomes [21, 24, 25]. ZIKV vaccines and viral inhibitory molecules (i.e., Chloroquine) became another means to attempt to control the disease, targeting at-risk individuals such as pregnant women [26, 27, 28, 29, 30]. Unfortunately, clinical trials stalled at Phase I/II and ZIKV treatments were not successfully distributed [31]. However, as other pathogen vaccines emerge, such as SARS-CoV-2, they can set a precedent for vaccines to reduce ZIKV infections.

1.1.2 ZIKV infection at a molecular level: Host and virus interactions

A window into ZIKV microscopically has mainly been based on other flaviviruses' properties, specifically Dengue virus [32, 33, 34]. The virus's 10,800 single-stranded RNA base-pair sequence genes code for proteins essential for viral replication and assembly [35]. Specifically, ZIKV has three structural proteins: the capsid, precursor membrane, and envelope [36, 37]. These proteins determine the shape of the virus and influence its selcetion of host receptors [38, 39, 40]. Additionally, seven nonstructural proteins (NS1, NS2A, NS2B, NS3, NS4A, NS4B, NS5) are expressed in ZIKV and involved in viral replication and host immune suppression [41, 42] (Figure 1.2A).

Because ZIKV has an envelope, the virus must undergo receptor-mediated endocytosis for the host to internalize the virus. Identified host receptors, such as the TIM and TAM family proteins, facilitate ZIKV infection [43]. After endocytosis, the endosome enzymes degrade the

protein coating of viral particles, releasing positive-sense, single-stranded RNA into the host cell. Structural and non-structural proteins are produced from viral RNA to create new viral particles [44, 45] (Figure 1.2B). Studies have shown that ZIKV cannot efficiently infect host cells lacking key components such as TAM receptors [43, 46]. Additionally, the upregulation of proviral factors increases the cell's susceptibility to ZIKV infection [46, 47, 48]. Efficient viral replication tools are present in their genome. Nevertheless, the virus uses the host transcriptional and translational machinery to assemble progeny, become secreted, and then infect neighboring cells [49, 50, 51].

Conversely, host cells contain innate defenses against viral infection, such as interferon-stimulated genes [52]. ZIKV-infected cells release interferons to warn neighboring cells by binding to receptors such as interferon-alpha receptor 1 (IFNAR1) [53, 54, 55]. Downstream of this signaling, genes are transcribed that are known to inhibit infection. These classes of interferon-stimulated genes (ISGs) are involved in multiple steps of the viral cycle from viral genome release to progeny release [56, 57, 58] (Figure 1.3). Studies have implicated interferon-induced genes, IFITs and IFITMs, in ZIKV infection inhibition in human embryonic stem cells [59]. The knowledge of both proviral and antiviral mechanisms in virus-host interactions can be utilized for elucidating mechanisms of infection in understudied cells and tissues.

1.1.3 ZIKV targets neural and placental cells during pregnancy

The structure, function, and epidemiology of ZIKV in humans have provided opportunities to study why some cells are targets of ZIKV and others are not. As previously discussed, the expression of putative ZIKV virus receptors have been an indicator of ZIKV susceptibility. For example, AXL, a phosphatidylserine receptor, is highly expressed in neural cells [60, 61, 62]. Coincidently, AXL is also a receptor for viruses such as ZIKV, and could facilitate viral-induced neural ailments such as Guillain-Barré syndrome in adults [4, 53, 63]. However, other organs, such as the skin, lack many proviral factors and are not highly infected [46].

Developing fetal neural tissues are vulnerable to ZIKV infection. Microcephaly, the malformation of the head, presents itself in varying degrees, and it is currently unknown why some exposed

babies are more impacted than others [6, 9]. However, it is hypothesized that viral-induced neural cell death causes microcephaly. Previous studies have shown that infected fetuses can experience brain cortex depletion and hindbrain apoptosis [54, 60]. Moreover, ZIKV infectivity is increased at a cellular level in neural progenitor cells compared to differentiated neural cells [61, 64, 65], suggesting that early development is more vulnerable to infection. In addition, even with less severe ZIKV infected fetuses, babies could experience other postnatal neurological effects, such as hearing loss and epileptic seizures [66, 67].

Another target of ZIKV infection is the placenta. The descending route of infection via the maternal-fetal interface has been widely studied [68, 69, 70]. Placental infection could cause abnormal pregnancies, such as preterm birth, leading to low birth weight and other comorbidities [71, 72, 73]. Like neural cells, placenta cells also expressed key proviral factors or ZIKV receptors such as AXL and MERTK [48, 74]. First-trimester placenta cells were more ZIKV-infected than third-trimester placenta cells due to higher AXL expression in first-trimester placenta cells, thus resulting in severe placental damage and fetal defects [48, 75, 76, 77].

More recently, pre-placental cells or trophectoderm cells in human preimplantation embryos have been shown to be a target of ZIKV infection via the ascending route or vaginal transmission [78]. However, ZIKV infection in embryos near fertilization and pre-fetus and pre-yolk sac cells, or the inner cell mass, has yet to be explored. The discovery of molecular targets of ZIKV infection, such as receptors and inhibitory mechanisms such as ISGs, may predict the ZIKV pathogenesis in early embryo, preimplantation, development.

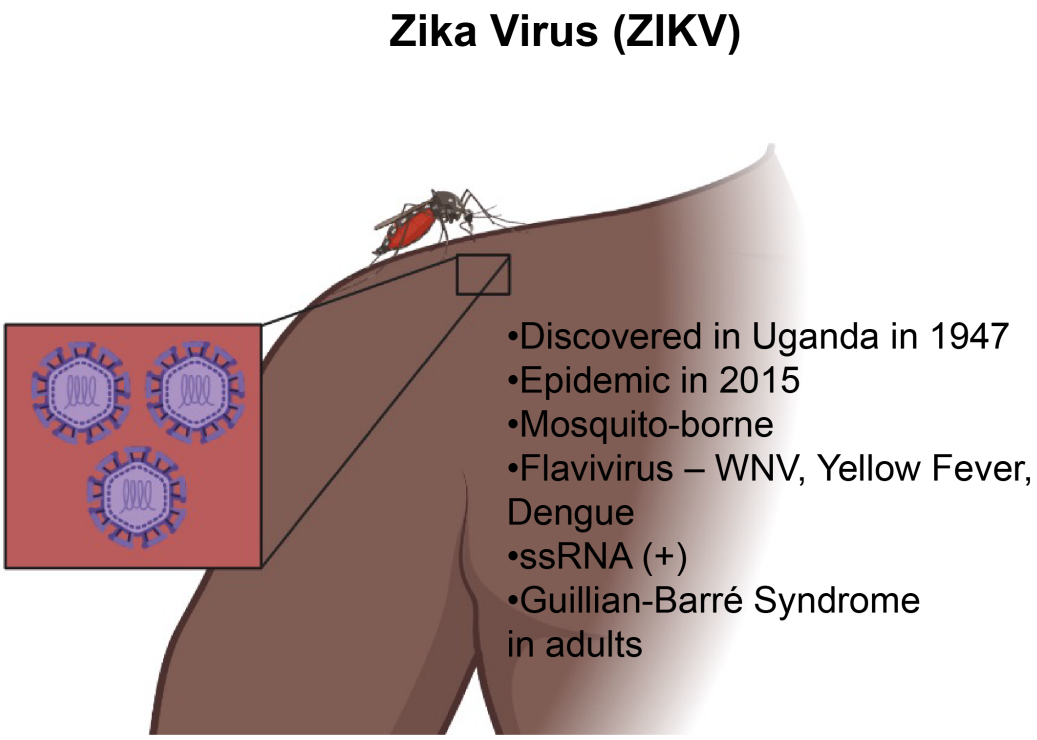

Figure 1.1: A cartoon of a mosquito-borne virus, Zika virus (ZIKV), with its transmission vector and the disease it causes. All introduction images were generated by biorender.com and/or illustrator.

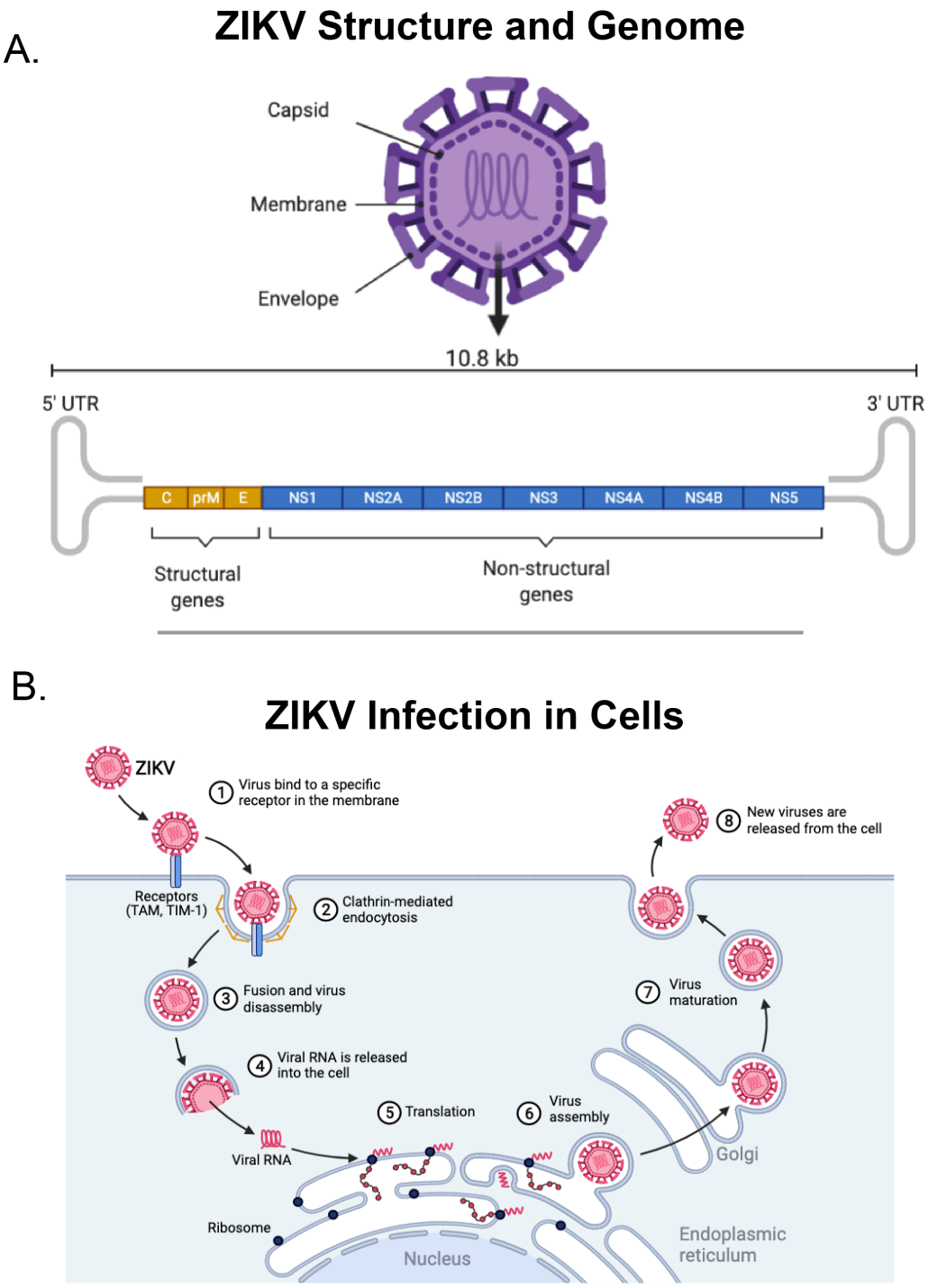

Figure 1.2: A cartoon of ZIKV structure and life cycle. A. A schematic of the ZIKV particle structure and the genome sequence of structural and non-structural genes **B.** A cartoon of the ZIKV life cycle in a host cell.

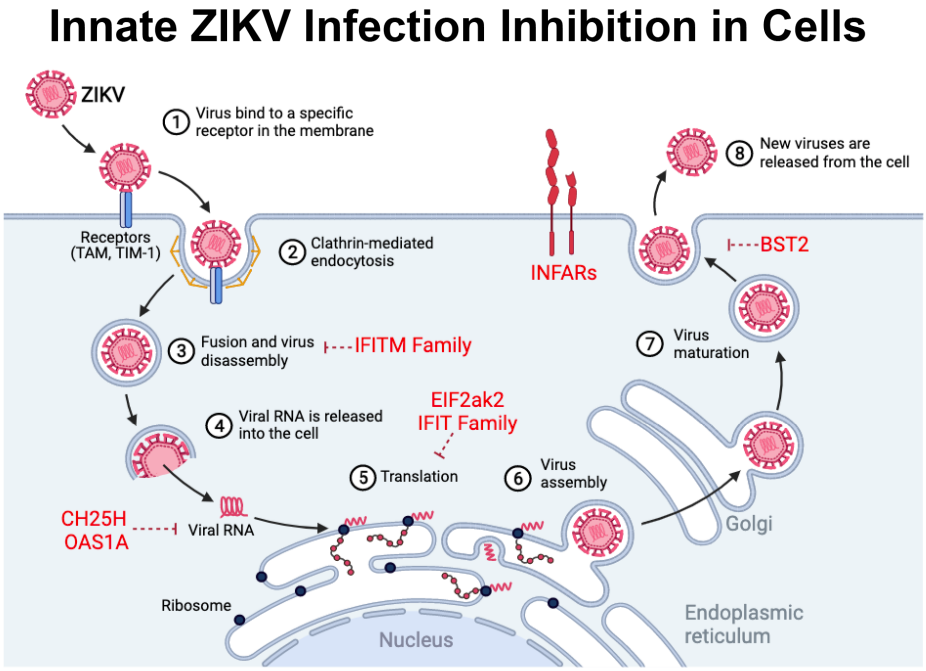

Figure 1.3: A cartoon of ZIKV infection inhibition by host cell antiviral mechanism molecules, interferon stimulated genes.

1.2 Preimplantation Development Overview

1.2.1 Fertilization to blastocyst: a mouse perspective

The mouse has served as a research organism for human development and disease. In preimplantation development, the similarities between mouse and human morphology and cell fate are remarkable [79, 80]. For decades, preimplantation development studies have led to an understanding of how one fertilized cell can develop complex tissues in the fetus. Many early discoveries are based on fundamental and exploratory science and, today, these early stages of development offer health-related insight into pregnancy. Therefore, studying ZIKV infection in early preimplantation could further the understanding of ZIKV-associated fetal outcomes. The preimplantation embryo stage starts at the fertilization of the egg to make a zygote, E0.5 or a half-day after insemination, which occurs in the oviduct (comparable to the fallopian tube in humans) [81]. At this stage, maternal transcripts and proteins are present in the zygote for embryo survival [82].

One day into embryo development, E1.5, the zygote cell divides into 2 to make up the two-cell stage within the oviduct. The two-cell mouse embryo (four-cell in humans) undergoes zygotic genome activation (ZGA) to make de novo transcipts while maternal transcipts and proteins start to degrade [83]. Due to two-cell embryos' transcriptional and translational needs, these embryos have an extended G2 phase [84].

After a few more cell divisions, two days into development, eight-cell embryos start to confront the first cell fate decision: the emergence of outside cells called the trophectoderm (TE) [85]. Eight-cell embryos then develop into the sixteen-cell stage embryo establishing the TE and developing inside cells called the inner cell mass (ICM). Finally, the embryo moves out of the oviduct and into the uterus at three days of development.

Between the 16-cell and 32-cell (early blastocyst) stage or E2.75-3.5, the embryo cavitates, and the newly formed blastocoel begins to expand. Epithelialized TE makes up the outer layer encapsulating the inner cell mass and cavity of the spherical blastocyst. Until this point, and for approximately four days of development, embryos have a zona pellucida (ZP) glycoprotein coat.

However, mid-blastocyst stage embryos begin to hatch out of the zona pellucida [86, 87]. Shortly after, the second cell fate decision occurs when the ICM delineates into two lineages: epiblast (EPI) and primitive endoderm (PE) [88]. Late blastocysts hatch out of the zona pellucida and are exposed to the uterine environment for implantation into the uterine wall (Figure 1.4A).

1.2.2 Preimplantation cell fate specification

Cell lineage specification is an essential process in preimplantation embryogenesis. From zygote to eight-cell embryos, all cells are totipotent. Evidence of totipotency in early preimplantation stages is shown by the ability of dissociated blastomeres to produce blastocysts in culture and complete organisms when derived from two to eight-cell stage embryos [89, 90, 91]

HIPPO signaling plays a role in determining the cell fate of outside and inside cells between eight to 16-cell stage embryos [92]. The apical membrane of outside cells expresses a membrane-bound protein atypical protein kinase C (aPKC). Downstream of aPKC, LATS2 is repressed, allowing YAP1/WWTR1/TEAD4 phosphorylation. The YAP1/WWTR1/TEAD4 complex promotes the expression of CDX2 and GATA3 proteins in mice, specifying TE cells [92, 93, 94, 95, 96]. Conversely, inside cells do not express CDX2 and express SOX2 in cells in the absence HIPPO signaling. In addition, loss of aPKC in embryos causes ectopic expression of SOX2 in outside cells [97].

The second cell fate decision occurs at mid-blastocyst, approximately four days into development, in the ICM. The ICM initially expresses SOX2 in all cells. However, during the second cell fate decision, SOX2 becomes restricted to half of the ICM cells, thereby specifying epiblast (EPI) fate. SOX17 expression emerges, specifying primitive endoderm (PE) within the other half of ICM cells [98, 99, 100]. Evidence shows that FGF4 and possibly BMP4 signaling is involved in the sorting of EPI and PE cells in blastocyst ICM [95, 101, 102, 103]. Remarkably, embryos undergo these lineage decisions autonomously by self-organization, and the loss of these cell fates leads to embryo demise and failure of implantation (Figure 1.4A).

1.2.3 Embryo-derived stem cells as a proxy for preimplantation development

Embryo-derived stem cells have served as a proxy for preimplantation development and the study of the cell lineage separately due to their transcriptional similarities to cells in the blastocyst (Figure 1.4B). Embryonic stem cells (ESCs) have been widely studied and informed how we understand the regulatory networks of pluripotency, the ability for cells to differentiate into adult cells [104, 105, 106]. These stem cells transciptionallhy resemble epiblast (EPI). Trophoblast stem cells (TSCs), resembling trophectoderm (TE) cells, are utilized to study placenta, an essential organ at the maternal-fetal interface [107, 108, 109]. In addition to programming, TSCs have also been utilized to understand placental disease states such as preeclampsia and viral infections [110, 111]. The latest and least studied stem cells are extraembryonic endoderm stem cells (XEN). XEN cells are derived from the primitive endoderm (PE) in blastocysts [112, 113]. Studies are underway to understand XEN cell line regulatory networks and multipotency [114, 115, 113]

All three embryo-derived stem cells can self-renew and differentiate into developed cell states. Since XEN and TSCs are multipotent, they differentiation into only a subset of terminal extraembryonic cell fates, including placental and yolk sac endoderm tissue, respectively [116, 117, 118, 119, 120]. In addition, embryonic stem cells can differentiate into embryos cell fates such as neurons and cardiomyocytes [121]. Evidence of embryo-derived stem cell potency has been determined by lineage tracing and chimera assays [108, 122, 123]. Thus, murine embryo-derived stem cells are a robust model for preimplantation development.

1.2.4 Mouse as a research organism for human development

The mouse has been a classical model for human development and disease. One of the ways the preimplantation mouse is similar to human preimplantation is the staging and morphology of embryos. However, the timing of the stages differs as mouse embryos take about four days in the preimplantation stage while human takes seven days [80, 97]. Although the timing of stages differs, the stages are comparable in cell number and size.

Cell fate specifications of EPI, PE, and TE between mice and humans are remarkably similar.

In particular, TE cell fate specification via HIPPO signaling is conserved between multiple species, showing the significance of this pathway in pre-placenta cell programming [97]. However, HIPPO signaling represses SOX2, a classically accepted pluripotency marker in mice. Conversely, in humans and cows, outside TE cells still express SOX2, giving new meaning to the proposed pluripotent marker in different species [124]. Thus, regardless of the initial expression of SOX2 in preimplantation development, SOX2 eventually becomes restricted to EPI cells, like mouse embryos.

What is the most different about mouse and human is the ability for their embryos to give rise to stem cells. Like mice, human ESCs (hESCs) have been used to understand pluripotency networks [125]. Recently, human TSCs (hTSCs) have been derived from embryos, making headway to understand the placental programming and *in vitro* model of placental differentiation [126]. Human XEN cells are yet to be derived from embryos, advancing studies to understand PE role in human embryo development [127]. Given the gaps in human embryo-derived cells, mouse embryo-derived stem cell lines are still a proxy for mouse and human development. Despite minor differences between human and mouse development, the similarities in preimplantation development between species are translatable. Therefore, the mouse is a good model for ZIKV infection (Figure 1.5A-B).

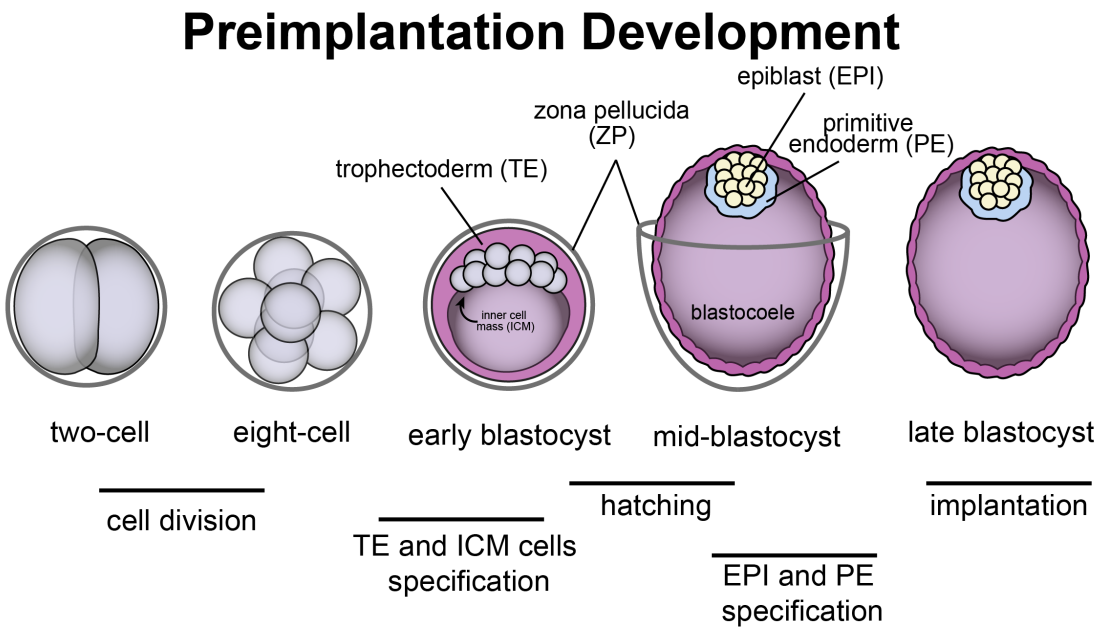

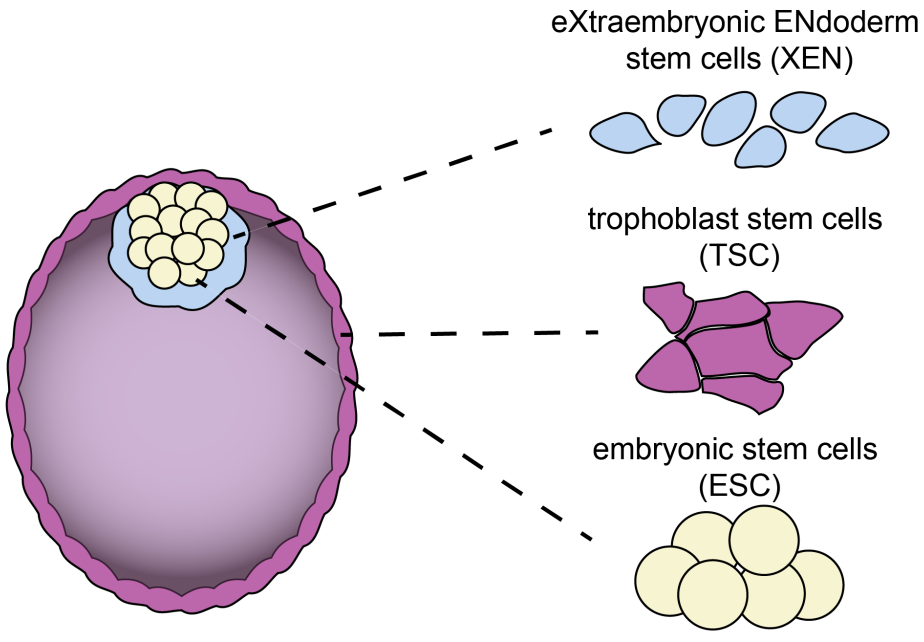

Figure 1.4: Mouse Preimplantation and stem cells. **A.** Mouse primplantation development illustrating the following: cleavage divisions, cell fate specification, and hatching. **B.** Three stem cell line can be derived from the mouse blastocyst *in vitro* are embryonic stem cells (ESC), trophoblast stem cells (TSC) and extraembryonic endoderm stem cells (XEN).

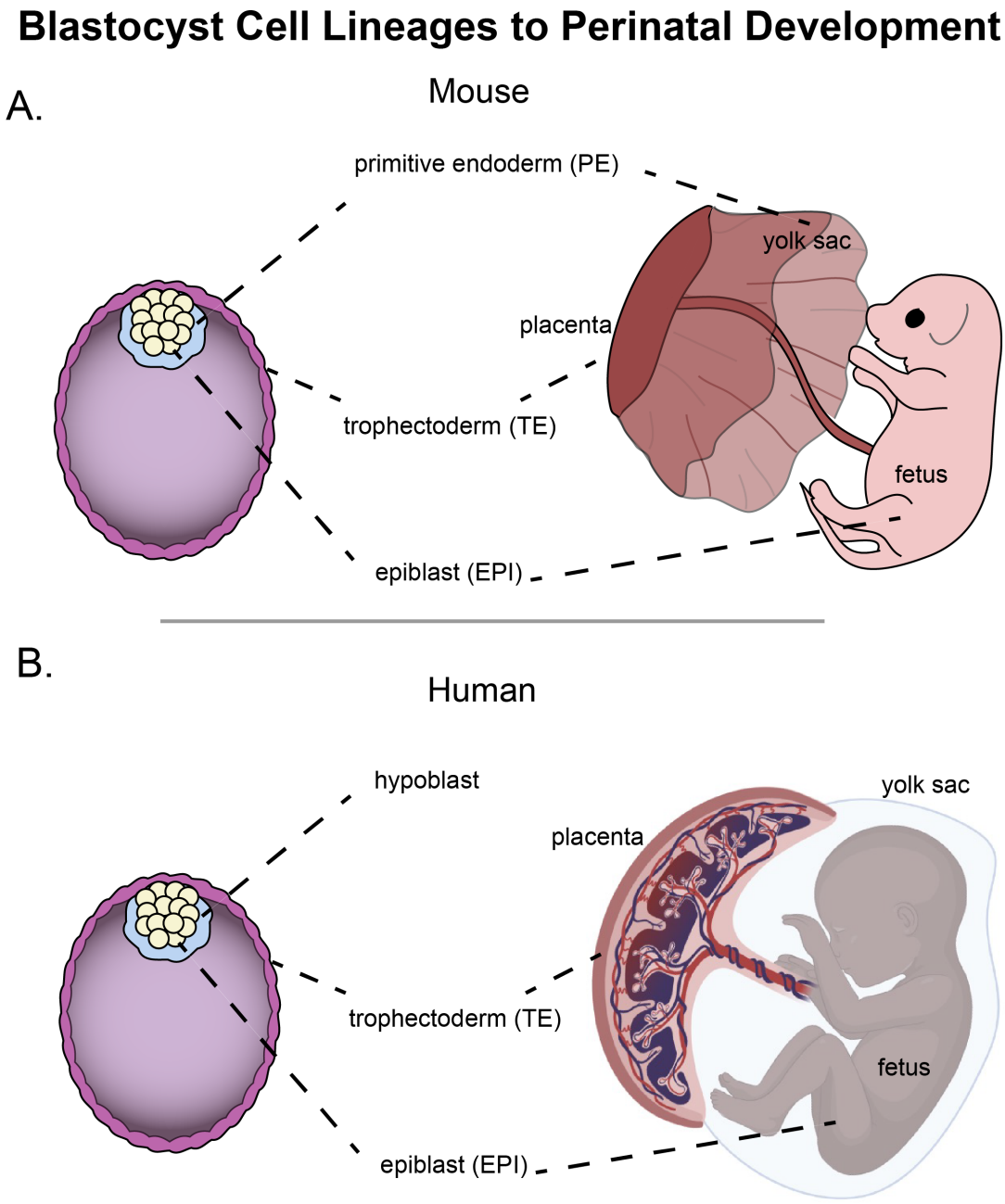

Figure 1.5: Preimplantation embryo cell lineages confer fetal development tissues similarly in A. mice and **B.** humans.

1.3 Infections during Pregnancy

1.3.1 ZIKV can affect mice

ZIKV is a significant health concern because fetal infections can result in microcephaly and miscarriage [6, 128]. Interestingly, some ZIKV-infected babies are seemingly healthy at birth, creating a gap in understanding why fetal ZIKV infection causes a spectrum of phenotypes (Figure 1.6). Most studies have examined the consequences of ZIKV infection of pregnant mothers via the descending route of infection (maternal blood to the placenta and then fetus) which provided essential insight into the effects of ZIKV on placental and neural tissues. However, the descending route paradigm assumes ZIKV infection occurs after the formation of the placenta, which is thought to transmit the virus from the mother's blood to the fetus [75, 64, 48]. At this stage, the neural tissues might be sufficiently well developed to resist infection. By contrast, relatively little is known about how earlier ZIKV infection would impact neural development. Arguably, the effects could be more deleterious if infection occurred earlier, but this would involve a placenta-independent route of infection. Sexual transmission provides an alternative route to the developing fetus, prior to the formation of the placenta. ZIKV infection via the ascending route is not well understood, nor is it understood how infection could impact the fetal lineage at very early stages, around the time of conception (Figure 1.7).

The mouse is a robust research organism for studying ZIKV infection for several reasons, such as embryonic similarities to human and *in vitro* embryo cell lineage models [79, 80, 129, 104, 115, 109, 130]. Most importantly, infected mouse fetuses exhibit similar phenotypes as humans infected with ZIKV (Figure 1.7). Fetuses from ZIKV infected pregnant dams via subcutaneous and intravenous exhibit placental and neural defects similar to infected humans fetuses [60, 6, 27, 54, 29, 128, 74]. The similarities in ZIKV-induced fetal effects are evidence that the mouse could model human infection. However, minimal studies have observed preimplantation infection and the effects on embryogenesis before neural and placenta specification [78, 131].

1.3.2 ZIKV persists in male and female reproductive tracts

In addition to being transmitted by mosquitos, ZIKV is sexually transmitted [132, 133, 55, 134] (Figure 1.7). This route of infection raises the possibility that embryos could become infected around the time of conception, a highly vulnerable developmental stage. Notably, there is evidence that ZIKV can persist in rodent and human male and female reproductive tracts and potentially infecting preimplantation embryos [135, 136, 137, 134]. An earnest effort has focused on how ZIKV affects the fetus via the descending route of infection. While these studies are essential in helping us understand how maternal infection impacts pregnancy, they do not help researchers understand the most severe defects. However, since this route of infection relies on a functional placenta for ZIKV transmission to the fetus, the descending route of infection encompasses a later window in fetal development, after specification of head and brain structures [53, 60, 64, 4, 47, 39, 61, 138] (Figure 1.7). Since ZIKV can be sexually transmitted and persist in male and female reproductive tracts, embryos could be exposed to ZIKV more directly and at much earlier developmental stages. Preimplantation embryo exposure to ZIKV may have more widespread and devastating effects on fertility and development. There is evidence that ZIKV infects trophectoderm cells in the blastocyst, and embryos fail to implant. However, it is unknown how ZIKV infection effects embryo stages between fertilization and blastocyst formation at a cellular level [78, 131]. our studies will shine light on infections that could lead to human-borne, ZIKV-induced sexually transmitted birth defects. Studies elucidating the effects of ZIKV infection in early pregnancy will inform epidemiologists and health care professionals about the fetal health risks in early ZIKV infection and why a spectrum of fetal phenotypes is observed (Figure 1.6).

1.3.3 Overview of viral infections in preimplantation development

Placental infection has been widely studied because there is evidence that viruses are transmitted via the maternal-fetal interface, also known as the descending route [68, 69, 139, 140, 141, 142]. However, there is an assumption that ZIKV infection occurs after placental specification. Before placental and neural specification, the preimplantation stage is a critical stage of pregnancy because

embryos possess few cells essential for tissues for later fetal development and formation of adult cells [143, 144]. Thus, ZIKV infection of these early stages could be detrimental to embryo health and potentially manifest only later in development.

Preimplantation embryos are vulnerable to certain viral infections (Table **??**) Two-cell and morula infection by a variety of viruses can cause developmental arrest, preventing development to blastocysts [145, 146, 147, 148, 149, 150, 151, 152]. The cause of viral-induced embryo demise is unknown. However, there is speculation that viruses can evade the innate cellular immune response and rewire the host machinery to induce cell [51, 153]. Since there are only a few cells in early preimplantation embryos and lack immune cells, infections could induce developmental arrest directly. In addition, blastocyst infection can cause implantation failure due to trophectoderm dysfunction and apoptosis of cells [78, 131]. Notably, some viruses cannot infect preimplantation embryos, which reveals embryo resistance to some viral infections [149, 154]. The presence of intrinsic factors could explain the viral resistance in embryos, such as interferon-stimulated genes, or the physical barrier provided by the zona pellucida [59, 155]. The zona pellucida is a glycoprotein layer that encapsulates preimplantation stage embryos until four days in mice [156]. While the structure of the zona pellucida, such as pore size and the thinning throughout embryogenesis, is controversial, there is evidence that the zona pellucida could provide a barrier to infection by some viruses [157]. Studies have shown that the artificial removal of the zona pellucida permitted viruses to infect embryonic cells [149, 148]. As a consequence of this infection, embryos did not develop into advanced preimplantation stages. Conversely, some viruses evade the zona pellucida layer and infect preimplantation embryos [147, 150]. Interesting that smaller viruses, averaging approximately 70 nm in diameter, can diffuse through the zona pellucida easier than larger viruses averaging more than 150 nm in diameter (Table **??**). It is currently unknown if ZIKV, a 45 nm in diameter virus, can infect embryos with and without the zona pellucida.

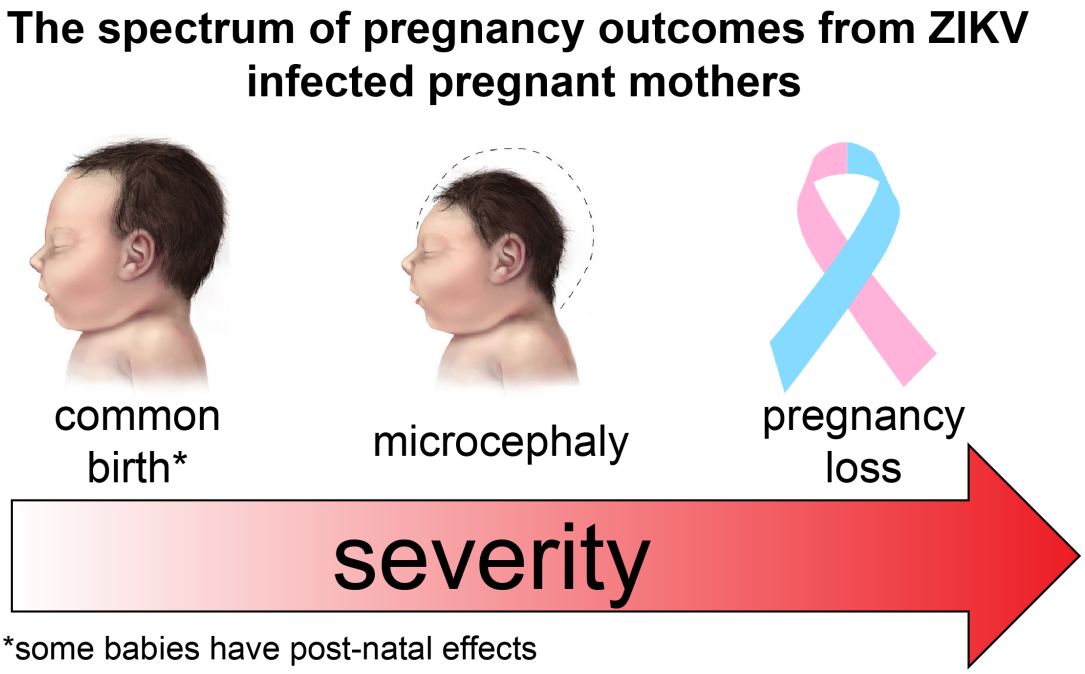

Figure 1.6: A cartoon of the spectrum of pregnancy outcomes from ZIKV-infected pregnant mothers: common birth, microcephaly, and pregnancy loss. The asterisk next to common birth reveals that some babies experience the postnatal diagnosis of neurological effects such as epilepsy and vision loss.

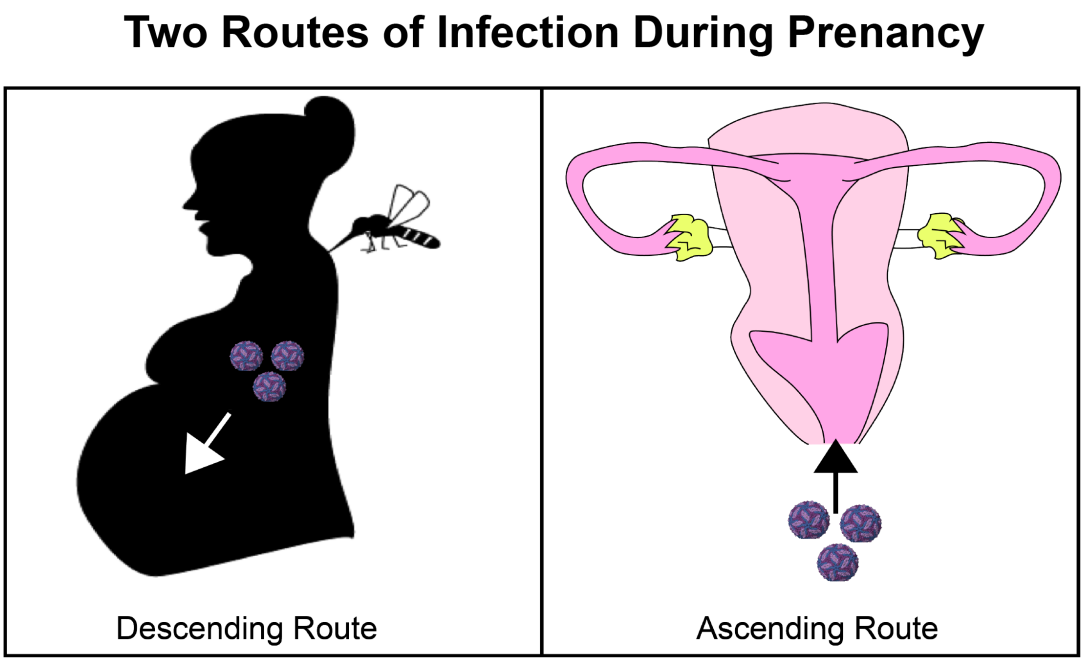

Figure 1.7: A cartoon of the two routes of ZIKV transmission: the descending route or maternal-fetal interface transmission and the ascending route or sexual transmission.

Table 1.1: Studies of preimplantation development viral infections

Embryo Stage Infected	Virus	Species	If any, genotype	Zona Pellucida?	Virus size (nm)	Passed through zona?	Citation
Blastocyst	$ZIKV^{UG}$	Mouse and Human	WT B6	zona-free	45	N/a	Tan et al. 2019
Morula	Sendai Virus	Mouse	ICR	zona-free	150-300	N/a	Lavilla-Apelo et al. 1991
Zygote, Blastocyst	$ZIKV^{PR}$	Rhesus Macaque	n/a	zona-free	45	N/a	Block et al. 2020
Blastocyst	SARS-CoV-2	Human	n/a	zona-free	50-200	N/a	Montano et al. 2021 bioRxIV
4-8C	A7 strain of Semliki Forest virus (SFV)	Mouse	Q/Fa	zona-free	50-70	N/a	Hearne et al., 1986
Blastocyst ICM	SFV and Rubella virus	Mouse	Q/Fa	n/a	60-70 (RV)	N/a	Hearne et al., 1986
2-4C, 5-8C, Morulae, Blast, Hatched Blastocyst	Pseudorabies strain 89V87	Pig	n/a	zona-free	200-250	N/a	Mateusen et al., 2007
2-4C, 5-8C, Morulae, Blast, Hatched Blastocyst	PRRSV	Pig	n/a	zona-free	45-70	N/a	Mateusen et al., 2007
2C	Mengovirus	Mouse	SWISS	zona-free	30	N/a	Gwatkin, 1963
2C, Morula	Mengovirus	Mouse	SWISS	zona-free	30	N/a	Gwatkin, 1966
Morula, Blastocyst	BHV-1	Cow	n/a	zona-free	120-200	N/a	Makarevich et al., 2007
2C, Morulae, Blastocyst, Isolated ICM/ TE	Reovirus (1 and 3)	Mouse	ICR	zona-free	81	N/a	Abramczuk et al., 1983
2C, Morulae, Blastocyst	SV40	Mouse	ICR	zona-free	45	N/a	Abramczuk et al., 1978
2C, Morulae, Blastocyst	Polyoma virus	Mouse	ICR	zona-free	50	N/a	Abramczuk et al., 1978
4-8C embryos	m-MuLv	Mouse	BALB/c	zona-free	120	N/a	Jaenisch et al., 1975
Embryo Stage Infected	**Virus**	**Species**	**If any, genotype**	**Zona Pellucida?**	**Virus size (nm)**	**Passed through zona?**	**Citation**
2C, 4C, 8C, Blastocyst	Sendai Virus	Mouse	ICR	zona-intact	150-300	no	Lavilla-Apelo et al. 1991
4-8C	A7 strain of Semliki Forest virus (SFV)	Mouse	Q/Fa	zona-intact	50-70	no	Hearne et al., 1986
2-4C, 5-8C, Morulae, Blast, Hatched Blastocyst	Pseudorabies strain 89V87	Pig	n/a	zona-intact	200-250	no	Mateusen et al., 2007
2-4C, 5-8C, Morulae, Blast, Hatched Blastocyst	PRRSV	Pig	n/a	zona-intact	45-70	no	Mateusen et al., 2007
2C	Mengovirus	Mouse	SWISS	zona-intact	30	yes	Gwatkin, 1963
2C, Morula	Mengovirus	Mouse	SWISS	zona-intact	30	yes	Gwatkin, 1966
Morula, Blastocyst	BHV-1	Cow	n/a	zona-intact	120-200	yes	Makarevich et al., 2007
Zygote, 2C, 4C	AAV	Mouse	C57BL/6 J	zona-intact	20-25	yes	Romeo et al., 2020

Table 1.2: Table of abbreviations

Abbreviations	Definition
ZIKV	Zika Virus
TS or TSCs	Trophoblast Stem Cells
ES or ESCs	Embryonic Stem Cells
XEN	eXtraembryonic ENdoderm Stem Cells
$ZIKV^{PR}$	Puerto Rican ZIKV Strain
$ZIKV^{UG}$	Ugandan ZIKV Strain
HCMV	Human Cytomegalovirus
MOI	Multiplicity of Infection
RTq-PCR	Real-Time Quantitative Polymerase Chain Reaction
ISGs	Interferon-Stimulated Genes
ZP	Zona Pellucida
DENV	Dengue Virus
POWV	Powassan Virus
WNV	West Nile Virus

1.4 Dissertation Objectives

Zika virus (ZIKV) infection causes detrimental fetal effects such as microcephaly and miscarriage. Previous studies focused on fetal infection through maternal blood via the placenta, the descending route of infection [54, 68, 76]. Additionally, ZIKV can infect developing neural cells which is hypothesized to cause microcephaly [62, 64]. However, ZIKV is sexually transmitted, suggesting that infection could occur during peri-conception or preimplantation development and cause more severe effects by an ascending route of infection. Recent studies of the ascending route of infection have shown the effects of ZIKV infection in blastocysts causing trophectoderm dysfunction [78, 131]. Although these findings provide insight into preimplantation infection, the effects of ZIKV infection in stages before blastocyst formation and lineage fates are still unknown.

The objective of my dissertation studies are to 1) identify proviral and antiviral intrinsically expressed in embryo-derived stem cells and embryos hosts to predict ZIKV infectivity, 2) examine ZIKV infection of embryo-derived stem cells *in vitro*, and lastly, to 3) explore the effects of ZIKV infection on embryos and its fetal lineages. In chapter 2, I determined the transcriptional profiles of proviral genes in mouse preimplantation embryos and embryo-derived stem cells, supporting ZIKV infectivity of early embryos. I also have shown the antiviral genes are expressed in human embryos, suggesting that these embryos could be resistant to infection. In chapter 3, I established infection protocols for embryo-derived stem cells. Additionally, I showed that all embryo-derived stem cells, embryonic stem cells, trophoblast stem cells, and extraembryonic endoderm stem cells are resistant to ZIKV infection and replication. In chapter 4, I showed that ZIKV could infect all cell lineages, trophectoderm, epiblast, and primitive endoderm, of murine blastocysts, resulting in the significant loss of these cell fates. We have also shown that two-cell embryos are vulnerable to infection regardless of ZIKV strain. Altogether, my studies will advance the knowledge of the consequences of ZIKV infection in pregnancy and human health.

CHAPTER 2

PRO- AND ANTI-ZIKA VIRUS FACTORS EXPRESSION IN EMBRYO-DERIVED STEM CELLS AND EMBRYOS

Jennifer L. Watts

This study was supported by the James K. Billman, Jr., M.D. Endowment at Michigan State University and National Institutes of Health awards R01 GM131759 and T32 HD087166.

2.1 ABSTRACT

Zika virus exploits host factors to survive and replicate within host cells. Conversely, the host can have protective measures to eliminate or inhibit further infection from viruses. The presence or the absence of these factors can be an indicator of the infectibility of cells or organisms. Previous studies have shown that proviral and antiviral factors can influence ZIKV infection in human cells, even in late-stage mouse development. However, it is unknown if these factors are also expressed in preimplantation development. This study will describe the expression of proviral and antiviral factors in embryo-derived stem cells and embryos using publicly available sequencing data to predict preimplantation susceptibility to ZIKV infection.

2.2 INTRODUCTION

Zika virus became an epidemic and major public health crisis in 2015 and 2016 in the Americas. The virus was typically understood as mosquito-borne and isolated in specific tropical regions. However, more recent findings implicates human transmission of ZIKV infection through the spread of sexual interactions [136, 137]. Adults contracting ZIKV experience mild symptoms of the virus, such as headaches and rashes, whereas fetuses exhibit more severe symptoms. These symptoms consist of mild growth restriction, microcephaly, or fetal demise [6, 67, 10].

Much of the knowledge of ZIKV infection is based on facts and studies performed on other flaviviruses, such as West Nile Virus (WNV) and Powassan Virus (POWV), which can infect developing fetuses and decrease fetal viability [34, 76], though the severity and prevalence of these viral fetal effects are lower. Nevertheless, like other flaviviruses, the most essential step of infection is the viral attachment via host receptors for downstream infection and replication. Previous studies in human cell lines revealed proviral factors that are sufficient and necessary for ZIKV infection [46]. Additionally, proviral factors such as AXL were expressed in mouse and human placentas, an organ known to transmit the virus to the baby [48, 74, 135]. These receptors, or proviral factors, promote infection in mammalian cells causing detrimental effects such as cell death [54, 60, 78].

In contrast to proviral factors that facilitate ZIKV infection, host cells also possess innate

survival mechanisms, known as antiviral factors. A particular class of antivirals known to inhibit flavivirus infection are interferon stimulated genes (ISGs) [57, 158]. In response to infection, cells transcribe ISGs to inhibit further infection in neighboring cells [52]. Functional studies of the interferon pathway and ISGs revealed that antiviral factors are necessary and sufficient for the protection of stem cells much like proviral factors [54, 55, 78, 159]

Currently, there is no comparative study of pro- and antiviral factors in preimplantation development. In this study, I used RNA-seq and microarray data to examine the expression patterns of proviral factors and INF pathway genes in embryo-derived stem cells and preimplantation embryos. Moreover, predictions made on infectivity throughout preimplantation development could corroborate early infection. These observations will reveal the risk of ZIKV infection at a cellular level in early pregnancy, explaining the spectrum of viral-induced congenital effects.

2.3 MATERIALS AND METHODS

2.3.1 Trophoblast Stem (TS) Cells Maintenance and Differentiation

Four-well Nunc plates with 30 nm coverslips or six-well plates were treated with 0.1% gelatin (Millipore, ES-006-B) and immediately aspirated. 100,000 TSCs (passage 23-28) for four-well or 600,000 TSCs for six-well are seeded in each well in 500 µL complete TSC media (70% feeder conditioned media and 30% incomplete media: RPMI, 20% FBS, 100 µM beta-mercaptoethanol, 2 mM L-glutamine or glutamax, 1mM sodium pyruvate and 50 µg/mL and penicillin/streptomycin) with 25 ng/mL of FGF4 and 1 u/mL of Heparin. TSCs were maintained in 5% CO_2 at 37°C and fed every two days while passaged every six days. To differentiate TSC, cells were plated on gelatin in complete TSC media (day 0). The following day, and for every day thereafter for six days, the media was replaced with incomplete TSC media. Morphological changes were observed between two and six days.

2.3.2 Extraembryonic Endoderm Stem (XEN) Cells Maintenance and Differentiation

CD-1 derived XEN cells (<38 passage) were plated gelatinized dishes in XEN Cell Medium (15% fetal bovine serum (FBS), 55 mM beta-mercaptoethanol (55x, Gibco), 0.1 mM nonessential amino acids, 1 mM sodium pyruvate, 2 mM L-glutamine or glutamax, 50 U or µg/mL pen/strep in DMEM) and incubated in 5% CO_2 at 37°C. To differentiate XEN cells to Visceral Endoderm like cells, culture dishes were treated with Poly-L-ornithine 0.01% solution (Sigma) for 30 minutes at room temperature and Laminin (Sigma L2020) at a concentration of 0.15 µg/cm^3. 2000 cell/mm^2 of XEN cells were cultured in each well in N2B27 Medium (50% DMEM-F12 mixture (Invitrogen), 50% Neural Basal Medium (Invitrogen), 100x N2 Medium (Invitrogen), 50x B27 (Invitrogen), 10000 U Pen/Strep and 55 mM beta-mercaptoethanol) and cultured overnight in 5% CO_2 at 37°C. N2B27 medium was replaced on the next day with N2B27 supplemented with 50 ng/mL BMP4 (R&D Systems) and every other day for 6-8 days.

2.3.3 Embryonic Stem Cell Maintenance

R1 ES cells were plated on 0.1% gelatin in ES medium (15% fetal bovine serum (FBS), 55 mM beta-mercaptoethanol, 0.1 mM nonessential amino acids, 1 mM sodium pyruvate, 2 mM L-glutamine or glutamax, 50 U or µg/mL pen/strep and 10 ng/mL LIF in DMEM) and cultured in 5% CO_2 at 37°C . ES cells underwent media change every and passaged every 2 days.

2.3.4 RT-qPCR

RNA was harvested using TriZol method (Thermo Fisher Scientific, 15596018, Pub No. MAN0001271) and made into cDNA using the QuantiTect Reverse Transcriptase kit (Qiagen, 205313). Newly produced cDNA was diluted 1:10. A master mix was made using Sybr Green PCR Master Mix (Applied Biosystems, 4309155), water, and each primer pair (Table 2.2). An auto-pipetter made four replicates of each well (resulting in 384 wells) and started the Light Cycler PCR machine for 50 cycles. We example the melt curve for primer dimers, amplification, and the program's standard

curve. From these results, we narrowed down the gene candidates. We used the same method but harvested RNA from D2, D4, D6 of TSC.

2.3.5 Immunofluorescence Assays

Cells were fixed in 4% formaldehyde for 10 minutes at room temperature, permeabilized with 0.5% Triton X-100 for 30 minutes at room temperature and blocked with 10% FBS and 0.1% Triton X-100 blocking buffer for 1 hour at room temperature or longer at 4°C. Primary antibodies were prepared in blocking buffer, and embryos and cells were incubated at 4°C overnight with the following primary antibodies (also, see table 2.3) : rabbit anti-MERTK (Abcam, ab95925), rabbit anti-Syntenin (Abcam, ab19903), rabbit anti-M6PR (Abcam, ab134153), goat anti-SOX2 (GT15098, Neuromics), mouse anti-mCDX2 (CDX2-88, BioGenex), and goat anti-mGata4 (sc1237, Santa Cruz Biotechnology Inc). Cells were washed with blocking buffer for 30 minutes, incubated with the following secondary antibodies for an hour: donkey anti-mouse/goat Alexa 488 (Invitrogen), donkey anti-rabbit/mouse CY3 (Jackson Immuno Research), and donkey anti-rabbit Alexa 647 (Jackson Immuno Research), and washed with blocking buffer for 30 minutes. Nuclei were stained with DRAQ5 (Cell Signaling, 40845) or Hoechst 33342 (Thermo Fisher Scientific, 62249). Embryo and cell images were captured on a Nikon A1 Confocal Laser Scanning Microscope using 60X Plan Apo IR Water Objective (NA 1.27 WI).

2.3.6 Image Analysis

Images were analyzed with FIJI Image J software. Graphs were generated with Prism GraphPad.

2.4 RESULTS AND DISCUSSION

2.4.1 Embryo-derived XEN cells express ZIKV receptor candidates

To predict ZIKV ability to infect preimplantation development cells, I first observed the expression of proviral factor genes in embryo-derived stem cells. Putative ZIKV receptors or proviral factors

were discovered in humans cells [43]. Moreover, the upregulation of these proviral factors increased ZIKV infection, whereas inhibition of receptors decreased ZIKV infection [46]. Therefore, I performed a qRT-PCR screen for proviral factors in trophoblast (TS) and extraembryonic endoderm (XEN) stem cells (Table 2.1). TSC and XEN cells are cell lines representative of trophectoderm and primitive endoderm in blastocysts and give rise to extraembryonic tissues such as the placenta and the yolk sac in fetal development. These tissues are also known to be infected by ZIKV [48, 74, 75, 128, 160, 161].

I found that seven proviral factor genes were expressed in embryo-derived stem cells. Specifically, XEN cells express *Icam2*, *M6pr*, *Sdcbp*, *Tyro3*, *Axl*, and *Mertk* genes, whereas TSCs express *M6pr*, *Sdcbp*, *Tyro3*, *Hla-G*, *Axl*, and *Mertk* genes. *Tim1* (*Havcr1* mouse variant) and *Icam5* (*Icam3* mouse variant) genes were not expressed in XEN and TS cells. Of the seven genes, only five proviral genes were common in both TS and XEN cells (Table 2.1). The five receptors are characterized into three categories: *Mertk*, *Tyro3*, and *Axl* genes encode phosphatidylserine receptors, *M6pr* gene encodes for a C-leptin type receptor, and *Sdcbp* encodes a glycosaminoglycan [43].

Next, I examined the transcript levels of the five verified proviral genes in all three embryo-derived stem cells, TS, XEN, and ES cells, using publicly available microarray data [162]. I examined embryo-derived stem cell specific genes such as *Nanog* and *Sox2* for ES cells, *Cdx2* and *Gata3* for TS cells, and *Sox17* and *Sox7* for XEN to show expression levels of functionally important genes (Figure 2.1A). Notably, *Mertk* expression is higher in XEN cells than in TS and ES cells (Figure 2.1A). Similarly, MERTK protein expression is higher in XEN cells than TS and ES cells (Figure 2.2A).

I then examined protein expression of other proviral factors that I previously verified. Specifically, TYRO3 presence correlated to high expression of *Tyro3* in XEN cells (Figure 2.1A, 2.5A). *Axl* gene expression was low in all embryo-derived stem cells (Figure 2.1A) and AXL protein was undetectable in all embryo-derived stem cells. Interestingly, *M6pr* gene expression was high in all three embryo-derived stem cells (Figure 2.1). However, M6PR protein was only detectable in ES and XEN cells (Figure 2.3A, 2.5A). Similarly, SDCBP protein was expressed in ES and XEN cells

(Figure 2.3A, 2.5A), although, Sdcbp expression levels in all three embryo dervied stem cells were moderate (Figure 2.1A). Based on the levels of proviral genes, XEN cells could be more susceptible to ZIKV infection than TS and ES cells.

2.4.2 ES cells express antiviral genes

Previously, I had shown that proviral factors are expressed in embryo-derived stem cells. However, antiviral factors could interfere with infection, decreasing the embryo-derived stem cell susceptibility to ZIKV. One of the classes of antiviral factors is called the interferon-stimulated genes (ISGs) [58]. There is evidence that specific antiviral genes, such as *Ifitm1* and *Bst2*, target flavivirus or ZIKV infection. In human embryonic stem cells (hESCs), basal ISGs activity, particularly within the IFITM family, plays a role in inhibiting ZIKV infection [59]. I, therefore, examined the expression of antiviral factors in three murine embryo-derived stem cells [162]. Remarkably, I found that more antiviral genes are expressed in mouse ESCs (mESCs) compared to TS and XEN cells, consistent with hESCs antiviral factor patterns (Figure 2.1A). These results, coupled with the decrease expression of proviral genes, suggest that ESCs are more resistant to ZIKV infection than other embryo lineages. Furthermore, the conservation of ISG patterns between species could be significant to protect pluripotent lineage [59, 143, 163, 164].

2.4.3 Murine preimplantation embryos express proviral genes

Previously, showed that individual embryo cell lineages dynamically express anti- and proviral factors and predict ZIKV infection in blastocysts. However, the expression of viral factors prior to blastocyst development has not been examined. I, therefore, examined the expression of pro- and antiviral factors to predict the infectability of ZIKV infection throughout preimplantation development.

To understand the susceptibility of preimplantation development to ZIKV infection, I examined the gene expression of proviral and antiviral factors such as ZIKV receptors and ISGs [165]. First, genes such as *Sox2* for Epiblast (EPI), *Cdx2* for Trophectoderm (TE), and *Sox17* for Primitive

endoderm (PE) were established to show functional transcript levels. I then observed that proviral factors were more highly expressed throughout preimplantation development than the antiviral genes (Figure 2.6A). However, there were no substantial differences observed across different preimplantation stages. These results suggest that mouse preimplantation embryos are susceptible to ZIKV infection.

To explore the localization of the proviral factors, I harvested mouse embryos at zero, one, two, and three-days post-conception (zygote, two-cell, eight-cell, and blastocyst), including the egg, and examined the protein expression of the putative proviral factors. I found that MERTK, SYTENIN (SDCBP), and AXL are expressed in embryos at the two-cell stage (Figure 2.8C, D, E-F), and MERTK, SDCBP, and TYRO3 are expressed in blastocyst (Figure 2.8A, D, E-F). M6PR was not detected in preimplantation embryos. The zygote and eight-cell embryos express the fewest proviral factors. Consistent with the localization of receptors, MERTK, AXL, SDCBP, and TYRO3 proteins localized near the cell surface of embryos (Figure 2.8A-F). These results suggest that two-cell and blastocyst stage embryos are more susceptible to ZIKV infection than other preimplantation stages.

2.4.4 Human preimplantation embryos express antiviral genes

While understanding the viral susceptibility in mice is relevant, there is little known about human preimplantation embryo susceptibility to ZIKV infection. Human preimplantation stages slightly differ in time. The first four days (E0-E4) of human development are fertilization and cleavage division into morula [80]. At five days of development/post-conception (E5), the embryo had developed into blastocyst and is prepared to implant into the uterine wall by day seven (E7) until about two weeks of pregnancy [80]. Mouse embryos, however, develop to blastocyst and implant within the first four days of development [79, 80]. Even with time differences between the species, preimplantation embryo stages are similar.

To characterize the expression of proviral and antiviral factor genes, I first observed functional genes during human preimplantation development using single-cell RNA-seq: *GATA3*, *SOX2*, and *SOX17* (Figure 2.7A) [129]. Contrary to mouse preimplantation development, more antiviral factor

genes were expressed in human embryos between E5-E7, particularly in epiblasts, than proviral factors (Figure 2.7A). These results are similar to their expression of antiviral genes in human and mouse ESC, an epiblast stem cell and *in vitro* model [59, 80, 104]. The expression patterns of ISGs could indicate the inhibition of ZIKV infection in preimplantation development, revealing the significance of viral protection of human pluripotent cells and early embryo development.

2.4.5 Undifferentiated embryo-derived stem cells express putative proviral factors

Previously, I have shown that proviral genes are expressed in mouse embryo-derived stem cells and embryos and can therefore predict embryonic cell's infectability to ZIKV. The basis of stem cells is that they can self-renew or differentiate into different cell types. Along with morphological differences, the gene expression changes through differentiation resembling more developed or mature cells. Therefore, I hypothesize that expression of gene encoding proviral factors changes throughout the differentiation of embryo-derived stem cells. Since the placenta and the yolk sac are the first lines of defense for infection in fetal development, I focused on TS and XEN cell differentiation for this [48, 49, 68, 166].

To predict the infectibility of differentiated TS cells, I differentiated TSCs for six days and harvested cells to examine proviral gene expression (Figure 2.9A). I examined multiple genes known to fluctuate during differentiation, such as *Gata3* and *Cdx2* to confirm differentiation (Figure 2.9C) [118]. As expected, *Cdx2* decreased, whereas *Gata3* increased during TSC differentiation. Furthermore, I observed morphological changes in cells where TSC transitioned from epithelial colonies to resembling post-implantation placental giant cells and syncytial trophoblasts (Figure 2.9A-B). I then examined the expression of proviral genes. I found that *Mertk* increases, whereas *Sdcbp* and *Axl* decreases as TSC cells differentiate (Figure 2.9D). *M6pr* and *Tyro3* proviral genes were dynamically expressed (Figure 2.9D). Overall, expression of proviral genes tended to decrease during differentiation (Figure 2.11A). These trends show that the undifferentiated TSC could be more susceptible to infection than differentiated TSC. This prediction is consistent with previous studies, where undeveloped placenta cells in the first trimester or trophectoderm cells were more

susceptible to infection than more developed third-trimester placental cells [48, 76, 78].

I previously studied how proviral gene expression fluctuates during the TSC differentiation of cells to study the windows of susceptibility to ZIKV infection. However, it is unknown if pre-yolk sac cells or XEN cells can be infected with ZIKV. Similarly, I studied the expression of proviral genes throughout XEN cell differentiation. Undifferentiated XEN cells have mesenchymal characteristics and differentiate to epithelial sheets, post-implantation visceral endoderm-like cells (Figure 2.10A-B). To verify the differentiation of XEN cells, I found that *Apoa1* and *Tnnc1* increases, consistent with previous studies (Figure 2.10C) [114, 116, 117, 122]. I then examined ZIKV receptor expression during XEN cell differentiation. I observed that *Mertk*, *Sdcbp*, and *Axl* were expressed at higher levels in undifferentiated XEN cells than differentiated XEN cells (Figure 2.10D). By contrast, *Tyro3* is expressed at higher levels in differentiated XEN cells while M6pr expression did not change over differentiation (Figure 2.10D). More proviral genes were expressed in undifferentiated XEN cells, while fewer receptors were expressed in differentiated XEN cells (Figure 2.11B). These results suggest that pre-yolk sac lineage cells are more susceptible to infection than developed yolk sac cells.

2.4.6 Conclusion

ZIKV infection is known to cause developmental conditions that can be devastating to families. Knowing the risk and the developmental windows of susceptibility to infection is crucial for epidemiology experts. Until recently, the focus has shifted towards preimplantation ZIKV infection, which is known to cause severe developmental arrest and cell apoptosis [78, 131]. While embryos can be infected, not all preimplantation developmental stages have been explored. It is imperative to understand the patterns of molecules that influence ZIKV infection: proviral and antiviral factors.

Here, I examined the expression levels of proviral and antiviral throughout preimplantation as well as differentiated tissues. I found that mouse ES cells may be more resistant to infection because they express antiviral factors, consistent hESCs and human epiblast cells in preimplantation development [59]. Additionally, undifferentiated extraembryonic lineage cells, TS and XEN cells,

express more proviral factors than their differentiated cell progeny. While the observed expression patterns of the pro- and antiviral genes could reveal the susceptibility of embryos to ZIKV infection, other important pathways may exist. Since viruses exploit the host machinery to survive and other genes, receptors and intracellular proteins could be involved in viral infection [167, 168]. Additionally, other antiviral factors outside of ISGs could inhibit ZIKV infection. Nevertheless, these observations of proviral genes could corroborate ZIKV infection in early mouse development.

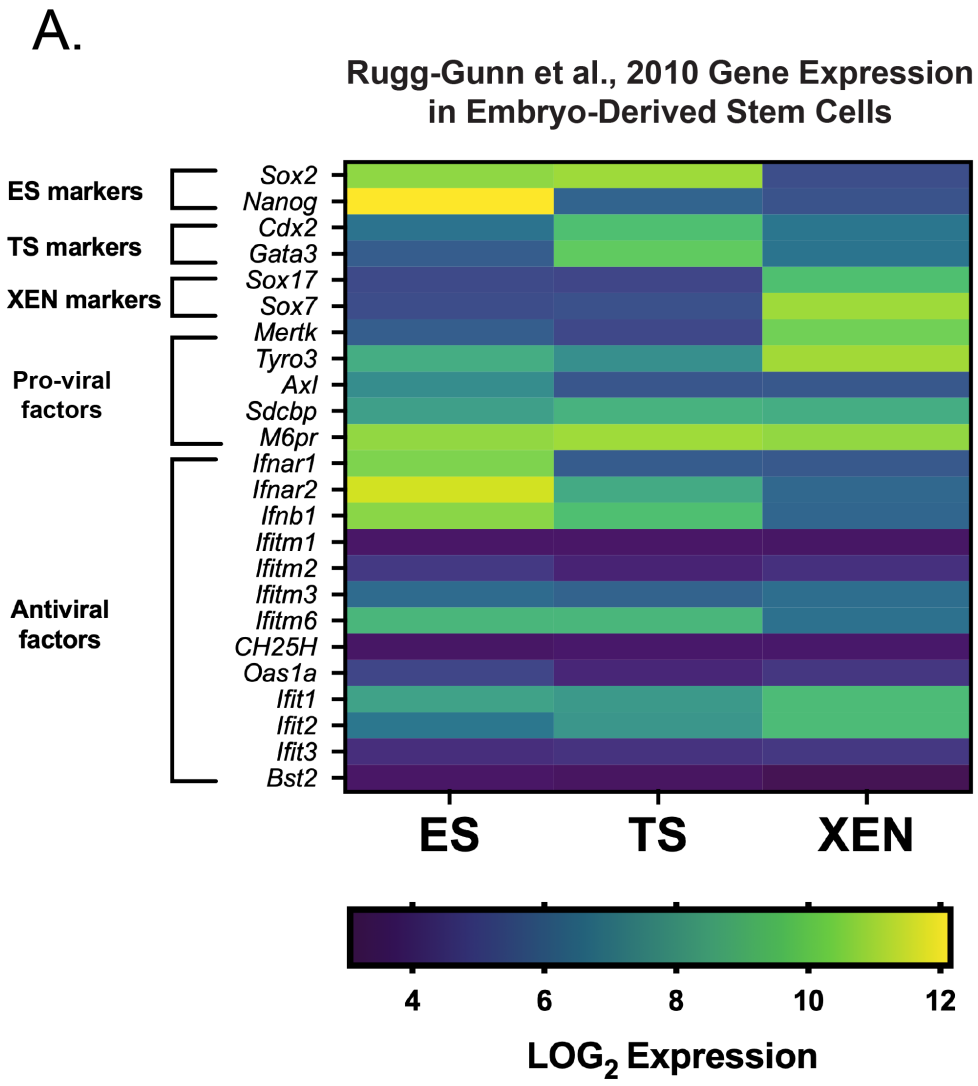

Figure 2.1: XEN cells express proviral factors. A. Heatmap displaying the Log_2 expression of Control, proviral factors, and antiviral factors genes in embryo-derived stem cell: Embryonic (ES), Trophoblast (TS), and Extraembryonic endoderm (XEN) stem cells.

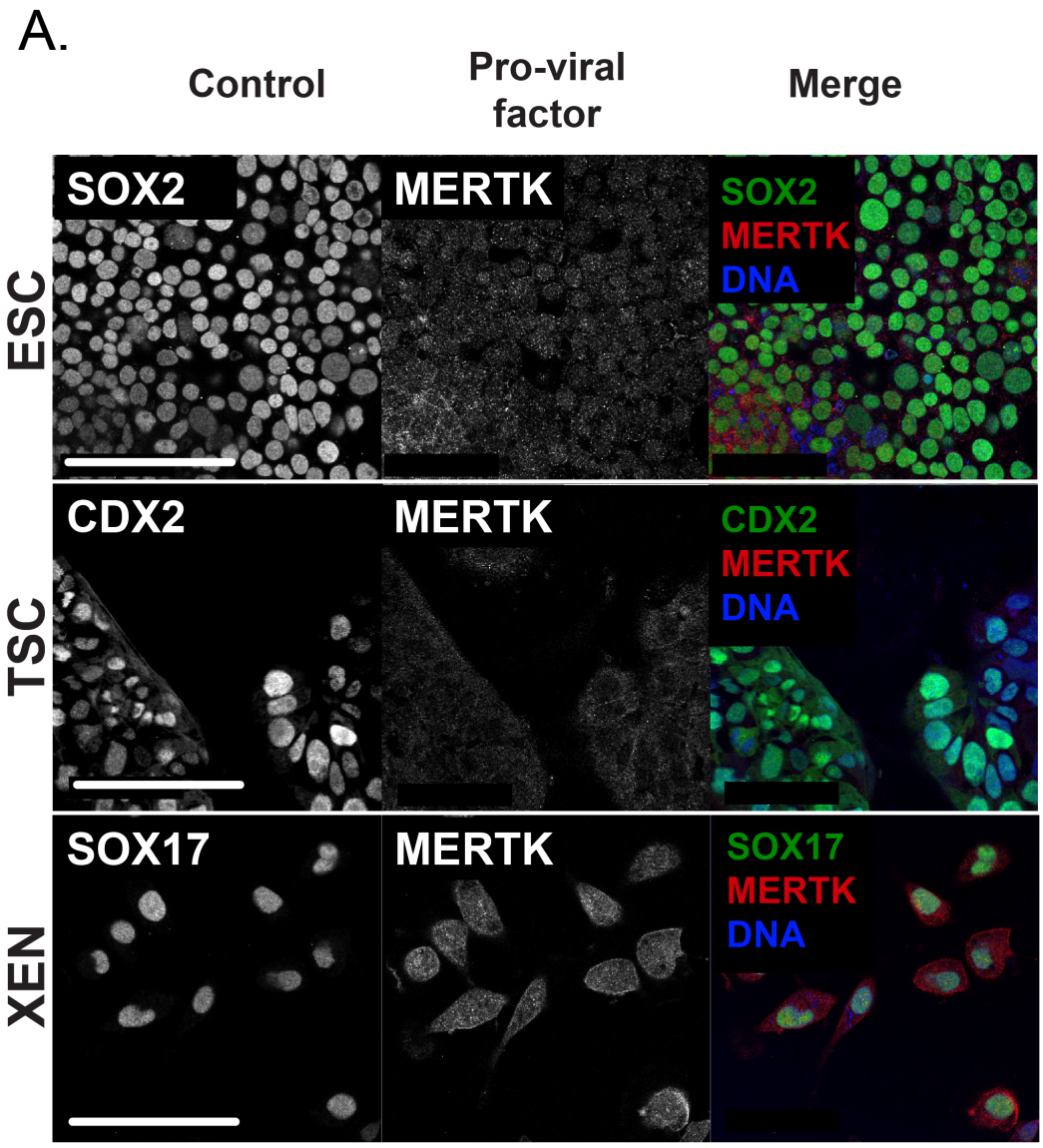

Figure 2.2: MERTK is detectable in XEN, but not in ES and TS cells. A. The protein expression of MERTK in embryo-derived stem cells: ES, TS, and XEN cells.Scale bar = 50 μm.

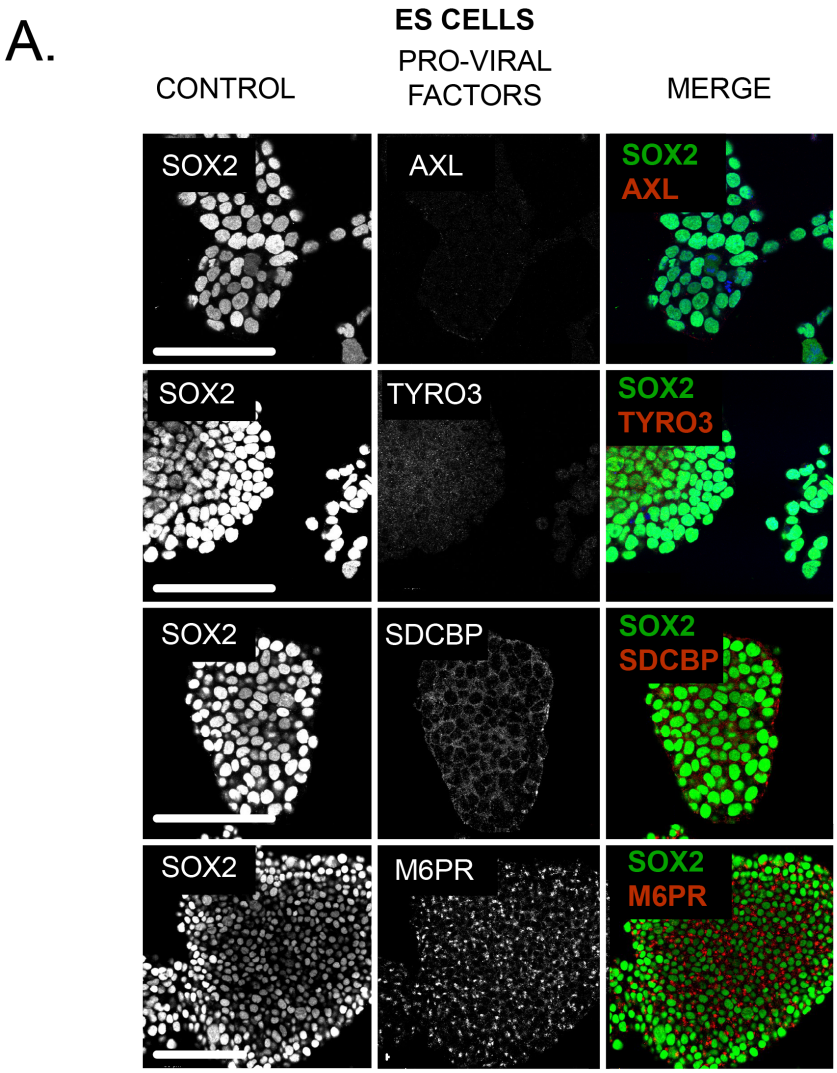

Figure 2.3: SDCBP and M6PR proviral proteins are detected in ES cells. A. Confocal imaging of ES cells immunostained for SOX2 and proviral factors, AXL, TYRO3, SDCBP, and M6PR. Scale bar = 100 µm.

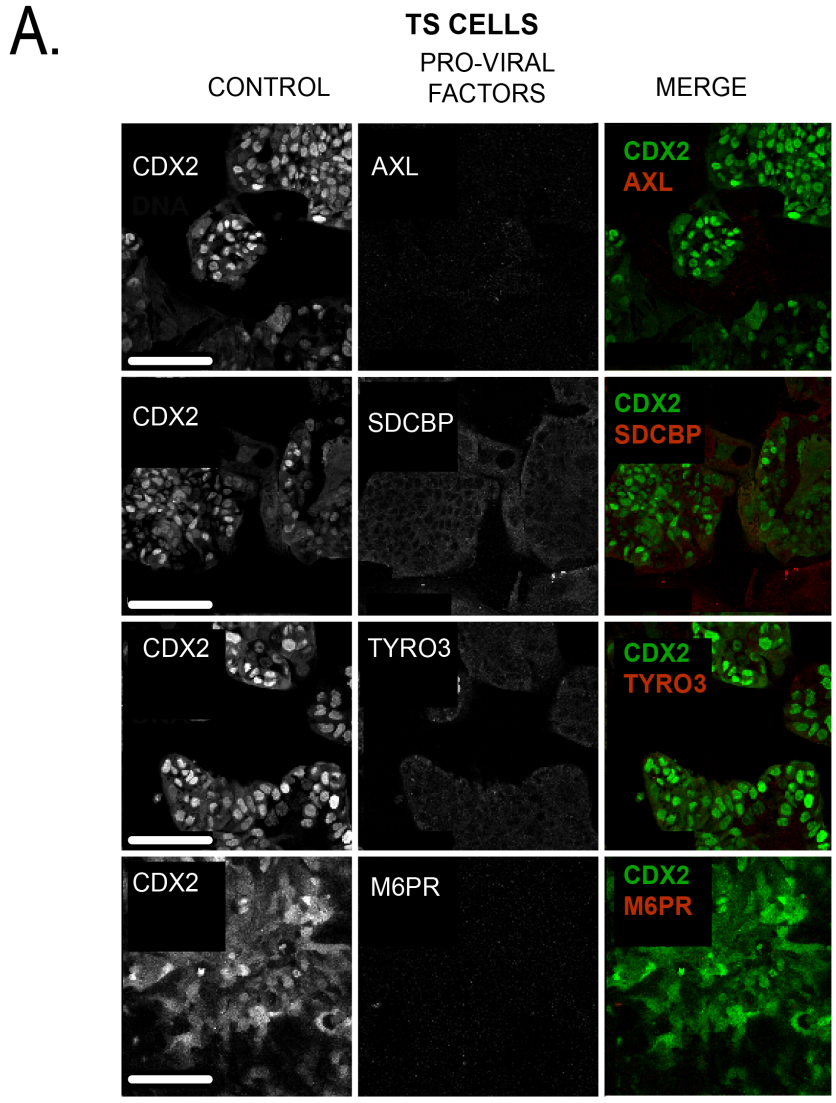

Figure 2.4: No proteins are detected in TS cells. A. Confocal imaging of TS cells immunostained for CDX2 and proviral factors, AXL, SDCBP, TYRO3, and M6PR. Scale bar = 100 µm.

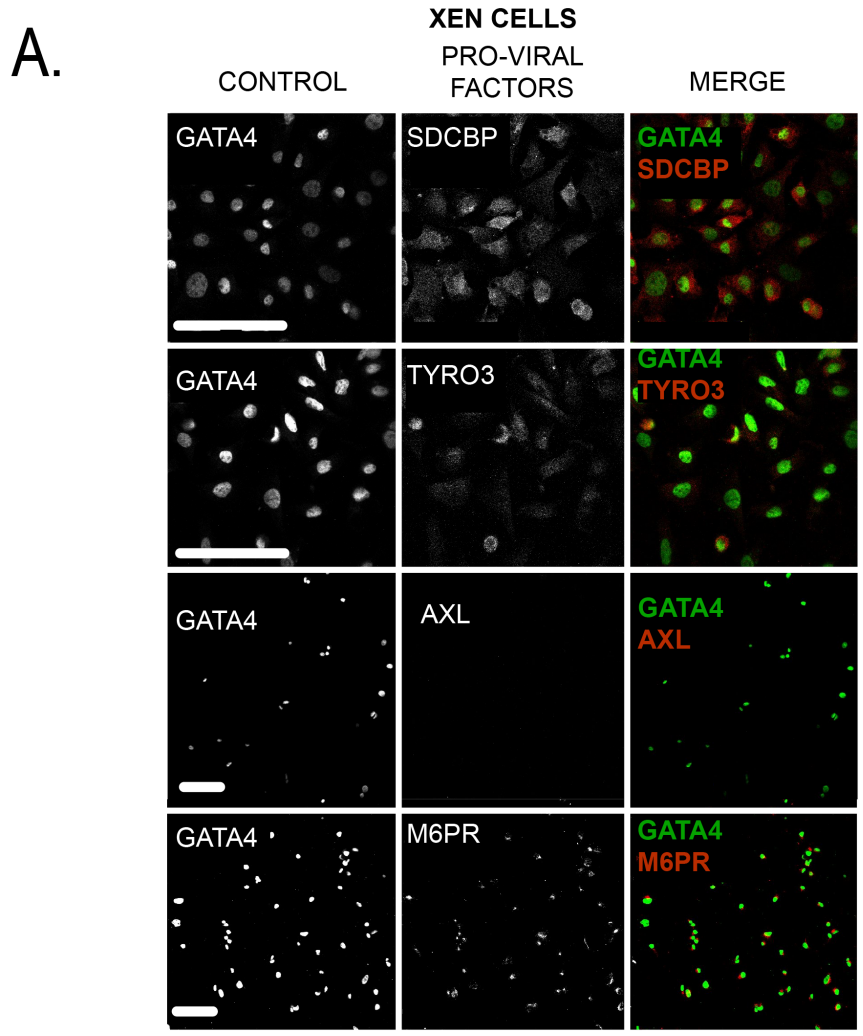

Figure 2.5: SDCBP and TYRO3 proviral proteins are detected in XEN cells. A. Confocal imaging of XEN cells immunostained for GATA4 and proviral factors, SDCBP, TYRO3, AXL, and M6PR. Scale bar = 100 μm

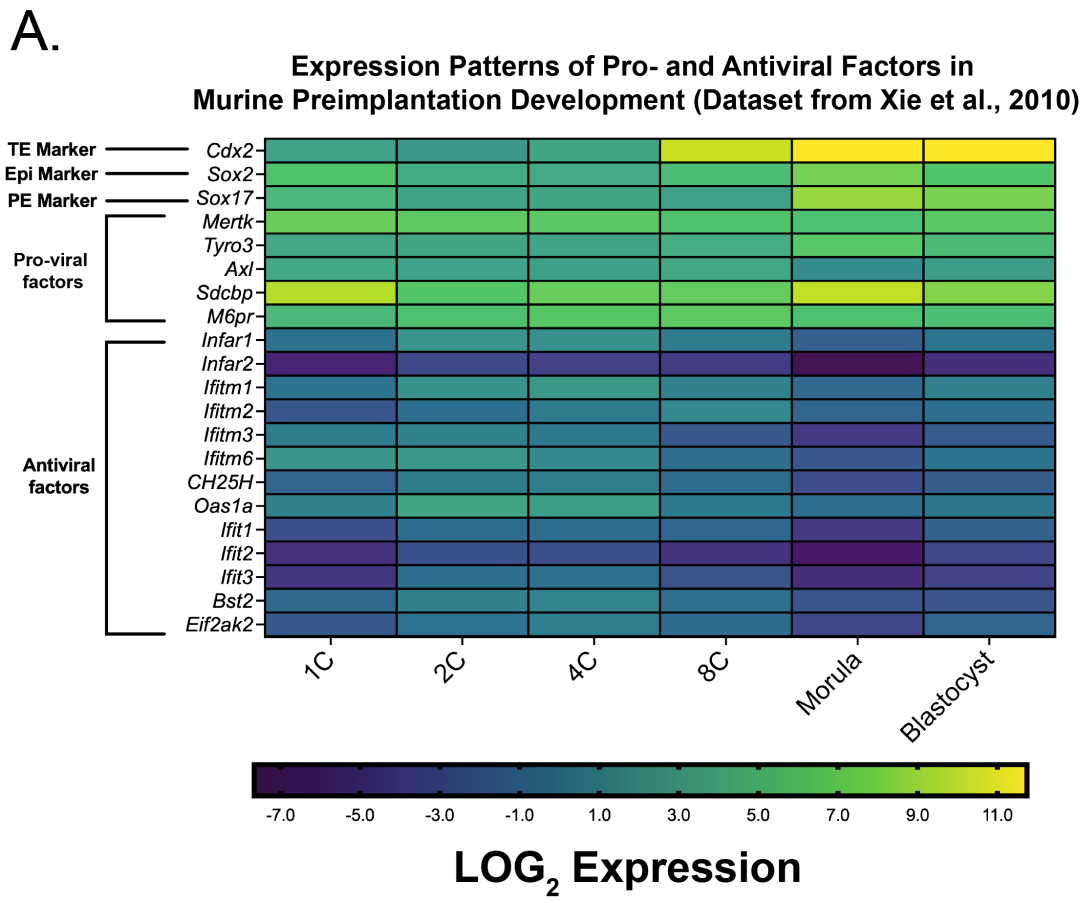

Figure 2.6: Mouse preimplantation embryos express proviral factors. A. A heatmap displaying the LOG_2 expression of three cell fates in blastocysts, proviral factors, and antiviral factors in murine preimplantation development.

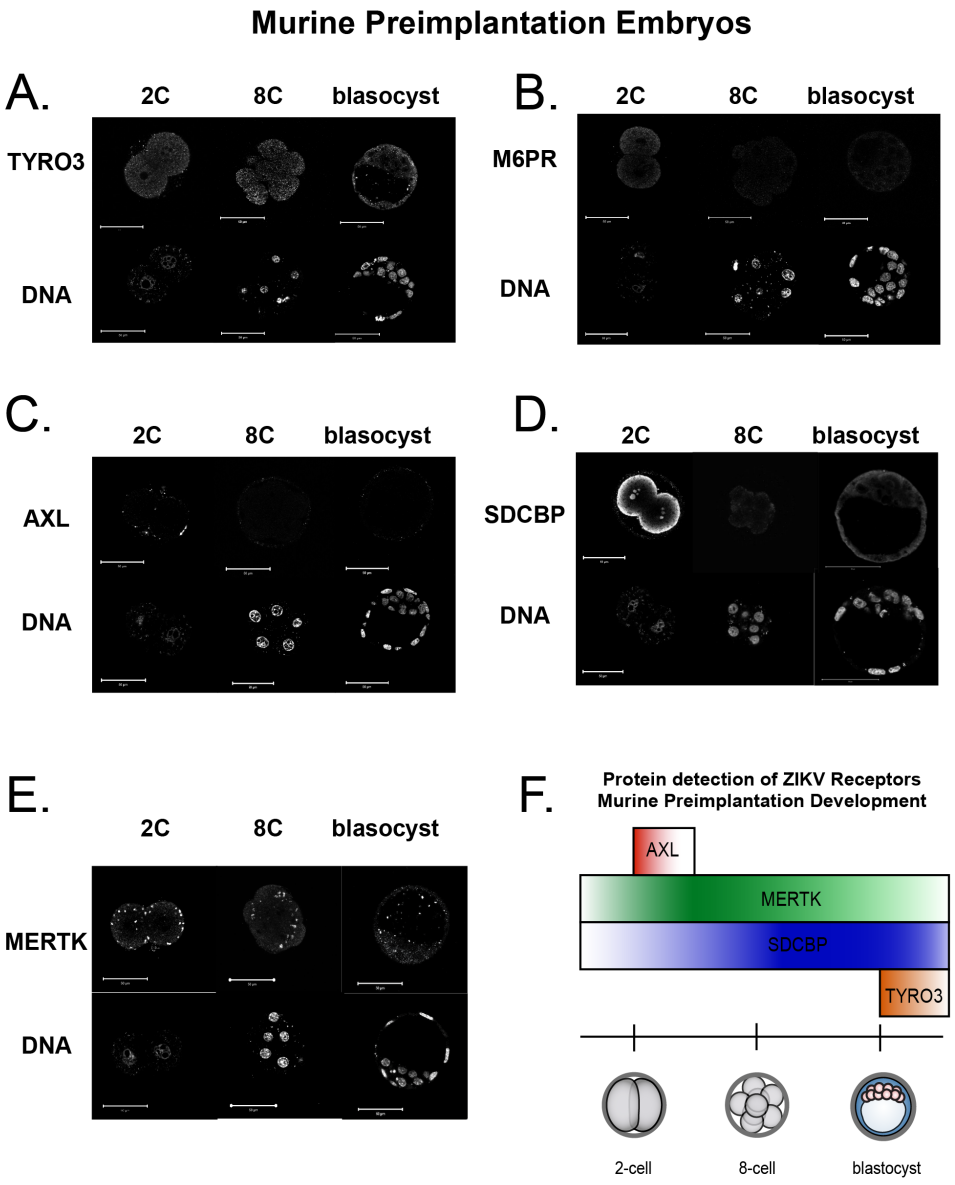

Figure 2.7: Protein expression of proviral factors at preimplantation two-cell (2C), eight-cell (8C), and blastocyst stages. **A.** Confocal imaging of TYRO3 immunofluorescence and nuclear stain. **B.** Confocal imaging of M6PR immunofluorescence and nuclear stain. **C.** Confocal imaging of AXL immunofluorescence and nuclear stain. **D.** Confocal imaging of SDCBP immunofluorescence and nuclear stain. **E.** Confocal imaging of MERTK immunofluorescence and nuclear stain. **F.** Summary of proviral proteins expressed in 2C, 8C, and blastocyst embryos. Scale bar for all confocal images = 50 μm.

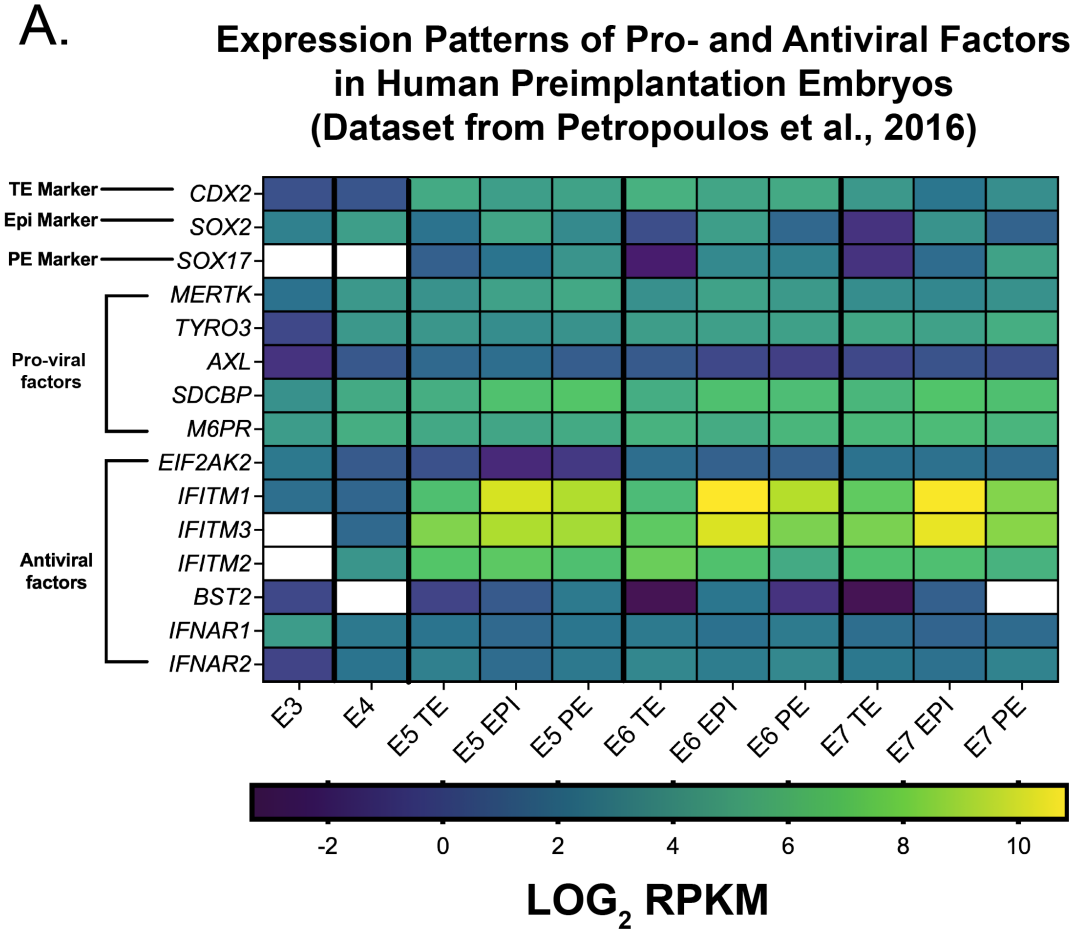

Figure 2.8: Human preimplantation embryos express antiviral factor genes. A. A heatmap displaying the Log_2 expression of cell fate, proviral factors, and antiviral factor genes in human preimplantation from E3 (morula) to E7 (late blastocyst) split into different cell lineages TE (trophectoderm), EPI (epiblast), and PE (primitive endoderm).

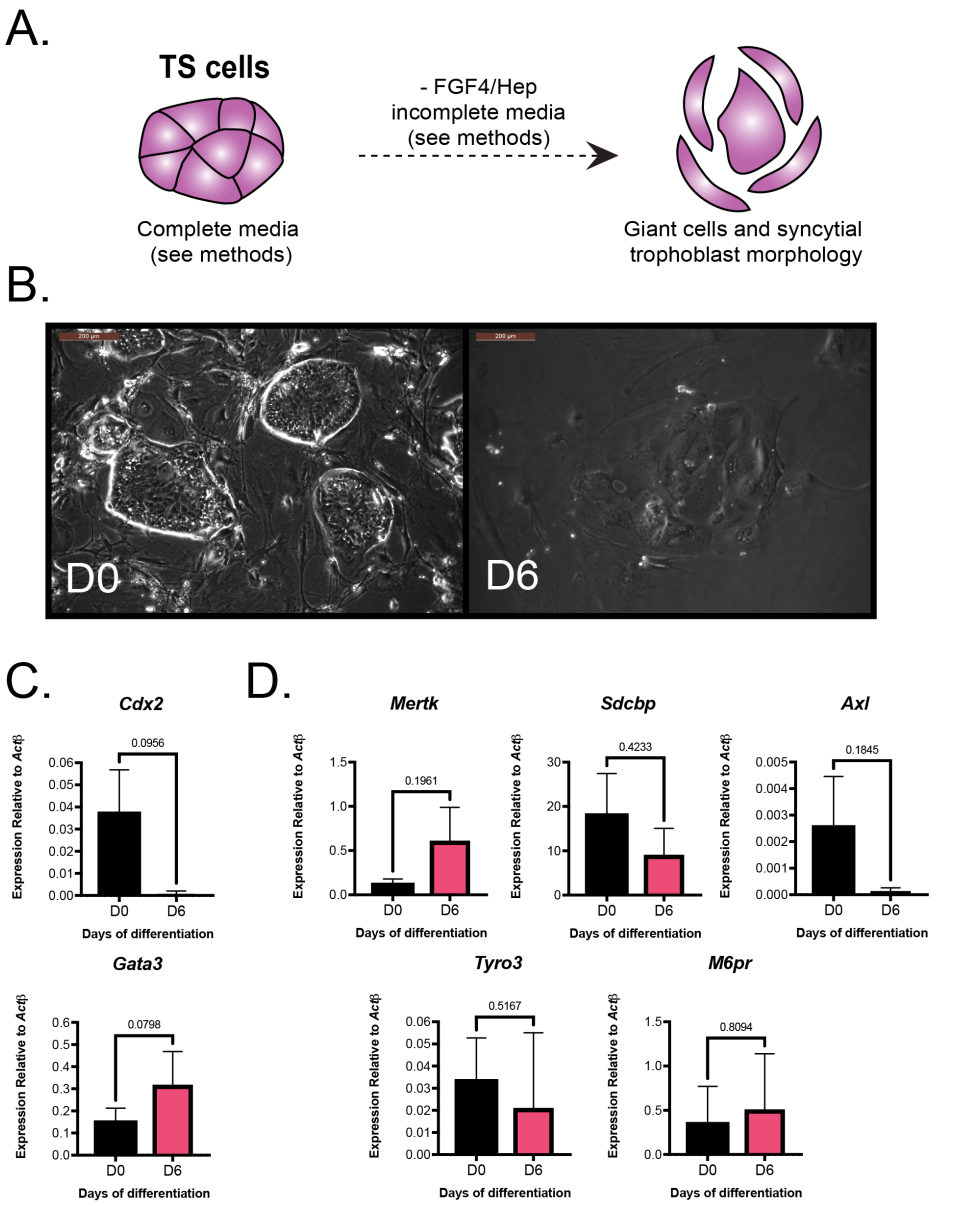

Figure 2.9: Undifferentiated TSCs express more proviral factors than differentiated TSCs. A. Experimental Design: The differentiation scheme of trophoblasts stem cells *in vitro* **B.** Brightfield images of undifferentiated TS cells (D0) and differentiated TS cell at Day 6 (D6). The morphological images shows that D0 TS cells grow in colonies whereas D6 TS cells transform to giant cells and syncytial trophoblast cells. **C.** Bar graphs show the expression of *Cdx2* and *Gata3* relative to *Actβ* at day 0 XEN (D0) and day 6 (D6) of XEN cells differentiation. **D.** Bar graphs show the expression of *Mertk*, *Sdcbp*, *Axl*, *Tyro3*, and *M6pr* genes relative to *Actβ* throughout XEN differentiation using RT-qPCR of three replicates. For all bar graph n=3 and statistics = paired t-test.

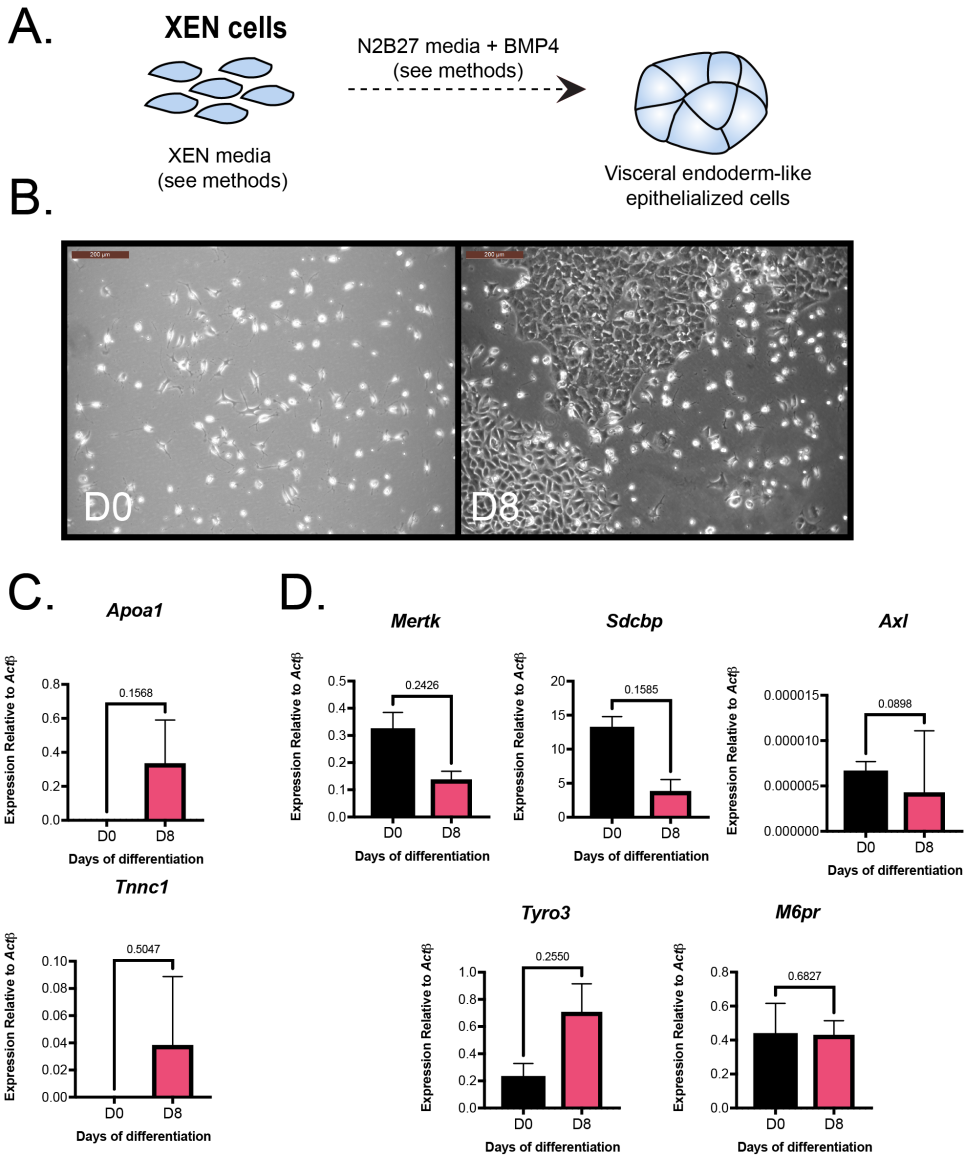

Figure 2.10: Undifferenitated XEN cells express more proviral factors than differentiated XEN cells. **A.** Experimental Design: The differentiation scheme of extraembryonic endoderm (XEN) cells in vitro **B.** Brightfield images of undifferentiated XEN cells and differentiated XEN cell (D0) at Day 8 (D8). D0 XEN cells grow in colonies whereas D8 XEN cells transform to epithelial sheet and visceral-like cells **C.** Bar graphs show the expression of *Tnnc1* and *Apoa1* relative to *Actβ* at day 0 XEN (D0) and day 8 (D8) of XEN cells differentiation. **D.** Bar graphs show the expression of *Mertk*, *Sdcbp*, *Axl*, *Tyro3*, and *M6pr* genes relative to *Actβ* throughout XEN differentiation using RT-qPCR of three replicates. For all bar graph n=2 or more and statistics = paired t-test

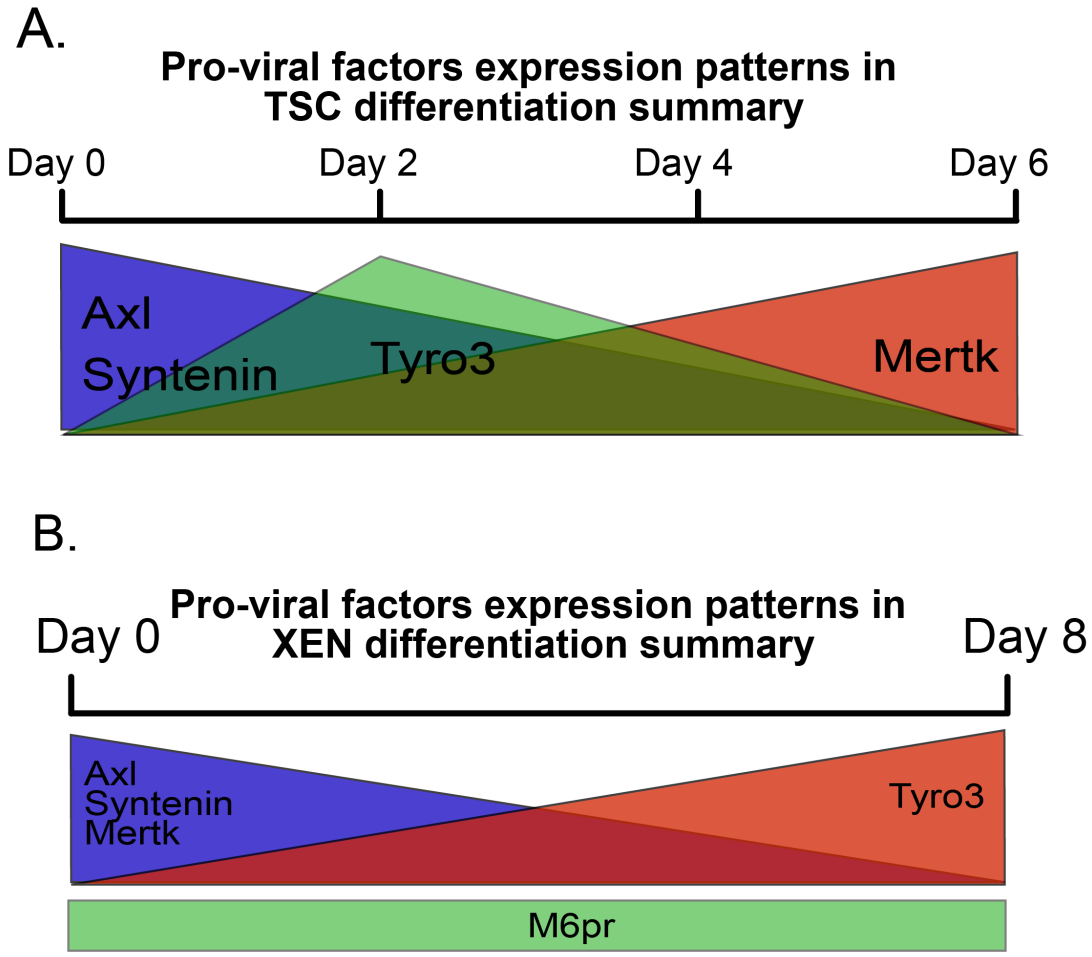

Figure 2.11: Summary of proviral factors dynamics throughout embryo-derived stem cell differentiation. **A.** Summary of the expression patterns of proviral factors throughout XEN differentiation using three replicates of RT-qPCR. **B.** Summary of the expression patterns of proviral factors throughout XEN differentiation using three replicates of RT-qPCR.

Table 2.1: Initial screen of candidate proviral genes in XEN and TS cells

Genes		*Icam2*	*M6pr*	*Sdcbp*	*Tyro3*	*Hla-G*	*Axl*	*Havcr1 (Tim1)*	*Mertk*	*Icam3 (Icam5)*
Cell types	**XEN**	X	X	X	X		X		X	
	TSC		X	X	X	X	X		X	

Table 2.2: ZIKV Receptor Primers

Marker types	Gene name	Forward Sequence (5'-3')	Reverse Sequence (5'-3')
Housekeeping	*beta-Actin*	F' CTGAACCCTAAGGCCAACC	R' CCAGAGGCATACAGGGACAG
TS Markers	*Cdx2*	F' AGACAAATACCGGGTGGTGTA	R' CCAGCTCACTTTTCCTCCTGA
	Gata3	F' GGGTTCGGATGTAAGTCGAG	R' CCACAGTGGGGTAGAGGTTG
XEN Markers	*Cldn6*	F' GCTCTGAACCACACAGCACA	R' AGACAAAGCTGACCGAGCAC
	Sox17	F' CTTTATGGTGTGGGCCAAAC	GCTTCTCTGCCAAGGTCAAC
	Tnnc1	F' CAGCAAAGGGAAGTCTGAGG	R' TAGTCAATTCGGCCATCGTT
Proviral factors	*M6pr*	F' CAAAGAACGAGGTGGCTCTC	R' CCCAACCACTGTCTCCTTGT
	Sdcbp	F' CAACGGACAGAACGTCATTG	R' GGTGTGATCCATCAGGCTTT
	Tyro3	F' GCGGGGACTATTATCGTCAG	R' GCTCGAGCACTGGTACATGA
	Axl	F' GTCAAGGAAATCGGCTGAAA	R' GTCAGCTGCAGTGAGACAGC
	Mertk	F' GACTCCCTATCCCGGAGTTC	R' CACAGAGAAGGTGGGTCGAT

Table 2.3: Antibodies

Marker Types	Antigen	Animal	Isotype	Source	Cat No./Clone	Working conc.
TE/TSC	mCDX2	mo	IgG1, kappa	BioGenex	CDX2-88	1 to 2000
EPI/ES	SOX2	goat	IgG	Neuromics	GT15098	1 to 2000
PE/XEN	hSOX17	goat	IgG	R&D Systems	AF1924	1 to 2000
	mGATA4	goat	IgG	Santa Cruz Biotechnology Inc	sc1237	1 to 2000
proviral factors	mAXL	rat	IgG2A	R&D Systems	MAB8541	1 to 500
	M6PR	Rabbit	IgG	Abcam	ab134153	1 to 200
	MERTK	Rabbit	IgG	Abcam	ab95925	1 to 400
	SYNTENIN	Rabbit	IgG	Abcam	ab19903	1 to 400
	TYRO3	Rabbit	IgG	Abcam	ab79778	1 to 500

CHAPTER 3

ZIKV INFECTIONS ARE LOW IN EMBRYO-DERIVED STEM CELLS

Jennifer L. Watts

This study was supported by the James K. Billman, Jr., M.D. Endowment at Michigan State University and National Institutes of Health awards R01 GM131759 and T32 HD087166.

3.1 ABSTRACT

Mammalian stem cells have been a robust *in vitro* model for infection in tissues. Preimplantation embryos develop three cells types at the blastocyst stage from which stem cells can be derived: trophoblast, extraembryonic endoderm, and embryonic stem cells. These *in vitro* representations of the blastocyst lineage can serve as a model of embryo cell population infection. However, ZIKV infection of all three embryo-derived stem cells have not been explored. I have discovered that candidate proviral factors are present in early embryos. Among these, MERTK and TYRO3 are present in both mouse embryo-derived stem cell lines and preimplantation embryos. Nevertheless, ZIKV did not highly infect undifferentiated embryo-derived stem cells compared to known infected cells. Moreover, ZIKV did not replicate in undifferentiated and differentiated embryo-derived cells were not infected. These results suggest that exposed preimplantation embryo cells *in vivo* will exhibit low infection and display less severe effects.

3.2 INTRODUCTION

ZIKV virus infection in pregnant mothers is known to cause severe congenital effects such as microcephaly and pregnancy loss. Efforts to understand ZIKV pathogenesis studies have examined fetal infection peri-placental and neural development using *in vitro* systems. Evidence shows that ZIKV can infect tissue-derived cells from placental and brain tissues via putative proviral factors such as AXL and MERTK [39, 48, 76, 169, 170, 166]. These *in vitro* studies are consistent with *in vivo* studies with more evidence of placental and neural damage [54, 60, 74]. While the studies on the pathology of ZIKV in fetal development are informative, there is an assumption that infection happens after the specification of placental and neural cells, about ten days post fertilization in mice and eight weeks in humans. However, ZIKV is sexually transmitted and affects embryos near conception, and it is unknown if implantation cells are infected by ZIKV.

There are very few studies capturing ZIKV infection in early pregnancy. Specifically, there is evidence that ZIKV infection can target preimplantation embryos up to four days post-fertilization in mice and one week in humans via ascending or sexual transmission [78, 131]. However, there

is little evidence of ZIKV infection in all embryo lineages. Embryo-derived stem cells, embryonic stem (ES) cells, trophoblast stem (TS) cells, and extraembryonic endoderm stem (XEN) cells serve as *in vitro* a proxy of epiblast (EPI), trophectoderm (TE), and primitive endoderm (PE) cells within the embryo, respectively [104, 109, 113]. Human embryonic stem cells and cultured TS cells have been modeled for ZIKV infection in early development. ES cells are resistant to ZIKV infection due to the antiviral gene expression of IFITs and IFITMs [59]. Conversely, TS cells were permissive to infection and expressed ZIKV receptors (proviral genes) such as AXL [78]. These findings of *in vitro* embryo-derived cell infections could provide insight to preimplantation development *in vivo* infections.

In human embryo-derived stem cells, ZIKV infection has been demonstrated in ES and TS cells . However, infection of human XEN cells is unknown because XEN cells have yet to be derived from human embryos. The challenges in human embryo-derived stem cells create a need for the study of mouse stem cell lines research organism. Previously, I found that antiviral genes are expressed at higher levels in mouse ES cells than in TS and XEN. Conversely, proviral genes were expressed higher in TS and XEN than in ES cells. I therefore hypothesize that ES cells will be more resistant to infection than TS and XEN cells. In this study, I infected all three embryo-derived stem cells with ZIKV to gain insight into how infection may happen in the three cells types in blastocysts. The gene expression of proviral and antiviral genes and proteins previously studied could corroborate ZIKV infectivity within stem cell progenitors in the embryo.

3.3 MATERIALS AND METHODS

3.3.1 Plaque Assay

Vero cells (ATCC, CRL-1586,) were cultured in 6-well plates to 100% confluency in 10% FBS EMEM in 5% CO_2 at 37°C. Cells were washed in EMEM without FBS and infected with $ZIKV^{PR}$ or PRVABC (ATCC, VR-1843) and $ZIKV^{UG}$ or MR776 (ATCC, VR-1838) diluted 10^2-10^6 in 500 mL of 2% FBS EMEM. Cells were infected or mock-infected for 15 minutes rocking at room temperature and incubated for 45 minutes in 5% CO_2 at 37°C. 4 mL of overlay (2% methylcellulose

prepared in 0% FBS EMEM) was added on top of inoculum in each well and incubated for 6-7 days. The overlay was then removed, and cells were fixed in 4% EM grade paraformaldehyde (Electron Microscopy Sciences, 15710). Vero cells were stained with 0.1% crystal violet solution prepared in 20% ethanol and 4% paraformaldehyde. Crystal violet stain was washed gently with water until the water was clear. Plaques were allowed to dry for 1-24 hours and counted under a transilluminator to determine viral titer (pfu/mL).

3.3.2 Chloroquine treatment

Cells were cultured in the incubator at 5% CO_2 at 37°C. Chloroquine (Invivogen, tlrl-chq) was prepared in XEN cell media at 0, 2, 20 and 200 μM. Cells were washed with PBS and treated with chloroquine for 1 hour. Chloroquine was rinsed with PBS and replaced with XEN cell media for toxicity experiment or infected with ZIKV and incubated for 24 hours.

3.3.3 Cell ZIKV infection

Vero, 293T (ATCC, CRL-3216), XEN (embryo-derived), ES (ATCC, SCRC-1036), and TS cells (passage <38) were cultured to 90-95% confluency in 12-well dishes in triplicates. Cells were washed with PBS (without Ca^{2+} and Mg^{2+}). Cells were inoculated with mock media or $ZIKV^{PR}$ in the appropriate cell media modified with 2% FBS. Cells were infected or mock-infected for 15 minutes rocking at room temperature and incubated for 45 minutes in 5% CO_2 at 37°C. Mock medium or ZIKV inoculum was removed, and cells were washed with PBS. The normal media for each cell type was added to the wells and incubated for 24, 48, and 96 hours.

3.3.4 Trophoblast Stem (TS) Cells Maintenance and Differentiation

Four-well Nunc plates with 30 nm coverslips or six-well plates were treated with 0.1% gelatin (Millipore, ES-006-B) and immediately aspirated. 100,000 TSCs (passage 23-28) for four-well plates or 600,000 TSCs for six-well plates were seeded in each well in 500 μL complete TSC media (70% feeder conditioned media and 30% incomplete media: RPMI, 20% FBS, 100 μM

beta-mercaptoethanol, 2 mM L-glutamine or glutamax, 1mM sodium pyruvate and 50 µg/mL and penicillin/streptomycin) with 25 ng/mL of FGF4 and 1 u/mL of Heparin. TSCs were maintained in 5% CO_2 at 37°C and fed every two days while passaged every six days. To differentiate TSC, cells were plated on gelatin in complete TSC media (day 0). The following day, and for every day thereafter for six days, media were replaced with incomplete TSC media. Morphological changes were observed between two and six days.

3.3.5 Extraembryonic Endoderm Stem (XEN) Cells Maintenance and Differentiation

CD-1 derived XEN cells (<38 passage) were plated gelatinized dishes in XEN Cell Medium (15% fetal bovine serum (FBS), 55 mM beta-mercaptoethanol (55x, Gibco), 0.1 mM non-essential amino acids, 1 mM sodium pyruvate, 2 mM L-glutamine or glutamax, 50 U or µg/mL pen/strep in DMEM) and incubated in 5% CO_2 at 37°C. To differentiate XEN cells to Visceral Endoderm like cells, culture dishes were treated with Poly-L-ornithine 0.01% solution (Sigma) for 30 minutes at room temperature and Laminin (Sigma L2020) at a concentration of 0.15 µg/cm^3. 2000 cell/mm^2 of XEN cells are cultured in each well in N2B27 Medium (50% DMEM-F12 mixture (Invitrogen), 50% Neural Basal Medium (Invitrogen), 100x N2 Medium (Invitrogen), 50x B27 (Invitrogen), 10000 U Pen/Strep and 55 mM beta-mercaptoethanol) and cultured overnight in 5% CO_2 at 37°C. N2B27 medium was changed on the next with N2B27 supplemented with 50 ng/mL BMP4 (R&D Systems) and every other day for 6-8 days.

3.3.6 Embryonic Stem Cell Maintenance

R1 ES cells are plated on 0.1% gelatin in ES medium (15% fetal bovine serum (FBS), 55 mM beta-mercaptoethanol, 0.1 mM non-essential amino acids, 1 mM sodium pyruvate, 2 mM L-glutamine or glutamax, 50 U or µg/mL pen/strep and 10 ng/mL LIF in DMEM. ES cells underwent a media change every and passaged every 2 days.

3.3.7 RT-qPCR

For each time point, RNA was harvested using TriZol (Thermo Fisher Scientific, 15596018, Pub No. MAN0001271) and then cDNA was prepared using the QuantiTect Reverse Transcriptase kit (Qiagen, 205313). Newly produced cDNA was diluted 1:10. A master mix was made using Sybr Green PCR Master Mix (Applied Biosystems, 4309155), water, and each primer pair (Table 3.1). The master mix and cDNA were added to the 96-well plate and analyzed using a QuantStudio3 instrument in technical triplicates.

3.3.8 Immunofluorescence and Confocal Microscopy

Cells were fixed in 4% formaldehyde for 10 minutes at room temperature, permeabilized with 0.5% Triton X-100 for 30 minutes at room temperature, and blocked with 10% FBS and 0.1% Triton X-100 blocking buffer for 1 hour at room temperature or longer at 4°C. Primary antibodies were prepared in blocking buffer, and embryos and cells were incubated at 4°C overnight with the ZIKV-E antibody (GTX133314, GeneTex). Embryos and cells were washed with blocking buffer for 30 minutes, incubated with the following secondary antibodies for an hour: donkey anti-mouse/goat Alexa 488 (Invitrogen), donkey anti-rabbit/mouse CY3 (Jackson Immuno Research), and donkey anti-rabbit Alexa 647 (Jackson Immuno Research), and washed with blocking buffer for 30 minutes. Nuclei were stained with DRAQ5 (Cell Signaling, 40845) or Hoechst 33342 (Thermo Fisher Scientific, 62249). Images were captured on a Nikon A1 Confocal Laser Scanning Microscope using 60X Plan Apo IR Water Objective (NA 1.27 WI). Each embryo was imaged entirely through a z-stack at 5 µm optical sections.

3.3.9 Image Analysis

Images were analyzed with FIJI Image J software cell counter. Cells were counted throughout the z-stack for total cells, each cell lineage marker, and ZIKV-E positive cells and imported into the Excel and GraphPad software. In addition to raw cell counts, the proportion of each cell lineage

marker and ZIKV infected cells were calculated relative to total cells. Graphs were generated with GraphPad.

3.4 RESULTS AND DISCUSSION

3.4.1 Determining Viral Titer of Infectious ZIKV

Before performing infection experiments, it is imperative to determine infectious viral titers to control the virus concentrations by performing plaque assays [171]. First, African green monkey cells or Vero cells were grown to 100% confluency. Then, I infected the cells with ZIKV in multiple serial dilutions, placed a CMC overlay, and incubated them for seven days. No plaques were observed in control or noninfected wells. However, increased concentrations exhibited increased number of plaques (Figure 3.2A). Plaques were counted from a desired well, and then used to calculate the viral titer for further experiments.

3.4.2 Reagent optimization for detecting ZIKV

Next, I optimized ZIKV infection protocols for embryo-derived stem cells. I used qPCR techniques because it is commonly used to detect ZIKV in human clinical infection [172]. I performed an initial infection comparing infection in human epithelial kidney (HEK 293T) cells and murine extraembryonic endoderm stem (XEN) cells with mock, one, and ten multiplicity of infection (MOI) concentrations of $ZIKV^{PR}$, I found that infection was hardly detectable with Cp values reaching 40 and above, the limit of detection (Fig. 3.2B). I therefore designed a new primer pair aligned to the $ZIKV^{PR}$ genome to test its efficiency in detecting viral RNA (Figure 3.2A-B). I then compared the detection of the original primer (primer pair 1) and the new primer pair (primer pair 2) and observed that primer pair 2 had a lower Cp value compared to primer pair 1 (Figure 3.1B). The results show that primer pair 2 significantly outperformed primer pair one. Primer pair 2 was used for further analyses.

Previously, I detected viral RNA. Antibodies can also detect ZIKV, particularly the emergence of new viral proteins. Initially, I used a flavivirus antibody verified in ZIKV infections but did not

exhibit specific immunofluorescence [75, 173]. Subsequently, I identified a polyclonal antibody verified to detect envelope protein of multiple strains of ZIKV in human astrocytes [47, 174]. I tested the antibody and found that it detected $ZIKV^{PR}$ in Vero cells (as shown in Figure 3.5A). The combination of optimized ZIKV RNA and ZIKV envelope detection allows adequate analysis of ZIKV infection in future studies.

3.4.3 Serum starved culture enhances ZIKV uptake in embryo-derived stem cells

Previously, I had optimized reagents to detect ZIKV for further analysis. Next, I attempted to optimize culture conditions for effective infection. Conventionally, less than 1 MOI has been used to infect cells [175]. However, I have shown that 1 MOI $ZIKV^{PR}$ was not detected in XEN cells, whereas 10 MOI of $ZIKV^{PR}$ exhibited detectable infection levels (Figure 3.2B). Therefore, I used 10 MOI infection for further experiments. I then compared 10 and 100 MOI $ZIKV^{PR}$ exposure to verify the correlation between viral exposure and intracellular infection. I compared 10 and 100 MOI ZIKV exposure and found that intracellular detection of ZIKV was significantly higher in XEN cells post 100 MOI $ZIKV^{PR}$ exposure than in 10 MOI exposed XEN cells (Figure 3.2C).

After considering the concentration of ZIKV infections, I became curious about how the serum content could affect infections. Serum-starved media was used to infect Vero cells to propagate fresh ZIKV particles [171]. However, in the initial infections of XEN cells, when ZIKV was not detected, serum was present. I then hypothesized that the serum hindered ZIKV infection. Subsequently, I inoculated XEN cells in normal serum (15% FBS) and serum-starved media (2% FBS) at 10 and 100 MOI ZIKV concentrations for 24 hours. I observed that serum-starved XEN cells were more highly infected than normal serum conditions, although the differences were not significant (Figure 3.2D). Subsequent experiments were performed in serum starved conditions nonetheless.

3.4.4 Chloroquine reduces ZIKV infection in embryo-derived stem cells

I previously optimized conditions for embryo-derived stem cells infection. Next, to confirm that intracellular ZIKV due to infection and viral uptake, I inhibited endocytosis of which is required for ZIKV entry. Chloroquine is a small molecule inhibitor of endocytosis and acidifies endosomes to destroy the endosome's cargo [176]. Initially, chloroquine was FDA-approved as an antimalaria drug, particularly for pregnant individuals, because the risk to fetuses is low [176, 177]. In addition to malaria treatment, chloroquine and its analogs have been suggested as a therapeutic for COVID-19 although it did not perform well in clinical trials [14, 178]. Conversely, published studies have shown that chloroquine has successfully reduced ZIKV infection in human cells and mouse embryos [26, 27, 29, 179].

Since chloroquine had been effective in preventing ZIKV infection in other cells types, I wanted to verify its effectiveness in embryo-derived stem cell infection. Therefore, I first performed a toxicity test in XEN cells using 0, 2, 20, and 200 μM concentration of chloroquine. I found 2 and 20 μM did not cause adverse effects on cell viability, and therefore used these concentrations for further experiments (Figure 3.3B). Next, I pre-treated XEN cells with cell viable doses of chloroquine, and then infected cells with $ZIKV^{PR}$ (Figure 3.3A). I found that intracellular ZIKV was significantly decreased in a dose-dependent manner compared to untreated infected cells (Figure 3.3C). These observations support the conclusion that XEN cells are susceptible to endocytosis-mediated ZIKV infection.

3.4.5 ZIKV infection is low in embryo-derived stem cells

Since I had optimized protocols for infection of embryo-derived stem cells, I examined $ZIKV^{PR}$ infection of embryo-derived stem cell lines. Therefore, I infected embryo-derived stem cells: embryonic (ES), trophoblast (TS) and extraembryonic endoderm (XEN) stem cells, and African green monkey cells (Vero) and human embryonic kidney cells (HEK 293T) with 10 and 100 MOI $ZIKV^{PR}$ (Figure 3.4A). After one, two, and four days post-infection, Vero and HEK 293T cells ZIKV infections were significantly higher compared to the embryo-derived stem cells throughout

the time course (Figure 3.4B). Interestingly, TS cells were the only cell lines that exhibited increased $ZIKV^{PR}$ after two days (Figure 3.4B).

Since most of the cells showed the highest levels of infection after two days, I performed an immunofluorescent assay to evaluate ZIKV envelope protein (ZIKV-E) in the five cell lines. I observed that Vero and 293T cells had exhibited higher immunofluorescence intensity than all three embryo-derived stem cells (Figure 3.5A-E). The immunofluorescence results were consistent with the $ZIKV^{PR}$ RNA results (Figure 3.4B). The expression of antiviral genes in ES cells could support ES cells' resistance to ZIKV infection (Figure 2.1A) [48, 59, 76, 78]. However, ZIKV also does not replicate in TS and XEN cells. These results could indicate that the blastocyst could exhibit low infection and resist replication in comparison to other more highly infected tissues.

3.4.6 Undifferentiated and differentiated embryo-derived stem cells cannot replicate ZIKV

Previously, I showed that all three embryo-derived stem cells are resistant to $ZIKV^{PR}$ infection, similar to what was reported for human ES cell infection [59]. However, these observations were surpising given the high expression levels of proviral factors in XEN and TS cells (Figure 2.5A-C, 2.7A-C). Furthermore, undifferentiated TS and XEN express more proviral genes than differentiated TS and XEN. Therefore, I sought to compare ZIKV infection between the two differentiation states to observe infection through development.

I cultured trophoblast stem cells with FGF4 and Heparin to initiate differentiation [118]. After six days of differentiation, where TS cells resemble more developed placental cells, cells were infected at 100 MOI for two days, and were then imaged (Figure 3.6A-B). ZIKV-E in undifferentiated TS cells (as shown in Figure 3.5C) was compared to ZIKV-E in differentiated TS cells. I observed no difference in the detection of ZIKV between undifferentiated and differentiated TS cells (Figure 3.6C), indicating that differentiated cells were resistant to infection. These results were unexpected because my previous analysis indicated that fewer proviral factors were expressed in differentiated TS cells than in undifferentiated TS cells (Figure 2.6C). Additionally, trophectoderm and 1st trimester placental cells are ZIKV infection in other published studies[180].

I then wanted to study the differences in infection of both undifferentiated and differentiated XEN cells. A case study following a miscarriage of a fetus showed positive ZIKV staining in the amnion during viral-induced pregnancy loss [128]. Interestingly, the primitive endoderm and their stem cell population, XEN, give rise to the yolk sac amnion, suggesting that ZIKV could infect the XEN cell lineage [99, 114]. To examine the infectivity of undifferentiated and differentiated XEN, I cultured XEN cells in N2B27 media with BMP4 to initiate differentiation [116, 117, 122]. After the eight days of differentiation, cells were ZIKV-infected for two days and were then imaged (Figure 3.7A-B). I found that ZIKV infection did not differ between the two differentiation states of XEN (Figure 3.7A-B). Furthermore, these results did not correlate with the increased levels of putative proviral factors in undifferentiated XEN cells than in differentiated XEN cells (Figure 2.8C). Overall, these results also reveal that the expression levels of putative proviral factors do not predict $ZIKV^{PR}$ infection in embryo-derived stem cells.

3.4.7 Conclusion

ZIKV can cause deleterious effects within several developmental structures. In the context of fetal infection, the primary known targets are placental and neural cells [48, 54, 60, 76]. However, infection of these targets must occur at a specific time in gestation, when placental and neural cell types have been specified. A few studies of preimplantation ZIKV infection have focused on the placenta/trophectoderm lineage, causing TE dysfunction [78, 131]. ZIKV infection of the other blastocyst cell lineages, however, has not been investigated.

In this study, I utilized embryo-derived stem cells to understand the effect of ZIKV infection of the three cell lineages. I reveal two significant findings: 1) ZIKV can infect all embryo-derived of the three cell lineages at low levels, and 2) there is little to no replication in ZIKV-exposed undifferentiated and differentiated TS and XEN cells. While the ZIKV resistance in ES has been established, TS and XEN low ZIKV infections are novel findings [59] and suggest other preimplantation embryo-derived stem cell lines will have this same low ZIKV infection. These observations, however, are not consistent with the observation of increased proviral gene expression

in embryo-derived stem cells. Therefore, the specific proviral and antiviral factors studied in Chapter 2 may be too limited. Other viral factors such as STAT2 and other viral replication mechanisms in control cell lines could promote infections that have not been studied [168, 167, 181] . Alternatively, other antivirals not studied could have reduce ZIKV infection in embryo-derived stem cells. ZIKV studies in preimplantation development are necessary to capture the vulnerability of embryos and their relation to human health.

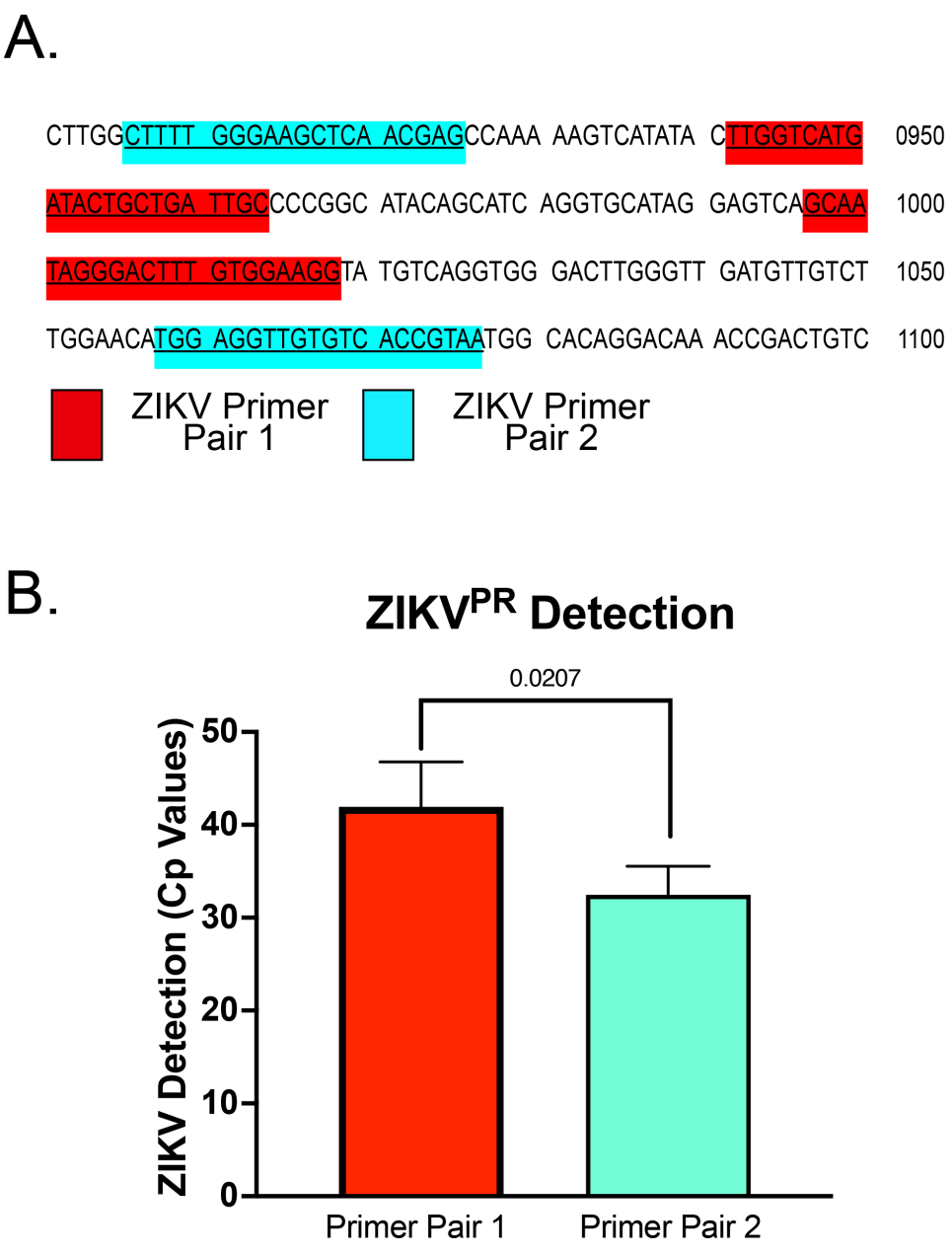

Figure 3.1: Newly designed primer pair detects virus. A. ZIKV primer pair 1 and 2 design aligned with the ZIKV Puerto Rican strain ($ZIKV^{PR}$) between the membrane and envelope exons. **B.** The average Cp values from primer pairs 1 and 2. Error bars = technical error and statistical test: unpaired t-test

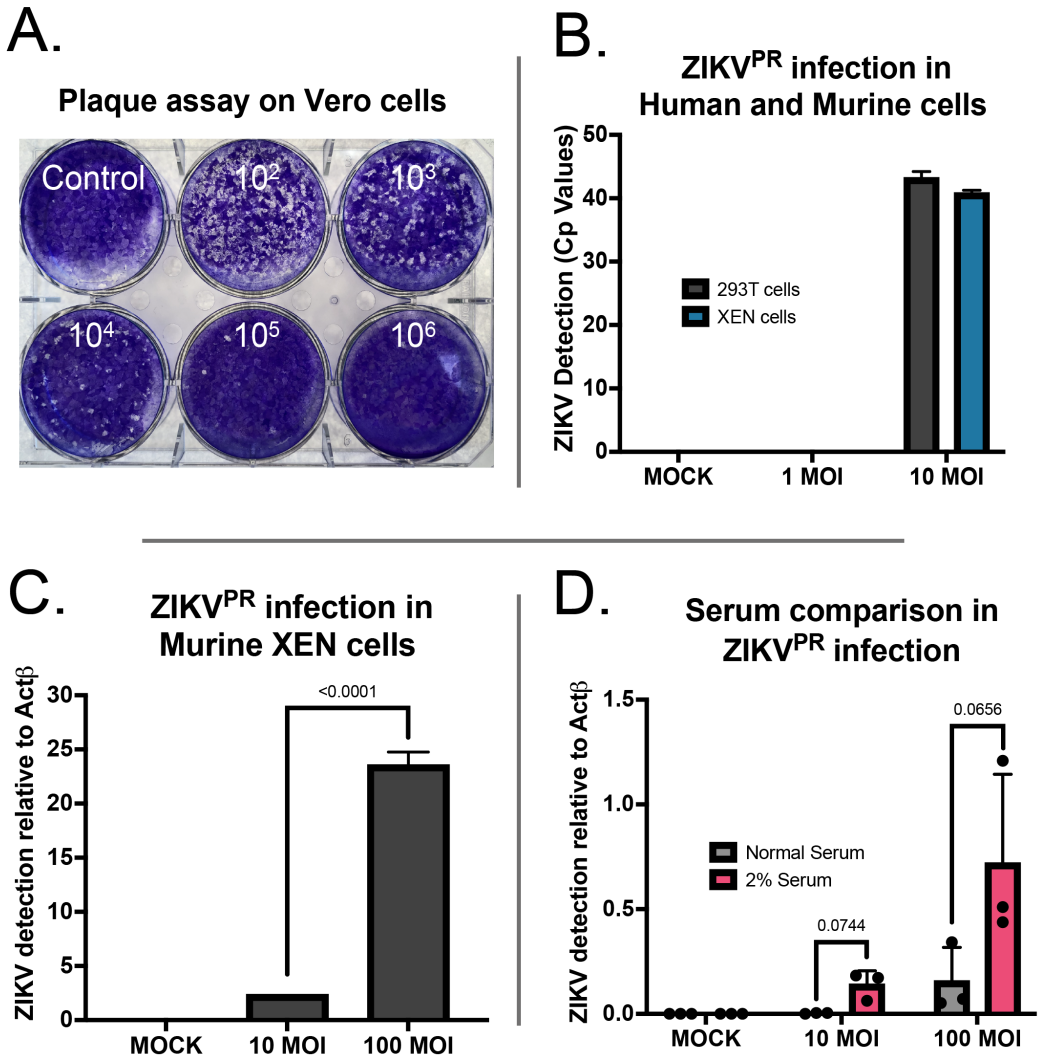

Figure 3.2: Optimization of ZIKV detection protocols and reagents. **A.** A plaque assay on Vero cells using control (MOCK) and ZIKV^{PR} dilution 10^2-10^6 after seven days. **B.** Bar graph of the average Cp values ZIKV^{PR} infection relative to *Actβ* of human embryonic kidney cells (HEK 293T) and mouse extraembryonic endoderm (XEN) cells at MOCK, 1 MOI, and 10 MOI after 24 hrs. **C.** Bar graph of the average ZIKV^{PR} infection relative to *Actβ* of XEN cells at MOCK, 10 MOI, and 100 MOI after 24 hrs. Error bars = technical error and statistical test: unpaired t-test. **D.** Bar graph of the average ZIKV^{PR} infection relative to *Actβ* of XEN in normal and serum-starved (2% FBS) medium at MOCK, 10 MOI, and 100 MOI after 24 hrs. Error bars = technical error and statistical test: unpaired t-test.

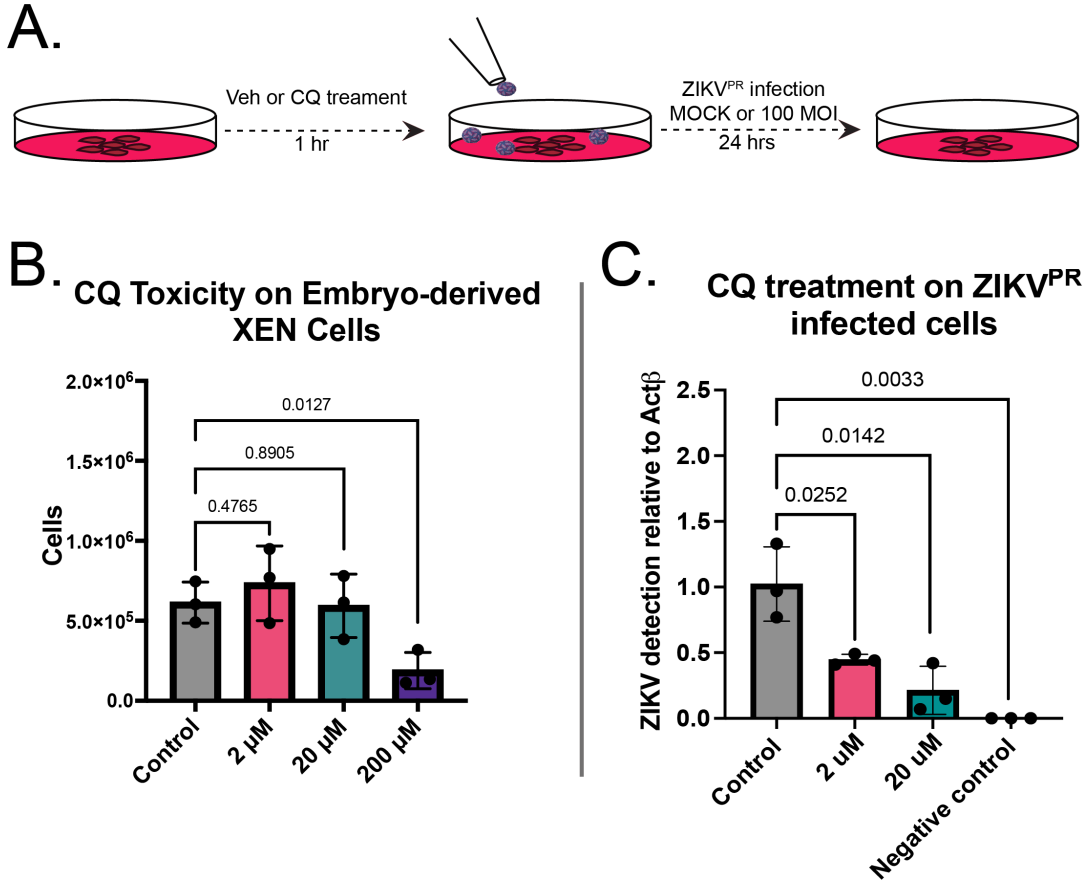

Figure 3.3: Chloroquine inhibits ZIKV^{PR} infection in embryo-derived stem cells. A. Experimental design: XEN cells were cultured and treated with Vehicle (Veh), 2 μM, and 20 μM of chloroquine (CQ) for 1-hr. Cells were then infected with MOCK or 100 MOI of ZIKV infection for 24-hrs and evaluated for infection. **B.** A bar graph of the average cell number after CQ treatment alone at Veh, 2, 20, and 200 μM for 24 hours. Error bars = SEM and Statistics = two-way ANOVA. **C.**Bar graph of the average ZIKV infection relative to *Actβ* of co-treated/infected XEN after 24 hrs. Error bars = SEM and statistics = two-way ANOVA.

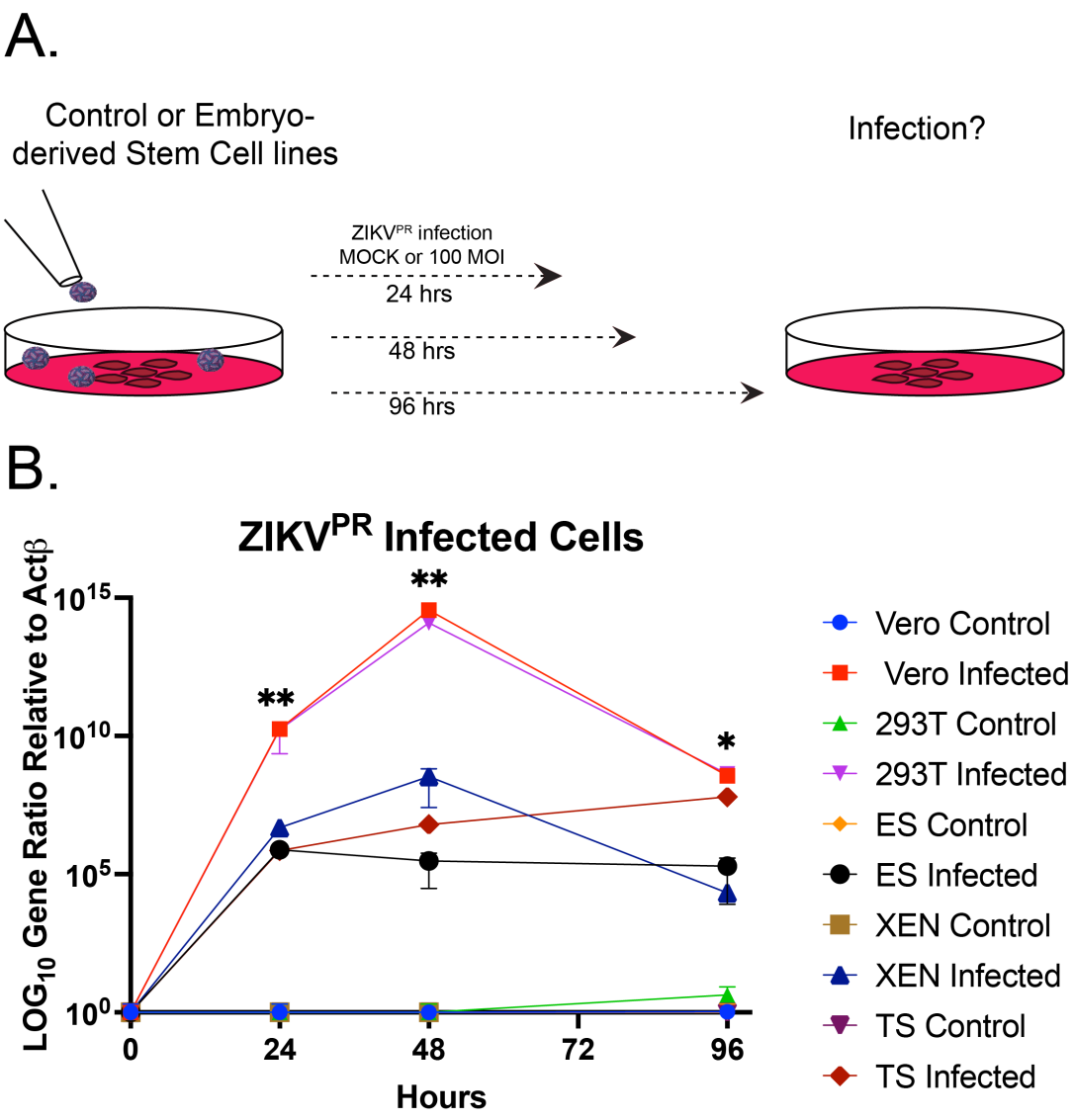

Figure 3.4: ZIKV infections are low in embryo-derived stem cells. A. Experimental design: Vero, 293T, ES, TS, and XEN cells were infected with MOCK or 100 MOI of ZIKV infection for 24, 48, and 96 hrs and evaluated for infection. **B.** A line graph depicting LOG_{10} ZIKV infection relative to *Actβ* over 24, 48, 96 hrs in Vero, 293T, ES, TS, and XEN cells. Error bars = SEM and statistics = ANOVA at each time point.

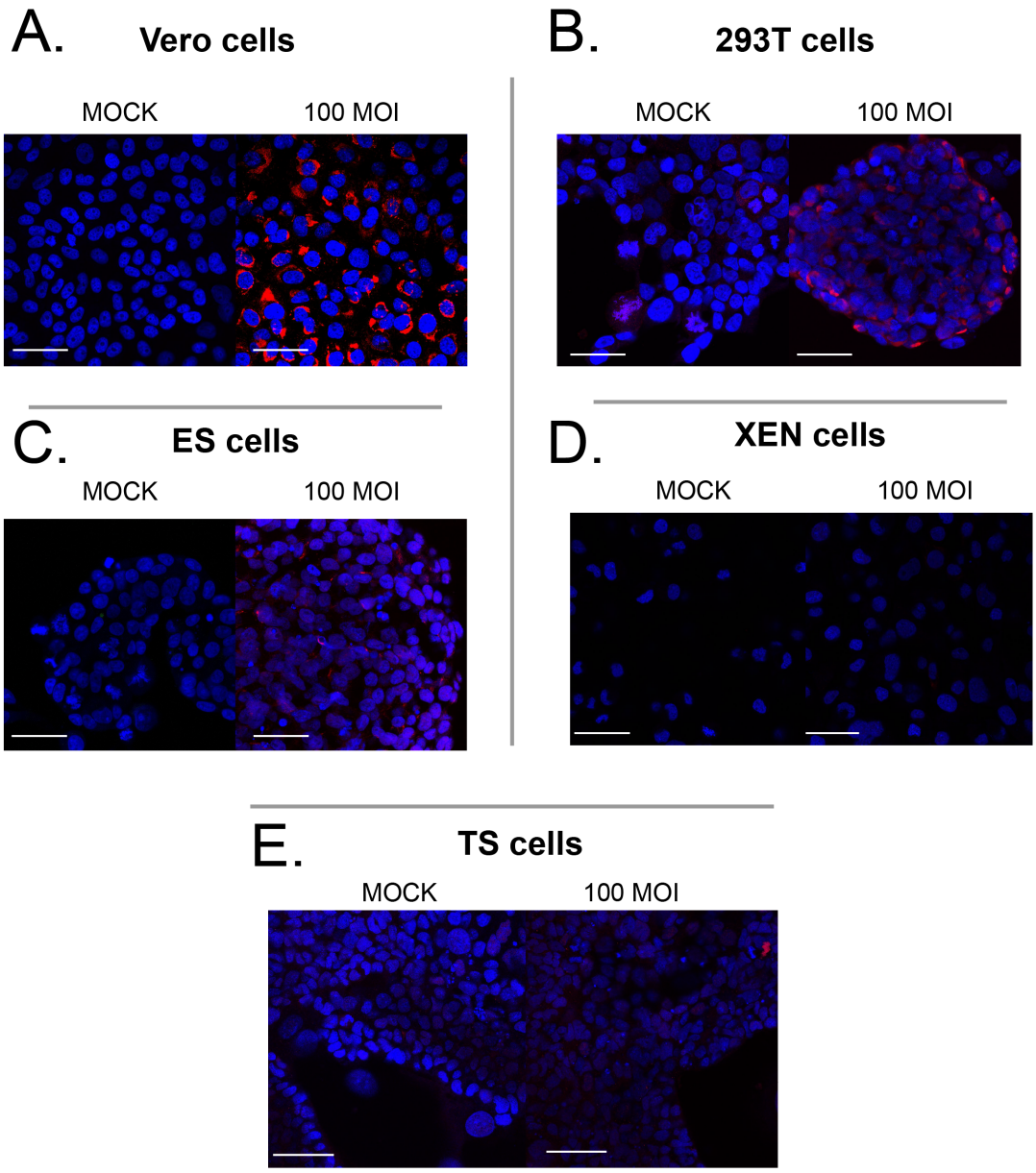

Figure 3.5: ZIKV does not replicate in embryo-derived stem cells. **A.** Confocal images with DNA and ZIKV-E stain on MOCK and 100 MOI ZIKV^{PR}-infected Vero cells. **B.** Confocal images with DNA and ZIKV-E stain on MOCK and 100 MOI ZIKV^{PR}-infected 293T cells. **C.** Confocal images with DNA and ZIKV-E stain on MOCK and 100 MOI ZIKV^{PR}-infected ES cells. **D.** Confocal images with DNA and ZIKV-E stain on MOCK and 100 MOI ZIKV^{PR}-infected XEN cells. **E.** Confocal images with DNA and ZIKV-E stain on MOCK and 100 MOI ZIKV^{PR}-infected TS cells.

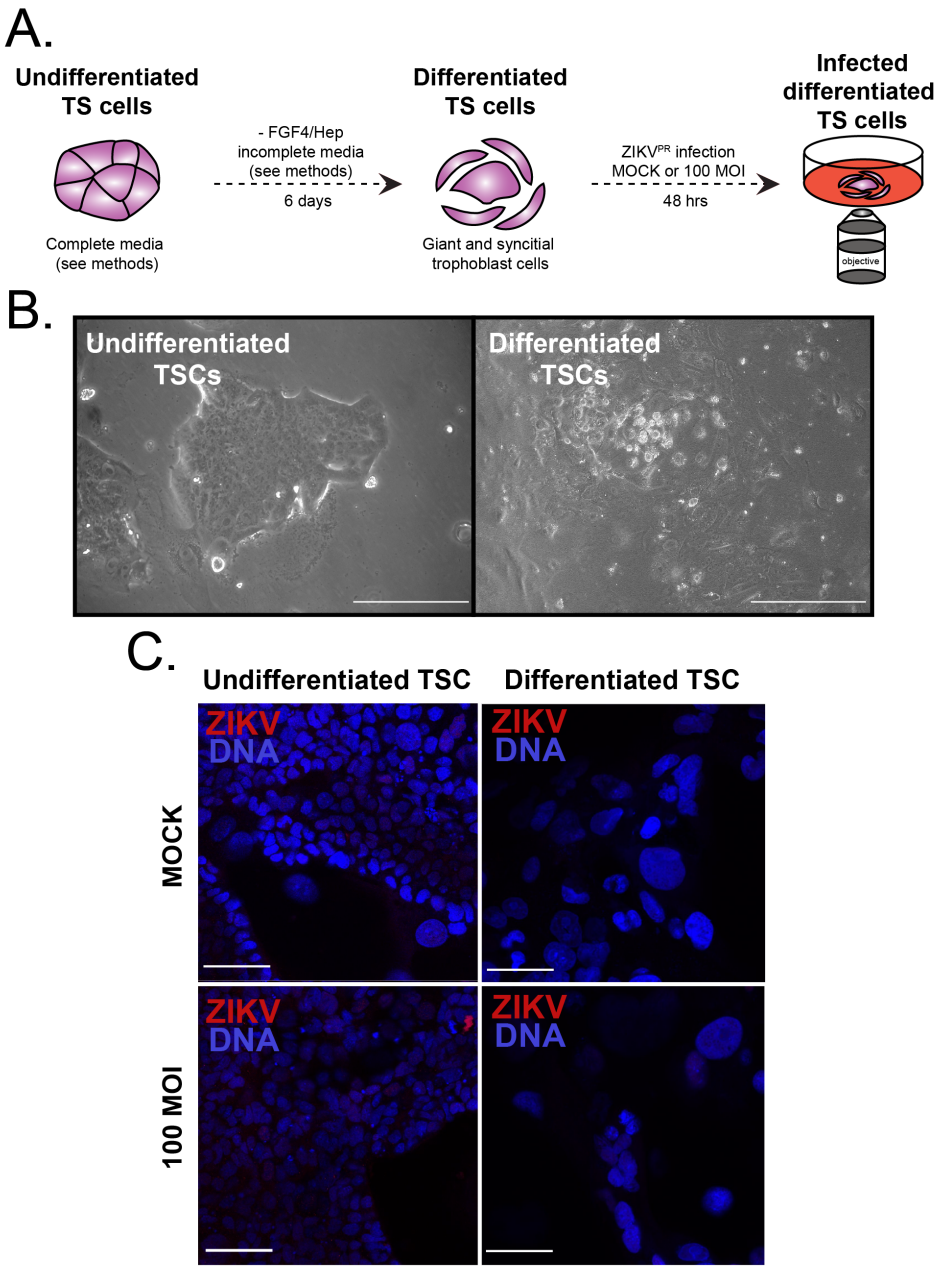

Figure 3.6: ZIKV does not replicate undifferentiated and differentiated TS cells. A. Experimental design: TS cell differentiation in culture absent of factors (see methods) to grow from colony morphology into giant and syncytial trophoblast morphology. After TS differentiation, cells were infected with mock or 100 MOI ZIKV^{PR} for 48 hrs and images for ZIKV detection. **B.** Brightfield images of undifferentiated and differentiated TS cells. **C.** Confocal images with DNA and ZIKV-E stain on MOCK and 100 MOI ZIKV^{PR}-infected undifferentiated (from Figure 3.5E) and differentiated TS cells.

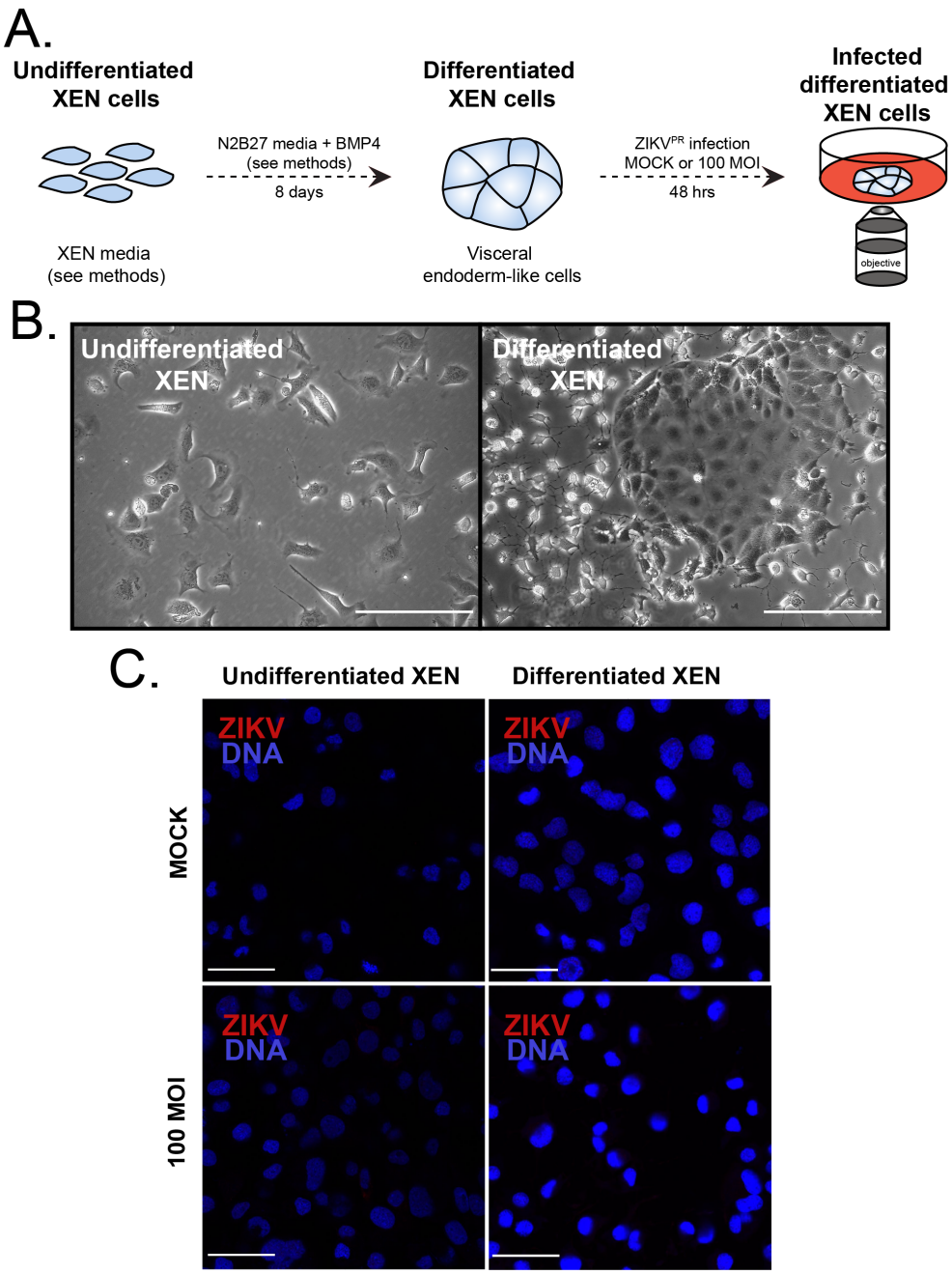

Figure 3.7: ZIKV does not replicate undifferentiated and differentiated XEN cells. A. Experimental design: XEN cells differentiation in culture in the presence of BMP4 (see methods) to grow from a mesenchymal morphology into visceral endoderm-like morphology. After XEN differentiation, cells were infected with mock or 100 MOI ZIKV^{PR} for 48 hrs and images for ZIKV detection. **B.** Brightfield images of undifferentiated and differentiated XEN cells. **C.** Confocal images with DNA and ZIKV-E stain on MOCK and 100 MOI ZIKV^{PR}-infected undifferentiated (from Figure 3.5E) and differentiated XEN cells.

Table 3.1: ZIKV Primers

Marker types	Gene name	Forward sequence (5'-3')	Reverse sequence (5'-3')
Housekeeping	mouse *beta-Actin*	F' CTGAACCCTAAGGCCAACC	R' CCAGAGGCATACAGGGACAG
	human *beta-Actin*	F' GAGCACAGAGCCTCGCCTTT	R' ACATGCCGGAGCCGTTGTC
	Vero *beta-Actin*	F' AAGGATTCATATGTGGGCGATG	R' TCTCCATGTCGTCCCAGTTGGT
ZIKV Primer Pair 1	*ZIKV*	F' TTGGTCATGATACTGCTGATTGC	R' CCTTCCACAAAGTCCCTATTGC
ZIKV Primer Pair 2	*ZIKV*	F' CTTTTGGGAAGCTCAACGAG	R' TTACGGTGACACAACCTCCA

CHAPTER 4

THE FETAL LINEAGE IS SUSCEPTIBLE TO ZIKA VIRUS INFECTION WITHIN DAYS OF FERTILIZATION

Jennifer L. Watts[1,2,3] and Amy Ralston, Ph.D.[2,3],

[1]Molecular, Cellular and Integrative Physiology Graduate Program, Michigan State University, East Lansing, Michigan, 48824, United States

[2]Reproductive and Developmental Biology Training Program, Michigan State University, East Lansing, Michigan, 48824, United States.

[3]Department of Biochemistry and Molecular Biology, Michigan State University, East Lansing, Michigan, 48824, United States

This study was supported by the James K. Billman, Jr., M.D. Endowment at Michigan State University and National Institutes of Health awards R01 GM131759 and T32 HD087166.

4.1 ABSTRACT

Adults contracting Zika virus (ZIKV) typically exhibit mild symptoms, yet the consequences of ZIKV infection can be much more severe for the newborn offspring of infected mothers sometimes resulting in severe birth defects. Many studies have focused on the role of maternal blood and the placenta in transmitting ZIKV to the fetus. Notably however, ZIKV is also transmitted sexually, raising the possibility that ZIKV could infect the embryo shortly after fertilization long before the placenta is established. Here, we evaluate the consequences of ZIKV infection in mouse embryos during the first few days of embryogenesis. We show that divergent strains of ZIKV can infect the fetal lineage and cause developmental arrest, raising concern for the developmental consequences of sexual ZIKV transmission.

4.2 INTRODUCTION

The Zika virus (ZIKV), a zoonotic member of the *Flaviviridae* family, is on the watch-list for preventing the next pandemic [182]. Mosquito-borne ZIKV infection of humans results in relatively mild symptoms including fever, rash and joint pain [3]. However, during pregnancy, vertical transmission of ZIKV from mother to fetus can result in outcomes ranging from normal development, to more severe outcomes such as microcephaly or fetal demise [77, 6, 19, 128, 10, 183]. The reasons for the widely varying pregnancy outcomes are unclear, but could include genetic or epigenetic variation among humans, prior priming of the immune system by exposure to ZIKV-related flaviviruses, or the timing of ZIKV infection during pregnancy [68, 70, 76].

Less commonly discussed is the role that the route of infection bears on pregnancy outcomes. Prior studies have primarily focused on the descending route of vertical transmission, from mother to fetus via the placenta [69]. By contrast, fewer studies have focused on the ascending route of infection, wherein virus is transmitted to developing offspring within the maternal reproductive tract [24, 134, 137, 184]. Since ZIKV is sexually transmitted [25, 161, 185], this raises the possibility that ZIKV infection around the time of conception could also impact pregnancy outcomes. In fact, sexual transmission of ZIKV reportedly increases the severity of adult infection [56, 132, 186],

raising major concern for the role of humans in the global spread of ZIKV [187]. Nevertheless, the effects of sexually transmitted ZIKV on embryonic development are still understudied.

The ascending route of viral transmission is concerning because, during the earliest stages of development, embryos lack both placentas and an adaptive immune system. For several days following fertilization, embryos develop as free-floating entities within the female reproductive tract. During these so-called preimplantation stages, critical developmental events occur, including establishment of the fetal, as well as crucial extraembryonic lineages, such as yolk sac and placenta [143]. During preimplantation development, the embryo is surrounded by a thick glycoprotein coat called the zona pellucida (ZP). However, it is currently unknown whether the ZP could help protect embryos from viral infection during this uniquely vulnerable preimplantation stage.

How ZIKV infection affects preimplantation development is still enigmatic; only two studies have explored this topic. One study evaluated the effects of a Puerto Rican strain of ZIKV on preimplantation rhesus monkey embryos [131], while another evaluated the effects of a Ugandan strain of ZIKV on mouse embryos [78]. While both studies generally concluded that ZIKV exposure can be harmful to preimplantation embryos, neither study evaluated infection of the fetal lineage directly. Moreover, the numerous differences in experimental design, including embryo species, presence/absence of the ZP, viral strain, and analysis endpoints, make it difficult to compare these studies to each other. Determining whether the fetal lineage is impacted by ZIKV infection requires not only a systematic experimental design, but also evaluation of lineage-specific, including markers of fetal and extraembryonic lineages, at the cellular level. Through this systematic experimentation, we demonstrate that ZIKV negatively impacts preimplantation development and possibly account for epidemiologically established viral-induced pregnancy loss outcomes.

4.3 MATERIALS AND METHODS

4.3.1 Animal Use

All animal research was conducted in accordance with the guidelines and approval of the Michigan State University Institutional Animal Care and Use Committee. Experiments were performed using

male and female CD-1 mice, at least 6-8 weeks of age. Animals were maintained on a 12-hour light/dark cycle with *ad libitum* access to food and water.

4.3.2 Virus propagation and preparations

Vero cells (ATCC, CRL-1586) were cultured in 75-cm^2 filtered cap flasks to 90-95% confluency in 10% FBS EMEM (ATCC, 30-2003) in 5% CO_2 at 37°C. Cells were washed with 5 to 10 mL of DPBS (Life Technologies, 14040133). Before infection, one flask was used to determine cell count. The remaining flasks of Vero cells were infected for 1 hour at an MOI of 0.01 in 5 ml of 2% FBS EMEM at 5% CO_2 at 37°C, rocking every 15 minutes, after which, 4 mL 10% FBS EMEM was added. Cell culture supernatants were collected 40-48 hours later, and then centrifuged for 10 minutes 1,300 x g at 4°C. Supernatants were pooled, and 1-mL aliquots were then stored at -80°C. For negative control experiments, Vero cell medium or Vero cell conditioned medium was used as has been done previously [131, 188, 167].

4.3.3 Plaque Assay

Vero cells (ATCC, CRL-1586) were cultured in a 6-well plate to 100% confluency in 10% FBS EMEM in 5% CO_2 at 37°C. Cells were washed in EMEM without FBS and infected with $ZIKV^{PR}$ or PRVABC (ATCC, VR-1843) and $ZIKV^{UG}$ or MR776 (ATCC, VR-1838) diluted to 10^2-10^6 in 500 mL of 2% FBS EMEM. Cells were infected or mock infected for 15 minutes, rocking at room temperature, and incubated for 45 minutes in 5% CO_2 at 37°C. 4 mL overlay (2% methylcellulose prepared in 0% FBS EMEM) was added on top of the inoculum in each well and incubated for 6-7 days. The overlay was then removed, and cells were fixed in 4% EM grade paraformaldehyde (Electron Microscopy Sciences,15710). Vero cells were stained with 0.1% crystal violet solution prepared in 20% ethanol and 4% paraformaldehyde. Crystal violet stain was washed gently with water until the water was clear. Plaques were allowed to dry for 1-24 hours and counted under a transilluminator to determine viral titer (pfu/mL).

4.3.4 Embryo ZIKV infection

Before embryo culture, KSOM media (Millipore, MR-121-D) and EmbryoMax Filtered Light Mineral Oil (Millipore, ES-005-C) were equilibrated overnight in 5% CO_2 at 37°C. CD-1 embryos were collected with M2 via the oviduct from E1.5 and E2.5 and via the uterine horn, 3.5 days post-copulatory plug. The zona pellucida remained intact or was removed two embryos at a time in 2-3 drops of 60 µL Tyrode's acid and washed in M2 media two times. Embryos were then cultured for 24, 48, or 96 hours in 5% CO_2 at 37°C in 20 µL KSOM with $ZIKV^{UG}$, $ZIKV^{PR}$, or equivalent concentration mock medium to create the inoculum. Final concentrations of $ZIKV^{UG}$ and $ZIKV^{PR}$ were 6 x 10^4 pfu/mL. Mock medium was either Vero cell medium or Vero cell conditioned medium no developmental differences were observed among embryos cultured in either control medium.

4.3.5 Immunofluorescence and confocal microscopy

Embryos were fixed in 4% formaldehyde for 10 minutes at room temperature, permeabilized with 0.5% Triton X-100 for 30 minutes at room temperature, and blocked with 10% FBS and 0.1% Triton X-100 blocking buffer for 1 hour at room temperature or longer at 4°C. Primary antibodies were prepared in blocking buffer, and embryos and cells were incubated at 4°C overnight with the following primary antibodies: goat anti-mouse anti-mCDX2 (CDX2-88, BioGenex), SOX2 (GT15098, Neuromics), goat anti-hSox17 (AF1924, R&D Systems), and ZIKV-E (GTX133314, GeneTex). Embryos and cells were washed with blocking buffer for 30 minutes, incubated with the following secondary antibodies for an hour: donkey anti-goat Alexa 488 (Invitrogen), donkey anti-rabbit/mouse CY3 (Jackson Immuno Research), and donkey anti-rabbit Alexa 647 (Jackson Immuno Research), and washed with blocking buffer for 30 minutes. Nuclei were stained with DRAQ5 (Cell Signaling, 40845) or Hoechst 33342 (Thermo Fisher Scientific, 62249). Embryo and cell images were captured on a Nikon A1 Confocal Laser Scanning Microscope using 60x Plan Apo IR Water Objective (NA 1.27 WI). Every embryo was imaged by collecting a complete z-stack, with 5 µm between each image.

4.3.6 Image analysis for embryos

Images were analyzed with FIJI Image J software. Cells were counted manually in each plane of each z-stack, and resulting data were and imported into Excel or GraphPad software. Graphs were generated with GraphPad. A chi-squared or an unpaired T-test was performed to examine significance.

4.4 RESULTS

4.4.1 ZIKV can infect all blastocyst lineages, including the fetal lineage

A prior study reported that wildtype mouse preimplantation embryos can be infected by exposing blastocysts (embryonic day E3.5) to 6 x 10^4 plaque forming units (pfu)/mL of a Ugandan strain of ZIKV ($ZIKV^{UG}$) at the blastocyst stage (embryonic day E3.5), when the ZP is removed [78]. Consistent with this observation, we observed significantly compromised developmental progression in ZP-removed embryos exposed to $ZIKV^{UG}$ on E3.5, compared with mock-infected ZP-removed embryos (Figure 4.5A-B).

Next, we evaluated the localization of the ZIKV viral envelope protein (ZIKV-E) within cells of the embryo, as a measure of infection [78]. Since the blastocyst contains three distinct cell types, we evaluated infection of each cell type individually. First, we focused on trophectoderm cells. The trophectoderm, which contains progenitors of the placenta, surrounds the blastocyst and is specifically labeled by the essential transcription factor CDX2 [119]. We detected ZIKV-E within CDX2-positive cells of blastocysts after $ZIKV^{UG}$ exposure (Figure 4.5C), and not in mock-infected, control blastocysts (Figure 4.2A-C), consistent with prior observations [78].

We then evaluated ZIKV-E within the epiblast lineage, which has not been previously examined in blastocysts. Epiblast cells are the pluripotent progenitors of the entire fetus and are located within the inner cell mass of the blastocyst. At this stage, epiblast cells comprise about half of all inner cell mass cells, and are intermixed with cells of the primitive endoderm [88], an extraembryonic lineage that is crucial for many developmental events [127]. Epiblast cells can be discerned within the inner

cell mass based on the expression of the pluripotency marker SOX2 [95]. Remarkably, ZIKV^{UG} was detected within SOX2-positive cells of blastocysts exposed to ZIKV^{UG} (Figure 4.5D). This is the first evidence that the fetal lineage can become infected by ZIKV during preimplantation.

Finally, we evaluated the expression of ZIKV-E within the primitive endoderm, which has not been previously examined. The primitive endoderm will give rise to crucial extraembryonic tissues including the anterior visceral endoderm, which plays critical roles in neural patterning [189]. In the blastocyst, primitive endoderm cells are interspersed with epiblast cells within the ICM at this stage [88], and can be identified on the basis of SOX17 expression [190]. We observed that ZIKV-E was detected in SOX17-positive primitive endoderm cells in blastocysts (Figure 4.5E). Therefore, all three blastocyst lineages are susceptible to infection during preimplantation.

4.4.2 ZIKV^{UG} infection disrupts cell fate specification in the blastocyst

In our previous analysis, as in the published study [78], we only examined whether CDX2-positive cells were also ZIKV-E-positive. We next evaluated whether ZIKV infection impacted the number of cells in embryos infected as in Figure 4.5A, which has not been reported. We observed a significant reduction in the average total number of cells across all ZIKV^{UG}-infected blastocysts (Figure 4.5A). Additionally, we observed a significant decrease in numbers of both trophectoderm and inner cell mass cells in infected blastocysts (Figure 4.5B-C). These results strongly suggest that ZIKV infection could disrupt cell fate specification in the blastocyst, a previously unexplored possibility.

To further investigate the ZIKV^{UG}-induced phenotype we next evaluated the expression levels of lineage-specific proteins. First, we quantified the number of cells within the outer layer of the blastocyst (as defined by position of nuclei) expressing CDX2 in embryos infected as in Figure 4.5A. In ZIKV^{UG}-exposed embryos, we observed a significant decrease in the average number of outside cells expressing CDX2, compared with mock-infected (Figure 4.5D). Moreover, the proportion of CDX2-positive cells was also significantly lower in ZIKV^{UG}-infected embryos (Figure 4.4A). The CDX2-negative trophectoderm cells could be considered to have morphological features of

trophectoderm differentiation (i.e., outside position), but they had lost or failed to express a key trophectoderm gene. Since *Cdx2* is essential for trophectoderm cell development [119], these data provide the first evidence that ZIKV infection interferes with trophectoderm cell fate specification.

We next investigated the effects of $ZIKV^{UG}$ on the inner cell mass cell lineages. In normal embryos, the epiblast marker SOX2 and primitive endoderm marker SOX17 are each detected in approximately half of all inner cell mass cells [95, 190]. We observed that the average number of SOX2-positive cells per embryo was significantly reduced in embryos exposed to $ZIKV^{UG}$ compared with mock-infected embryos (Figure 4.5E). In addition, we noted a significant decrease in the average number of SOX17-positive cells per embryo compared with mock-infected embryos (Figure 4.52F). The proportion inner cell mass cells expressing either marker was also lower than expected in infected embryos (Figure 4.4B-C), consistent with a failure to specify or maintain cell fates, rather than a change in cell fate or failure to developmentally progress [95, 99, 191] . Since expression of both SOX2 and SOX17 were reduced by $ZIKV^{UG}$ infection and since both *Sox2* and *Sox17* are required for the development of their respective lineages [99, 192], we conclude that $ZIKV^{UG}$ infection is detrimental to inner cell mass cell fate specification.

4.4.3 $ZIKV^{UG}$-induced lethality of mouse embryos at multiple preimplantation stages

Up to this point, we had focused on the susceptibility of mouse blastocysts to ZIKV, starting on day three of embryo development. However, the effects of ZIKV exposure on embryos during earlier development has not been reported. We therefore evaluated the *ex vivo* development of embryos exposed to $ZIKV^{UG}$ in the absence of ZP starting from earlier stages of development.

We first exposed embryos to $ZIKV^{UG}$ at the eight-cell stage (E2.5), and then cultured these to the same endpoint as for our prior studies (Figure 4.5A). For this and subsequent experiments, embryos were cultured in 6 x 10^4 pfu/mL, as for previous experiments. Although embryo cell number increases during preimplantation development, cell divisions proceed by cleavage, halving cell size so that the embryo maintains the same diameter. Therefore, we reasoned that the effective multiplicity of infection (MOI) would remain comparable during the course of each experiment.

Following infection at the eight-cell stage, we observed a significant decrease in embryo viability after $ZIKV^{UG}$ exposure, compared with mock-infected embryos (Figure 4.5B). However, we note that the degree of the $ZIKV^{UG}$-induced lethality was lower at this stage than it had been when embryos were exposed starting on E3.5.

Next, we examined the viability of $ZIKV^{UG}$-infected embryos at the two-cell stage (E1.5) (Figure 4.5C). At the two-cell stage, removal of the ZP decreased viability of cultured two-cell embryos, as anticipated [193]. In $ZIKV^{UG}$-exposed embryos, viability was dramatically decreased, compared with mock-infected embryos (Figure 4.5D). Notably, the degree of the $ZIKV^{UG}$-induced lethality at this stage was similar in degree to what we had observed at the blastocyst stage. These observations indicate that multiple preimplantation stages are susceptible to $ZIKV^{UG}$-induced lethality in the absence of the ZP.

Finally, we evaluated the levels of transcripts encoding several known flavivirus entry proteins [43] in mouse and human preimplantation embryo gene expression data [165, 129]. Among commonly studied flavivirus entry proteins, *Tyro3*, and *Mertk* were more abundant than *Axl* (Figure 4.6A). Similarly, expression of *TYRO3* and *MERTK* is elevated during human early embryonic development (Figure 4.6B). Our observations indicate that mouse embryos are susceptible to ZIKVUG-induced lethality at multiple stages, and implicate TYRO3 and MERTK as ZIKV entry targets for future study.

4.4.4 The zona pellucida fails to protect embryos from ZIKV-induced lethality

During preimplantation, the embryo resides within the ZP until around E4.5, when the embryo hatches from the ZP [156]. The results presented above, in addition to published evidence [131, 78], raise concern for the susceptibility of ZP-free preimplantation embryos to ZIKV infection. However, several viruses have been observed to penetrate the ZP and infect preimplantation embryos [147, 150, 194, 195], including viruses that are larger in diameter than ZIKV. Whether $ZIKV^{UG}$ is capable of penetrating the ZP of preimplantation embryos has not been examined.

To evaluate whether the ZP can protect preimplantation embryos from $ZIKV^{UG}$-induced lethal-

ity, we exposed ZP-intact embryos of multiple stages to ZIKV^{UG}, and then observed their *ex vivo* development, similar to previous experiments (Figure 4.5E). We noted a small but significant decrease in the viability ZP-intact blastocysts exposed to of ZIKV^{UG} compared to mock-exposed controls (Figure 4.5F). However, the viability of ZP-intact eight-cell embryos was unaffected by ZIKV^{UG}-exposure (Figure 4.5G). Strikingly, the viability of ZP-intact two-cell embryos was severely compromised by ZIKV^{UG} exposure compared to controls, with around half of infected embryos arresting around the 4-cell stage, in spite of the ZP (Figure 4.5H). We conclude that the ZP is not a complete barrier to ZIKV^{UG}-induced lethality.

4.4.5 Two-cell embryos are vulnerable to multiple ZIKV strains

We and others [78] have observed that an African strain of ZIKV (ZIKV^{UG}) can impact the development of preimplantation mouse embryos, but it is unknown whether other strains may affect mouse embryo development. A recent study showed that non-human primate preimplantation embryos are vulnerable to a ZIKV strain of Asian lineage [131], but a comparative study of the two lineages has not been performed during preimplantation in any species. We felt that it was important to perform this comparison because studies have shown that ZIKV strains of both African and Asian lineage can affect fetal and adult tissues [38, 39, 40, 196], with no clear consensus on which strain is the more virulent. We therefore evaluated whether the Asian-derived Puerto Rican strain of ZIKV (ZIKV^{PR}) would affect the development of preimplantation mouse embryos.

For this comparison, we focused on two-cell embryos with and without ZP (Figure 4.7A), since this appeared to be a uniquely susceptible stage. We noted that ZIKV^{PR} disrupted development of two-cell embryos lacking the ZP (Figure 4.7B), as well as two-cell embryos retaining their ZP (Figure 4.7C). These observations indicate that two-cell embryos are vulnerable to ZIKV strains from different viral lineages.

4.5 DISCUSSION

According to the World Health Organization, ZIKV presents a major threat to human health, and its epidemic potential is widely recognized [8]. Disturbingly, the *Aedes* mosquitoes that transmit ZIKV are considered among the top invasive, dangerous species in the world [197, 198]. Moreover, ZIKV can be transmitted sexually [25, 161, 185], providing a second mechanism of global expansion. Indeed, the capacity of human-borne pathogens to spread beyond control are unfortunately all too familiar. ZIKV vaccines are under development, but are not yet widely available [31].

Although ZIKV infection asymptomatic in many individuals, the consequences can be more severe for some, for reasons that are still under active investigation. Of particular concern is the effects of ZIKV on unborn babies. We have identified new developmental windows of embryo susceptibility to ZIKV (Figure 4.6D). We do not yet understand why the two-cell stage is particularly vulnerable to infection, but we consider several possible mechanisms, including ultrastructural changes to the ZP, which could be initially more permeable to ZIKV, heightened expression of novel ZIKV entry proteins, and/or proximity to the maternal-to-zygotic transition in gene expression.

We have shown that all three blastocyst lineages are susceptible to infection, including the fetal lineage. Importantly, a prior study reported increased levels of apoptosis in ZIKV-infected mouse blastocysts [78], providing a possible mechanism for the observed disruptions to cell fate. These observations reinforce the concern that human-borne ZIKV infection poses a significant threat to human embryo viability [132, 186].

ZIKV infection of the primitive endoderm could create additional developmental complications. In mouse, the primitive endoderm-derived extraembryonic endoderm plays critical roles in the development of the brain, intestine, heart, germ cells, and blood [189, 199, 200, 201, 202, 203]. In human embryos, the epiblast and primitive endoderm (known as hypoblast) are physically adjacent as in mouse [127], suggesting conservation of function. However, whether hypoblast damage results in severe birth defects, such as microcephaly or other defects, has not been investigated.

These observations provide rationale for examining the susceptibility of human epiblast and

primitive endoderm to ZIKV infection. As in mouse, epiblast, primitive endoderm (hypoblast), and trophectoderm are specified by blastocyst stage in human embryos [204]. However, it remains unknown whether ZIKV can infect human epiblast or hypoblast and whether ZIKV can pass through the ZP of human embryos. Since studies of human preimplantation embryos are, necessarily performed *ex vivo*, our findings and conditions are directly applicable to this artificial, experimental setting. Nevertheless, elucidating the impact of sexually transmitted ZIKV on human pregnancy will require special epidemiological attention.

An additional benefit of *ex vivo* embryo study is that it permits evaluation of the effects of viral infection on embryos without influence of the maternal immune system. This is important because maternal immune response to ZIKV can vary among species and individuals [56, 205]. Our observations establish the intrinsic susceptibility of preimplantation embryos to infection by both Asian and African ZIKV lineages, and warrant follow-up studies to determine whether and how sexually transmitted ZIKV may impact human fertility and pregnancy outcomes.

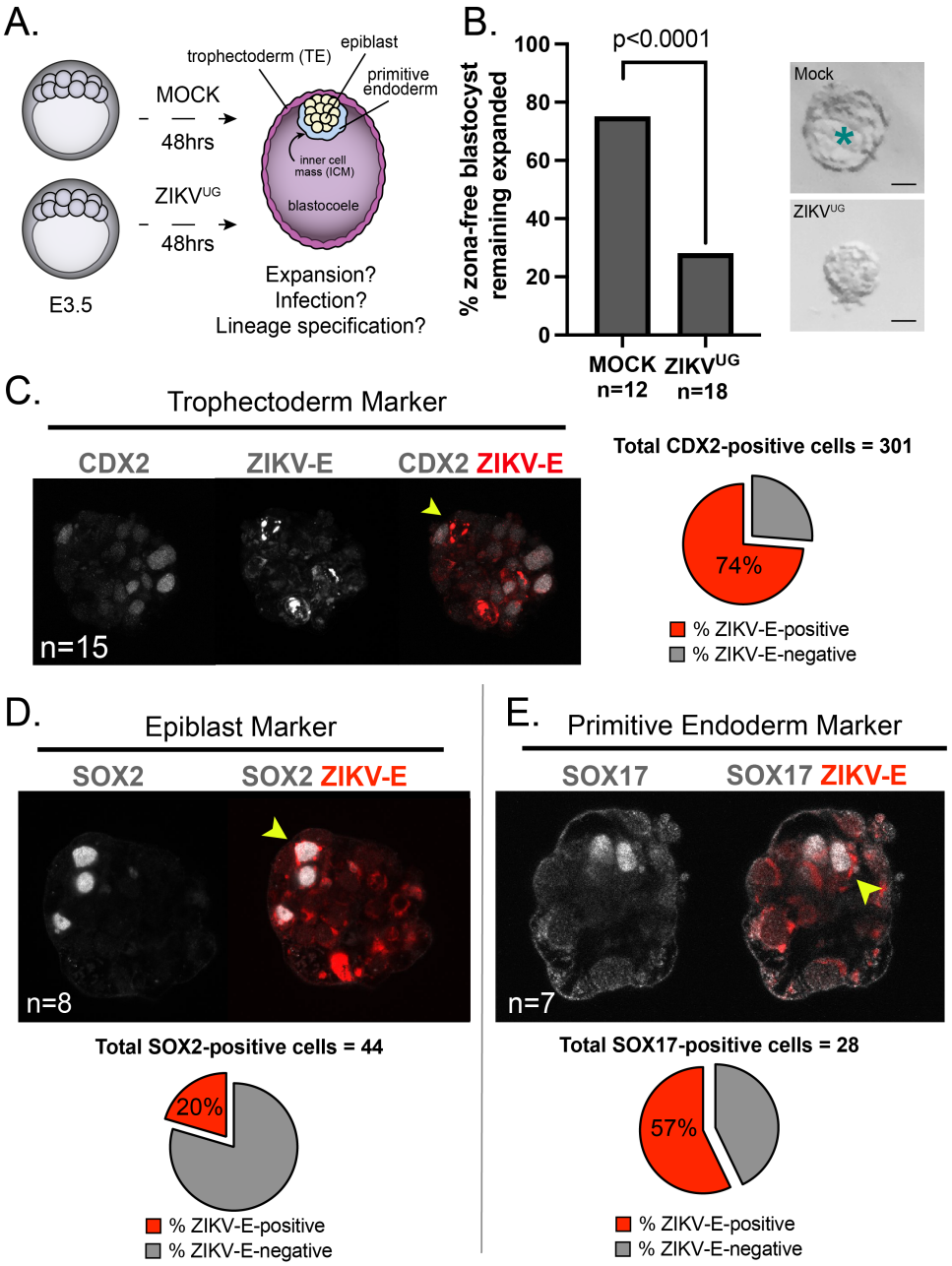

Figure 4.1: ZIKV^{UG} causes defects in blastocyst development. A. Experimental design: embryos were harvested on day three of development (blastocyst stage). ZP were removed, embryos were transferred to embryo culture medium containing ZIKV^{UG} or mock medium, and then allowed to develop for indicated period of time, when endpoint analyses were performed. **B.** The proportion of blastocysts remaining expanded, with representative images. Asterisk indicates expanded blastocoel. Statistical test: Chi-squared. Scale bar = 20 µm **C.** Max projection of all sections of z-stack confocal imaging of CDX2 and ZIKV-E immunofluorescence of a representative ZIKV^{UG}-infected blastocyst. Arrowhead indicates a ZIKV-E-positive cell. Pie chart shows proportion of ZIKV-E-positive/negative CDX2-positive cells across all embryos examined (*see next page*).

Figure 4.1 (cont'd) **: D.** Max projection of all sections of z-stack confocal imaging of SOX2 and ZIKV-E immunofluorescence of a representative $ZIKV^{UG}$-infected blastocyst. Arrowhead indicates a ZIKV-E-positive cell. Pie chart shows proportion of ZIKV-E-positive/negative SOX2-positive cells across all embryos examined. **E.** Max projection of all sections of z-stack confocal imaging of SOX17 and ZIKV-E immunofluorescence of a representative $ZIKV^{UG}$-infected blastocyst. Arrowhead indicates a ZIKV-E-positive cell. Pie chart shows proportion of ZIKV-E-positive SOX17-positive/negative cells across all embryos examined. For all panels, n= the number of embryos examined.

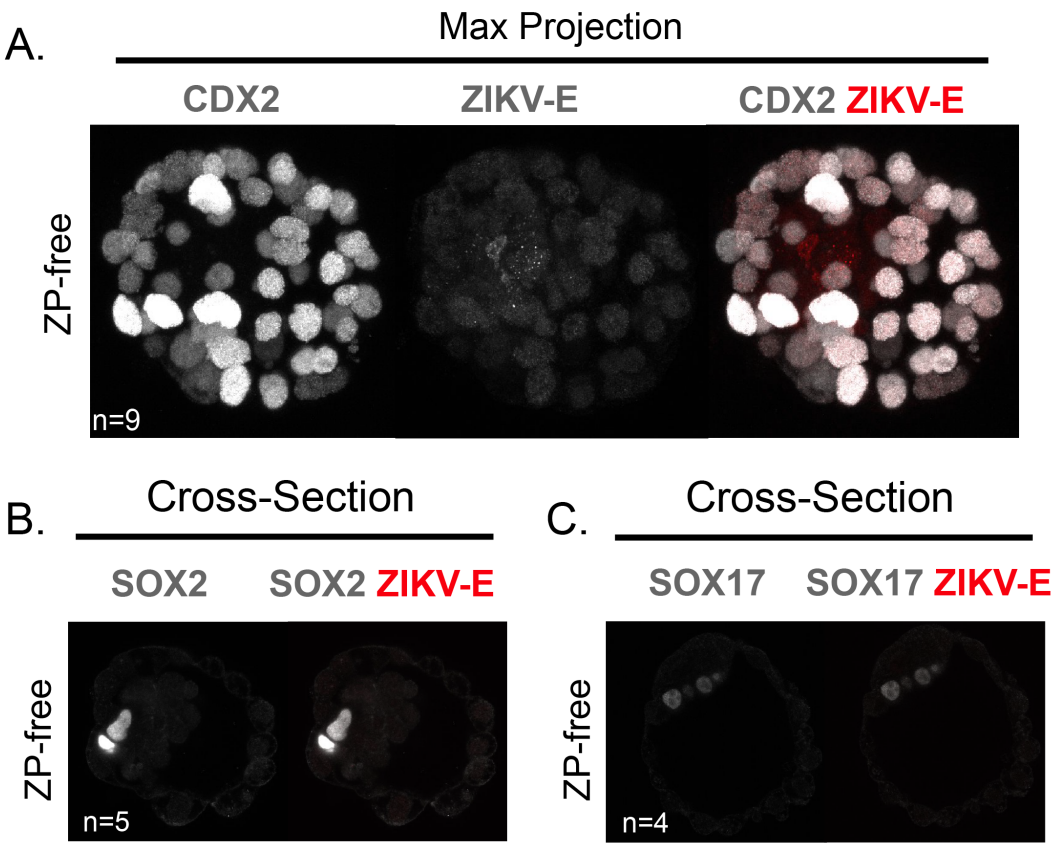

Figure 4.2: Negative control for ZIKV-E immunofluorescence experiments. A. Embryos were not exposed to ZIKV, and were then immunofluorescently stained with antibodies to detect CDX2 and anti-ZIKV-E, demonstrating ZIKV-dependent ZIKV-E signal detected in Fig. 4.5. **B.** Similar to panel A, uninfected embryos were immunofluorescently stained with antibodies to detect SOX2 and anti-ZIKV-E. **C.** Uninfected embryos were immunofluorescently stained with antibodies to detect SOX17 and anti-ZIKV-E.

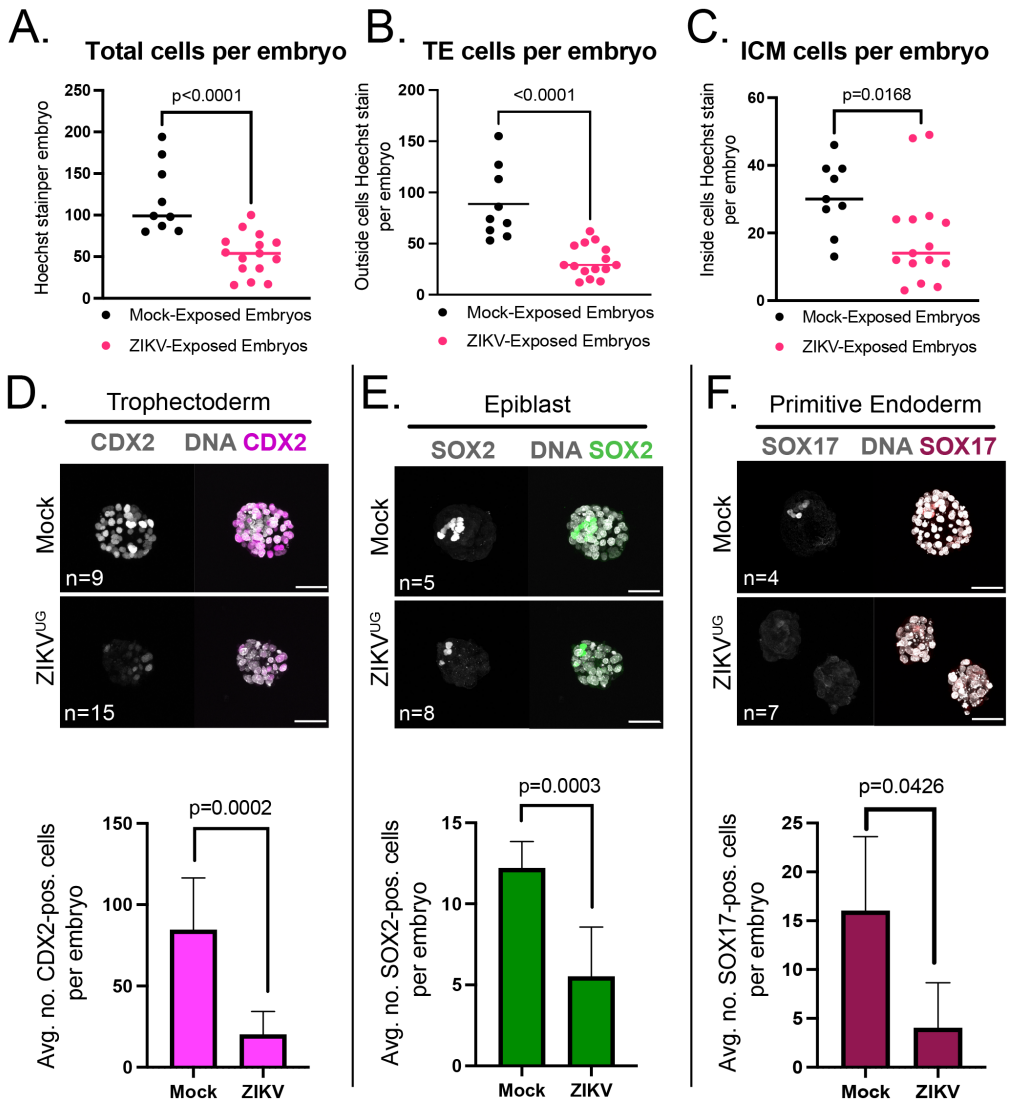

Figure 4.3: ZIKV^{UG} disrupts cell fate specification in the blastocyst. **A.** Number of cells in each blastocyst after 48 hr from E3.5 in mock and ZIKV-infected conditions. Statistical test: unpaired t-test. **B.** Number of trophectoderm (TE) cells in each blastocyst after 48 hr from E3.5 in mock and ZIKV^{UG}-infected conditions. Statistical test: unpaired t-test. **C.** Number of inner cell mass (ICM) cells in each blastocyst after 48 h from E3.5 in mock and ZIKV^{UG}-infected conditions. Statistical test: unpaired t-test. **D.** Max projection of all sections of z-stack confocal imaging of CDX2 immunofluorescence and nuclear stain for a representative mock-infected and a representative ZIKV^{UG}G-infected blastocyst. Column chart shows average number of CDX2-positive cells in all embryos (sample sizes provided in the image panels) for each condition. Statistical test: unpaired t-test (*see next page*).

Figure 4.3 (cont'd) **E.** Max projection of all sections of z-stack confocal imaging of SOX2 immunofluorescence and nuclear stain for a representative mock-infected and a representative $ZIKV^{UG}$-infected blastocyst. Column chart shows average number of SOX2-positive cells in all embryos (sample sizes provided in the image panels) for each condition. Statistical test: unpaired t-test. **F.** Max projection of all sections of z-stack confocal imaging of SOX17 immunofluorescence and nuclear stain for a representative mock-infected and a representative $ZIKV^{UG}$-infected blastocysts. Column chart shows average number of SOX17-positive cells in all embryos (sample sizes provided in the image panels) for each condition. Statistical test: unpaired t-test. For all images, scale bar = 50 μm, n = number of embryos.

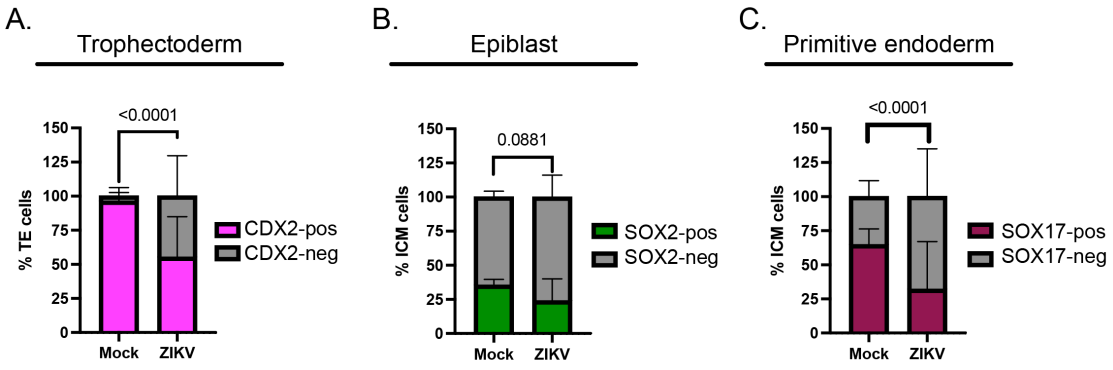

Figure 4.4: Lineage marker expression as a proportion of cells in each lineage. **A.** Proportion of outside cells in which CDX2 was detected among blastocysts described in Fig. 4.5. TE=trophectoderm, statistical test: Chi-squared. **B.** Proportion of inner cell mass (ICM) cells in which SOX2 was detected among blastocysts described in Fig. 4.5. Statistical test: Chi-squared. **C.** Proportion of inner cell mass (ICM) cells in which SOX17 was detected among blastocysts described in Fig. 4.5. Statistical test: Chi-squared.

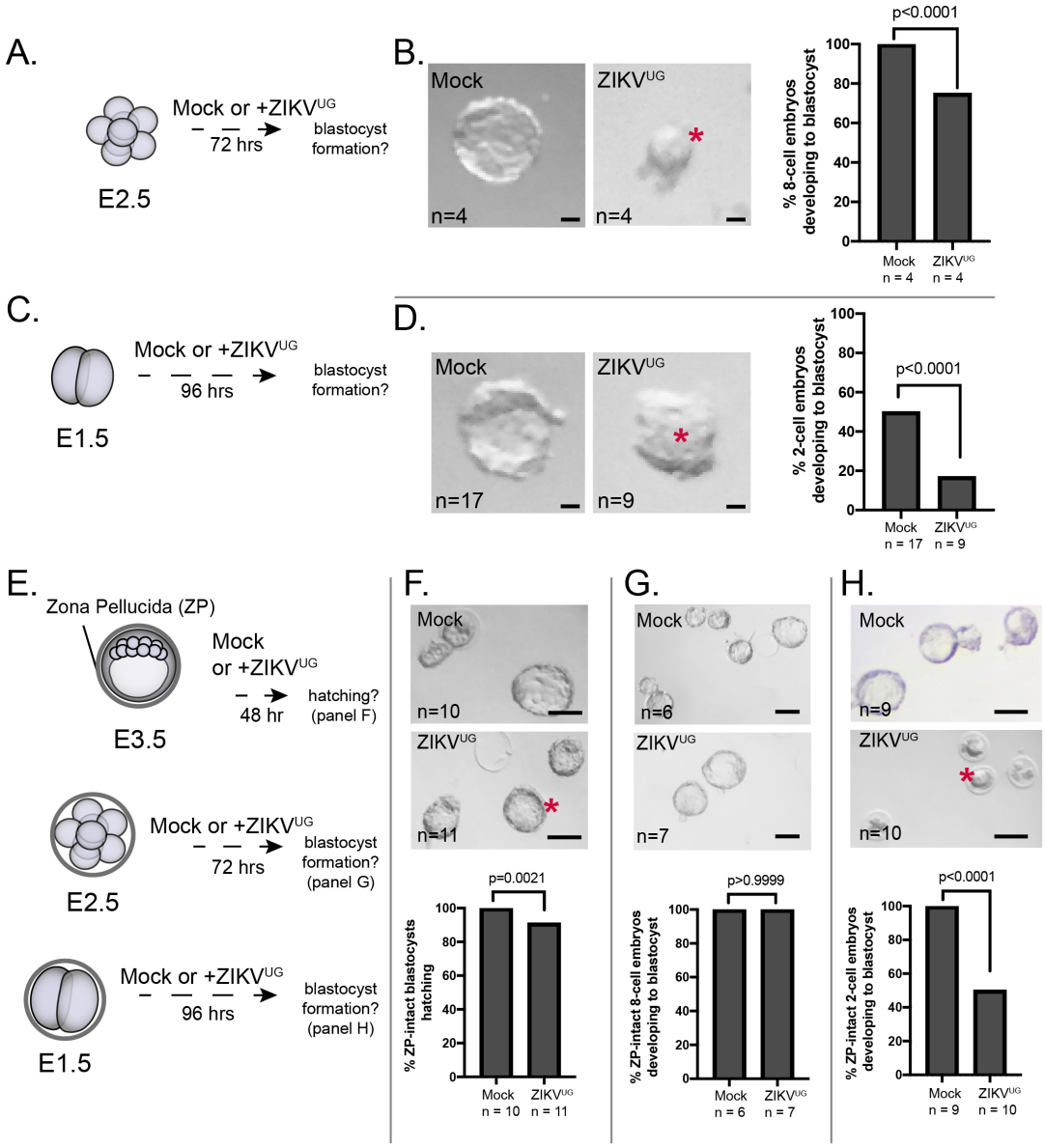

Figure 4.5: ZIKV^{UG} infects embryos at multiple stages, and the ZP fails to protect embryos from ZIKV^{UG} at all stages. A. Experimental design: embryos were collected at the 8-cell stage (E2.5), ZP removed, and then cultured for 72 hr in ZIKV^{UG} or mock medium. **B.** Representative images of embryos cultured as described in panel A. Column chart shows the proportion of embryos progressing to blastocyst stage. Statistical test: unpaired t-test. Scale bar = 20 µm. **C.** Experimental design: embryos were collected at the 2-cell stage (E1.5), ZP removed, and then cultured for 96 hr in ZIKV^{UG} or mock medium. **D.** Representative images of embryos cultured as described in panel C. Column chart shows the proportion of embryos progressing to blastocyst stage. Statistical test: unpaired t-test. Scale bar = 20 µm. **E.** Experimental design: embryos were collected at indicated stages, ZP were left intact,and then embryos were cultured until the same developmental endpoint (*see next page*).

Figure 4.5 (cont'd) **F.** Representative images of embryos cultured as described in panel E. Column chart shows the proportion of embryos progressing, evidenced by hatching from the ZP. Statistical test: unpaired t-test. Scale bar = 100 μm. **G.** Representative images of embryos cultured as described in panel E. Column chart shows the proportion of embryos progressing to blastocyst stage. Statistical test: unpaired t-test. Scale bar = 100 μm. **H.** Representative images of embryos cultured as described in panel E. Column chart shows the proportion of embryos progressing to blastocyst stage. Asterisks indicates developmentally arrested embryos. Statistical test: unpaired t-test. Scale bar = 100 μm. For all panels, n = number of embryos.

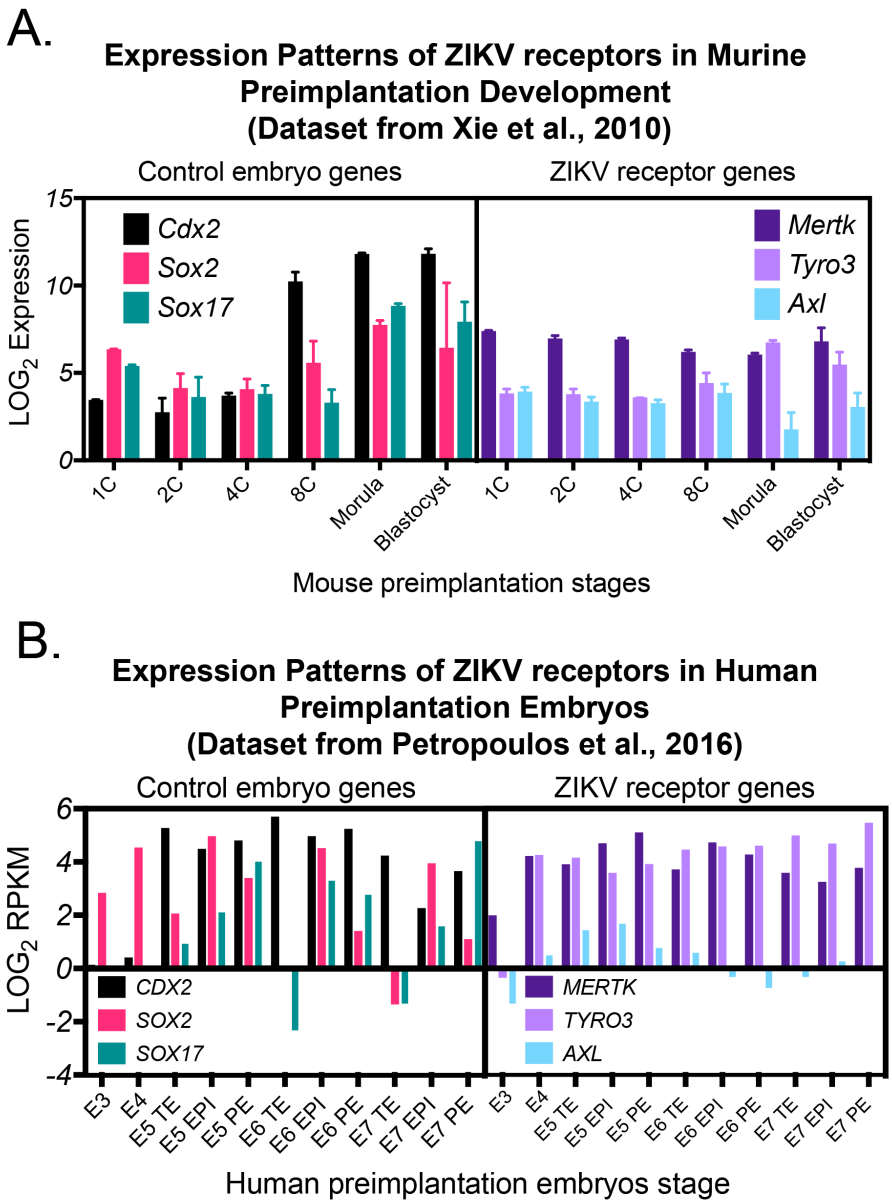

Figure 4.6: *Mertk* and *Tyro3*, but not *Axl*, are highly expressed ZIKV enrty factors in mouse and human preimplantation embryos. A. Column chart shows average LOG2 gene expression of embryo control genes, *Cdx2*, *Sox2*, and *Sox17*, and ZIKV entry factors, *Mertk*, *Tyro3*, and *Axl* throughout mouse preimplantation development (one-cell to blastocyst). Error bars = standard deviation. **B.** Column chart shows absolute LOG2 RPKM values of embryo control genes, *CDX2*, *SOX2*, and *SOX17*, and ZIKV entry factors, *MERTK*, *TYRO3*, and *AXL* throughout human preimplantation development (E3-E7).

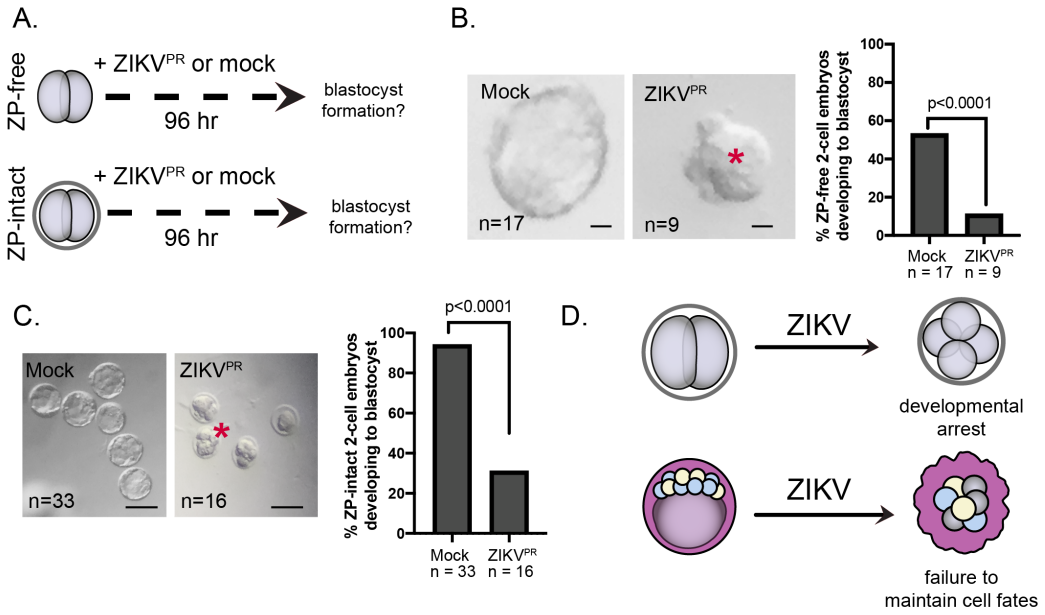

Figure 4.7: Two-cell embryos are susceptible to the Asian lineage-derived ZIKV^{PR}. A. Experimental design: embryos were harvested at the two-cell stage, and ZP either removed or left intact. Embryos were then exposed to ZIKV^{PR} for 96 hr. **B.** Representative images of ZP-free embryos cultured as described in panel A. Column chart shows the proportion of embryos progressing to blastocyst stage. Statistical test: unpaired t-test. Asterisk indicates developmentally arrested embryo. Scale bar = 20 µm. **C.** Representative images of ZP-intact embryos cultured as described in panel A. Column chart shows the proportion of embryos progressing to blastocyst stage. Statistical test: unpaired t-test. Asterisks indicates developmentally arrested embryo. Scale bar = 100 µm. For all panels, n = number of embryos. **D.** Summary of key findings.

CHAPTER 5

GENERAL DISCUSSION

5.1 Dissertation summary

5.1.1 Chapter 2 Summary

In chapter 2, I evaluated the expression levels of genes encoding proviral and antiviral factors in early preimplantation development. I utilized mouse embryo-derived stem cells, a proxy for embryo cells, and publicly available transcriptome data to examine the gene expression of ZIKV receptors, viral infection facilitators, and viral inhibitory factors of the interferon pathway [43, 57, 129, 162, 165]. I found that proviral factors were expressed in extraembryonic endoderm (or primitive endoderm-like) cells and trophoblast stem (or trophectoderm-like) cells. Similarly, mice express higher levels of proviral than antiviral factors throughout preimplantation development (zygote to blastocyst) (Figure 5.1A). These results suggest that embryonic cells, particularly primitive endoderm and trophectoderm cells, could be ZIKV-infected. Conversely, I found that mouse embryonic stem (or epiblast-like) cells and human preimplantation embryos (E3.0-E7.0) expressed antiviral factors, revealing that epiblast and human embryos could be resistant to ZIKV infection. Altogether, the expression patterns of proviral and antiviral genes could predict ZIKV infectivity in early development and possible human preimplantation development

5.1.2 Chapter 3 Summary

Previously, I showed that proviral factors are expressed in embryos and embryo-derived stem cells, suggesting ZIKV infectibility. To test this hypothesis, I first had to optimize protocols to ensure accurate detection of ZIKV infection. In addition, I found that chloroquine can inhibit ZIKV infection in stem cells. I then infected embryo-derived stem cells, trophoblast stem cells, extraembryonic stem cells and found that ZIKV does not highly infect these stem cells compared to

Vero and human cells. In addition to low infection, ZIKV could not replicate in all embryo-derived stem cell lines (Figure 5.1B). The presence of proviral genes in the stem cells did not indicate high ZIKV infection. Since these stem cells are a proxy for embryonic cells in the blastocyst [106, 108, 107], these results suggests that embryos will also exhibit low infection.

5.1.3 Chapter 4 Summary

Despite low infection of embryo-derived stem cells, there is evidence that ZIKV infects mouse and human blastocysts [78, 131]. In chapter 4, I showed that ZIKV exposure in ZP-removed preimplantation embryos caused developmental arrest. In addition, all three blastocyst cell lineage fates, epiblast, primitive endoderm, and trophectoderm were significantly reduced. However, ZP-intact embryos developed normally except for two-cell embryos. Lastly, I showed that two different ZIKV strains have the same deleterious effects in two-cell embryo development. These results reveal that two-cell embryos are most vulnerable to infection, and the blastocyst fails to maintain cell fates after infection (Figure 5.1C). These infection results are supported by the presence of proviral factors. Altogether, preimplantation ZIKV infection can lead to embryo demise and contribute to the miscarriage phenotype found in human infections.

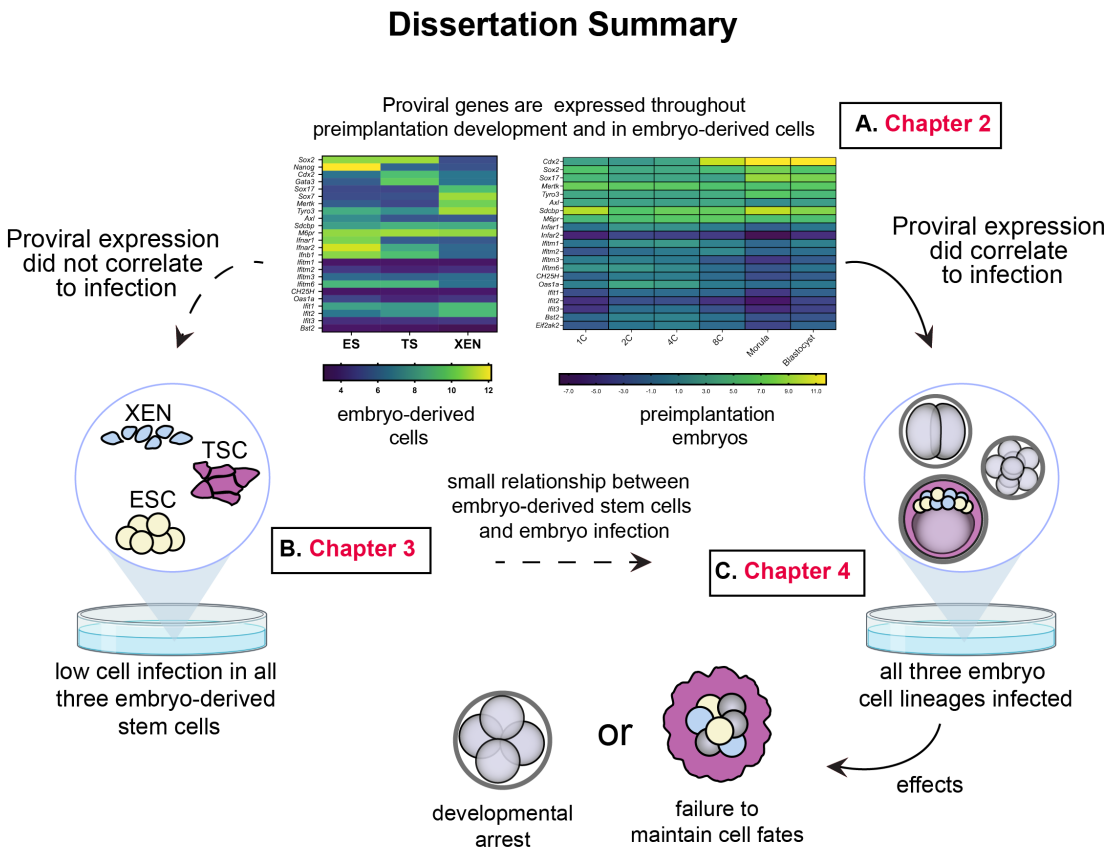

Figure 5.1: A schematic of the chapter findings. **A.** proviral genes are expressed in embryo-derived stem cells and thoughout preimplantation development. **B.** ZIKV-exposed embryo-derived stem cells were not infected. **C.** ZIKV-infected preimplantation embryos resulted in developmental arrest or failure to maintain embryo cell fates.

5.2 Concluding remarks

The shift in focus from the descending route of ZIKV infection to the ascending route offers an opportunity to understand infections in preimplantation development, developmental stages in which the mother would not know they are pregnant. Since ZIKV causes embryo demise, miscarriage could be undetected and epidemiologically underestimated. My dissertation studies are significant to human health because it advances the knowledge on ZIKV infection impact on early pregnancy outcomes. There are still questions to inquire about the oviduct/uterine environment effects on embryo infection and the long-term outcomes of ZIKV-exposed preimplantation embryos.

The oviduct houses early preimplantation stages (approximately 3-4 days post fertilization) across multiple species. Previous studies have shown oviduct cells have intrinsic expression of immune factors to support bovine embryo development during preimplantation stages, some of which include antiviral genes [206, 207]. However, it is unknown how oviduct antiviral factors effect embryo infections. Since antiviral factors reduce viral susceptibility, I speculate that ZIKV-induced antiviral factors will cross-talk with preimplantation embryos, protecting them from the virus. Alternatively, resident oviduct immune cells may attack preimplantation embryos due to pathogen-induced and embryo death observed in Chapter 4 and other studies [78, 131]. Even with the expression of antiviral genes in the oviduct, there is evidence that ZIKV persists in female reproductive tracts [136, 134]. This suggests that proviral factors are expressed in the uterus. However, the expression pattern of the proviral factors in the oviduct and uterus has not been fully explored during to ZIKV infection.

The correlation between infections in embryo-derived stem cells and embryos was starkly different. Since embryo-derived stem cells (TS, ES, and XEN cells) are a proxy to the preimplantation embryo, initially these cells were thought to be a predictor of *in vivo* embryo infection. However, infection was low in all embryo-derived stem cells and new ZIKV particles were not produced (Chapter 3). Conversely, infection was higher in embryos (Chapter 4). One major difference between the embryo *in vitro* system and the *in vivo* embryo is the homogeneity of the cells in culture. Embryonic cells, however, are intrinsically heterogeneous [94]. Additionally, the expression

of antiviral and proviral genes could differ between embryo-derived cells and embryos. These differences could result in infection differences between these two systems. Embryo-derived stem cell co-cultures or synthetic embryos (warmflash) could more accuratley recapitulates the embryo and enable cross-talk between distinct lineages which would be required for high ZIKV infection and replication.

Lastly, the long-term effects of preimplantation ZIKV infection are left to be investigated. While infected embryos exhibited reduced development to later preimplantation stages, a small proportion of embryos survive. It is unknown if these ZIKV-exposed preimplantation embryos survive post-implantation or exhibit ZIKV syndrome phenotypes at birth. An ideal experiment would be to infect embryos in culture, and then introduce them to a pseudopregnant recipient females [208]. After allowing embryos to grow in utero, the embryos can be examined in the perinatal stages to determine if preimplantation ZIKV infection manifests defects later in development. If fetuses exhibit fetal demise, microcephaly, or growth restriction phenotypes, then preimplantation ZIKV exposure may impact later development. Alternatively, if fetuses are born normally, then preimplantation exposure does not impact late fetal development.

This thesis sets a precedent to study other pathogens, bacteria and viruses, that affect newborn children post preimplantation embryo exposure. Particularly, Human Cytomegalovirus (HCMV), in the *Herpesviridae* family, and ZIKV have strikingly similar effects such as microcephaly, intrauterine growth restriction, and fetal loss [209, 210] . Both can also be transmitted via placenta and sexual contact [211, 212, 213]. Interestingly, the prevalence of congenital HCMV-related birth defects according to the US Centers of Disease Control and Prevention is 20% while ZIKV is less than 10%. With this growing concern for future emerging pathogens, studies of HCMV or other viral infections in early development will be necessary to understand the full spectrum of viral-induced birth defects.

BIBLIOGRAPHY

BIBLIOGRAPHY

[1] Mary Kay Kindhauser et al. “Zika: the origin and spread of a mosquito-borne virus”. In: *Bull. World Health Organ.* (2016).

[2] Simon Cauchemez et al. “Association between Zika virus and microcephaly in French Polynesia, 2013-15: A retrospective study”. In: *Lancet* 387.10033 (2016), pp. 2125–2132.

[3] Srilatha Edupuganti et al. “Biphasic Zika Illness With Rash and Joint Pain”. In: *Open Forum Infectious Diseases* (2017).

[4] Jernej Jorgaevski et al. “ZIKV Strains Differentially Affect Survival of Human Fetal Astrocytes versus Neurons and Traffic of ZIKV-Laden Endocytotic Compartments”. In: ().

[5] Antonino Uncini, Nortina Shahrizaila, and Satoshi Kuwabara. “Zika virus infection and Guillain-Barré syndrome: A review focused on clinical and electrophysiological subtypes”. In: *J. Neurol. Neurosurg. Psychiatry* 88.3 (2017), pp. 266–271.

[6] Miguel del Campo et al. “The phenotypic spectrum of congenital Zika syndrome”. In: *Am. J. Med. Genet. A* 173.4 (2017), pp. 841–857.

[7] Rachel Lowe et al. “The zika virus epidemic in brazil: From discovery to future implications”. In: *Int. J. Environ. Res. Public Health* 15.1 (2018).

[8] Theodore C Pierson and Michael S Diamond. “The emergence of Zika virus and its new clinical syndromes”. In: *Nature* 560.7720 (2018), pp. 573–581.

[9] Hugo A Arroyo. “Microcephaly”. In: *Medicina* 78.Cdc (2018), pp. 94–100.

[10] Margaret A Honein et al. “Birth Defects Among Fetuses and Infants of US Women With Evidence of Possible Zika Virus Infection During Pregnancy”. In: *JAMA* 317.1 (2017), p. 59.

[11] American Academy et al. “Practice Parameter : Diagnostic assessment of the child with Report of the Quality Standards Subcommittee of the American Academy of Neurology and the Practice Committee of the Child Neurology Society”. In: (2010).

[12] Dianne Abuelo. “Microcephaly Syndromes”. In: *Semin. Pediatr. Neurol.* 14.3 (2007), pp. 118–127.

[13] S Stoler-Poria et al. “Developmental outcome of isolated fetal microcephaly”. In: *Ultrasound Obstet. Gynecol.* 36.2 (2010), pp. 154–158.

[14] Elangovan Manivannan et al. “The Rise and Fall of Chloroquine/Hydroxychloroquine as Compassionate Therapy of COVID-19”. In: *Front. Pharmacol.* 12 (2021), p. 1057.

[15] Didier Musso, Albert I Ko, and David Baud. “Zika Virus Infection — After the Pandemic”. In: *N. Engl. J. Med.* 381.15 (2019), pp. 1444–1457.

[16] Theodore C Pierson and Michael S Diamond. “The continued threat of emerging flaviviruses”. en. In: *Nat Microbiol* 5.6 (June 2020), pp. 796–812.

[17] Dawn M Dudley et al. “Miscarriage and stillbirth following maternal Zika virus infection in nonhuman primates”. en. In: *Nat. Med.* 24.8 (Aug. 2018), pp. 1104–1107.

[18] Bruno Hoen et al. “Pregnancy Outcomes after ZIKV Infection in French Territories in the Americas”. en. In: *N. Engl. J. Med.* 378.11 (Mar. 2018), pp. 985–994.

[19] Oscar Pacheco et al. “Zika Virus Disease in Colombia — Preliminary Report”. In: *N. Engl. J. Med.* (2016), NEJMoa1604037.

[20] Maria G Teixeira et al. “The epidemic of Zika virus-related microcephaly in Brazil: Detection, control, etiology, and future scenarios”. In: *Am. J. Public Health* 106.4 (2016), pp. 601–605.

[21] Phillipe Boeuf et al. “The global threat of Zika virus to pregnancy: epidemiology, clinical perspectives, mechanisms, and impact”. eng. In: *BMC Med.* 14.1 (Aug. 2016), p. 112.

[22] Babak Shadgan et al. “Zika and Rio Olympic Games”. In: *Curr. Sports Med. Rep.* 15.4 (2016), pp. 298–300.

[23] Flavio Codeço Coelho et al. “Higher incidence of Zika in adult women than adult men in Rio de Janeiro suggests a significant contribution of sexual transmission from men to women”. In: *Int. J. Infect. Dis.* 51 (2016), pp. 128–132.

[24] Michel Jacques Counotte et al. “Sexual transmission of Zika virus and other flaviviruses: A living systematic review”. In: *PLoS Med.* (2018).

[25] Franca Grischott et al. “Non-vector-borne transmission of Zika virus: A systematic review”. In: *Travel Med. Infect. Dis.* (2016).

[26] Rodrigo Delvecchio et al. “Chloroquine, an endocytosis blocking agent, inhibits zika virus infection in different cell models”. In: *Viruses* (2016).

[27] Chunfeng Li et al. “Chloroquine, a FDA-approved Drug, Prevents Zika Virus Infection and its Associated Congenital Microcephaly in Mice”. In: *EBioMedicine* (2017).

[28] Pinar Mesci et al. “Blocking Zika virus vertical transmission”. In: *Sci. Rep.* 8.1 (2018), pp. 1–13.

[29] Sergey A Shiryaev et al. “Repurposing of the anti-malaria drug chloroquine for Zika Virus treatment and prophylaxis”. In: *Sci. Rep.* (2017).

[30] Chunpeng Yang, Rui Gong, and Natalia de Val. “Development of Neutralizing Antibodies against Zika Virus Based on Its Envelope Protein Structure”. In: *Virol. Sin.* 34.2 (2019), pp. 168–174.

[31] Aryamav Pattnaik, Bikash R Sahoo, and Asit K Pattnaik. “Current status of zika virus vaccines: Successes and challenges”. In: *Vaccines* 8.2 (2020), pp. 1–19.

[32] Yuxia Hu and Lei Sun. “Systematic Analysis of Structure Similarity between Zika Virus and Other Flaviviruses”. In: *ACS Infectious Diseases* 5.7 (2019), pp. 1070–1080.

[33] San Suwanmanee and Natthanej Luplertlop. “Dengue and Zika viruses: lessons learned from the similarities between these Aedes mosquito-vectored arboviruses”. In: *J. Microbiol.* 55.2 (2017), pp. 81–89.

[34] Fabio Zanini et al. “Single-cell transcriptional dynamics of flavivirus infection”. In: *Elife* 7 (2018).

[35] Anyou Wang et al. “Emerging Microbes & Infections (2017) 6, e13”. In: (2017).

[36] Peter Nambala and Wen Chi Su. “Role of Zika virus prM protein in viral pathogenicity and use in vaccine development”. In: *Front. Microbiol.* 9.AUG (2018), pp. 1–6.

[37] Ter Yong Tan et al. “Capsid protein structure in Zika virus reveals the flavivirus assembly process”. In: *Nat. Commun.* 11.1 (2020), pp. 1–13.

[38] Zhen Gong, Xiaoyu Xu, and Guan Zhu Han. “The diversification of Zika virus: Are there two distinct lineages?” In: *Genome Biol. Evol.* (2017).

[39] Qiang Shao et al. “The african zika virus mr-766 is more virulent and causes more severe brain damage than current asian lineage and dengue virus”. In: *Development* (2017).

[40] Yannick Simonin et al. “Zika Virus Strains Potentially Display Different Infectious Profiles in Human Neural Cells”. In: *EBioMedicine* (2016).

[41] Volha A Golubeva et al. “Network of Interactions between ZIKA Virus Non-Structural Proteins and Human Host Proteins”. In: *Cells* 9.1 (2020), pp. 1–18.

[42] Brett D Lindenbach and Charles M Rice. “Genetic Interaction of Flavivirus Nonstructural Proteins NS1 and NS4A as a Determinant of Replicase Function”. In: *J. Virol.* 73.6 (1999), pp. 4611–4621.

[43] Manuel Perera-Lecoin et al. *Flavivirus entry receptors: An update*. 2013.

[44] M G Bueno et al. “Animals in the Zika Virus Life Cycle: What to Expect from Megadiverse Latin American Countries”. In: *PLoS Negl. Trop. Dis.* 10.12 (2016), pp. 1–13.

[45] Devika Sirohi and Richard J Kuhn. “Zika Virus Structure, Maturation, and Receptors”. In: *J. Infect. Dis.* 216.Suppl 10 (2017), S935–S944.

[46] Rodolphe Hamel et al. “Biology of Zika Virus Infection in Human Skin Cells”. In: *J. Virol.* 89.17 (2015), pp. 8880–8896.

[47] Chet Raj Ojha et al. “Toll-like receptor 3 regulates Zika virus infection and associated host inflammatory response in primary human astrocytes”. In: *PLoS One* 14.2 (2019), pp. 1–26.

[48] Takako Tabata et al. “Zika Virus Targets Different Primary Human Placental Cells, Suggesting Two Routes for Vertical Transmission”. In: *Cell Host Microbe* 20.2 (2016), pp. 155–166.

[49] Brooke Liang et al. *Host and viral mechanisms of congenital Zika syndrome*. 2019.

[50] Shivani K Thaker, James Ch’ng, and Heather R Christofk. *Viral hijacking of cellular metabolism*. 2019.

[51] Shashi Kant Tiwari et al. “Zika virus infection reprograms global transcription of host cells to allow sustained infection”. In: *Emerg. Microbes Infect.* (2017).

[52] William M Schneider, Meike Dittmann Chevillotte, and Charles M Rice. “Interferon-stimulated genes: a complex web of host defenses”. eng. In: *Annu. Rev. Immunol.* 32 (2014), pp. 513–545.

[53] Stephanie L Cumberworth et al. “Zika virus tropism and interactions in myelinating neural cell cultures: CNS cells and myelin are preferentially affected”. In: *Acta neuropathologica communications* 5.1 (2017), p. 50.

[54] Jonathan J Miner et al. “Zika Virus Infection during Pregnancy in Mice Causes Placental Damage and Fetal Demise”. In: *Cell* 165.5 (2016), pp. 1081–1091.

[55] Clayton W Winkler et al. “Sexual and Vertical Transmission of Zika Virus in anti-interferon receptor-treated Rag1-deficient mice”. In: *Sci. Rep.* 7.1 (2017), pp. 1–13.

[56] Shahzada Khan et al. “Dampened antiviral immunity to intravaginal exposure to RNA viral pathogens allows enhanced viral replication”. In: *J. Exp. Med.* 213.13 (Dec. 2016), pp. 2913–2929.

[57] John W Schoggins et al. “A diverse range of gene products are effectors of the type I interferon antiviral response”. eng. In: *Nature* 472.7344 (Apr. 2011), pp. 481–485.

[58] John W Schoggins. “Interferon-Stimulated Genes: What Do They All Do?” In: *Annual Review of Virology* 6 (2019), pp. 567–584.

[59] Xianfang Wu et al. “Intrinsic Immunity Shapes Viral Resistance of Stem Cells”. In: *Cell* 172.3 (2018), 423–438.e25.

[60] Fernanda R Cugola et al. “The Brazilian Zika virus strain causes birth defects in experimental models”. In: *Nature* 534.7606 (2016), pp. 267–271.

[61] Jason Dang et al. “Zika Virus Depletes Neural Progenitors in Human Cerebral Organoids through Activation of the Innate Immune Receptor TLR3”. In: *Cell Stem Cell* 19.2 (2016), pp. 258–265.

[62] Hengli Tang et al. “Zika Virus Infects Human Cortical Neural Progenitors and Attenuates Their Growth”. en. In: *Cell Stem Cell* 18.5 (May 2016), pp. 587–590.

[63] Claudia Sánchez-San Martn et al. “Differentiation enhances Zika virus infection of neuronal brain cells”. In: *Sci. Rep.* 8.1 (Dec. 2018).

[64] Brandon W Hughes et al. “Infectivity of Immature Neurons to Zika Virus: A Link to Congenital Zika Syndrome”. In: *EBioMedicine* 10 (2016), pp. 65–70.

[65] Mao-Xing Tang et al. “What are the roles of macrophages and monocytes in human pregnancy?” In: *J. Reprod. Immunol.* 112 (Nov. 2015), pp. 73–80.

[66] Cl??udia Collucci. *Babies with microcephaly in Brazil are struggling to access care*. 2016.

[67] Alessandra Peloggia et al. *Zika virus exposure in pregnancy and its association with newborn visual anomalies and hearing loss*. 2018.

[68] Bin Cao, Michael S Diamond, and Indira U Mysorekar. *Maternal-fetal transmission of zika virus: Routes and signals for infection*. 2017.

[69] Camila Zanluca, Lucia de Noronha, and Claudia Nunes Duarte dos Santos. *Maternal-fetal transmission of the zika virus: An intriguing interplay*. 2018.

[70] Carmen D Zorrilla et al. “Zika Virus Infection in Pregnancy: Maternal, Fetal, and Neonatal Considerations”. In: *J. Infect. Dis.* (2017).

[71] James P Boardman. “Preterm Birth: Causes, Consequences and Prevention”. In: *J. Obstet. Gynaecol.* (2008).

[72] Stephanie E Purisch and Cynthia Gyamfi-Bannerman. *Epidemiology of preterm birth*. 2017.

[73] Surendra Sharma, Jessica E Thaxton, and Tania A Nevers. *TLR-mediated preterm birth in response to pathogenic agents*. 2010.

[74] Meghan S Vermillion et al. “Intrauterine Zika virus infection of pregnant immunocompetent mice models transplacental transmission and adverse perinatal outcomes”. In: *Nat. Commun.* 8 (2017).

[75] Kjersti M Aagaard et al. “Primary Human Placental Trophoblasts are Permissive for Zika Virus (ZIKV) Replication”. In: *Sci. Rep.* 7 (2017).

[76] Derek J Platt et al. “Zika virus-related neurotropic flaviviruses infect human placental explants and cause fetal demise in mice”. In: *Sci. Transl. Med.* (2018).

[77] Antonio Soares de Souza et al. “Fetal Infection by Zika Virus in the Third Trimester: Report of 2 Cases”. In: *Clin. Infect. Dis.* 63.12 (2016), pp. 1622–1625.

[78] Lei Tan et al. “Pre- and peri-implantation Zika virus infection impairs fetal development by targeting trophectoderm cells”. In: *Nat. Commun.* (2019).

[79] Katie Cockburn and Janet Rossant. *Making the blastocyst: Lessons from the mouse*. 2010.

[80] Kathy K Niakan et al. “Human pre-implantation embryo development”. eng. In: *Development* 139.5 (Mar. 2012), pp. 829–841.

[81] Shuai Li and Wipawee Winuthayanon. “Oviduct: Roles in fertilization and early embryo development”. In: *J. Endocrinol.* 232.1 (2017), R1–R26.

[82] Mark B Dworkin and Eva DworkinRastl. “Functions of maternal mRNA in early development”. In: *Mol. Reprod. Dev.* 26.3 (1990), pp. 261–297.

[83] Keith E Latham and Richard M Schultz. “EMBRYONIC GENOME ACTIVATION”. In: *Front. Biosci.* 6.d (2001), pp. 748–759.

[84] Bin Gu, Eszter Posfai, and Janet Rossant. “Efficient generation of targeted large insertions by microinjection into two-cell-stage mouse embryos”. In: *Nat. Biotechnol.* 36.7 (2018), pp. 632–637.

[85] Chunmeng Yao, Wenhao Zhang, and Ling Shuai. “The first cell fate decision in pre-implantation mouse embryos”. In: *Cell Regeneration* 8.2 (2019), pp. 51–57.

[86] Karolis Leonavicius et al. “Mechanics of mouse blastocyst hatching revealed by a hydrogel-based microdeformation assay”. In: *Proc. Natl. Acad. Sci. U. S. A.* 115.41 (2018), pp. 10375–10380.

[87] Henry Sathananthan, Judith Menezes, and Sulochana Gunasheela. “Mechanics of human blastocyst hatching in vitro”. In: *Reprod. Biomed. Online* 7.2 (2003), pp. 228–234.

[88] Claire Chazaud et al. “Early Lineage Segregation between Epiblast and Primitive Endoderm in Mouse Blastocysts through the Grb2-MAPK Pathway”. In: *Dev. Cell* 10.5 (May 2006), pp. 615–624.

[89] E Casser et al. “Totipotency segregates between the sister blastomeres of two-cell stage mouse embryos”. en. In: *Sci. Rep.* 7.1 (Aug. 2017), p. 8299.

[90] J Rossant. “Postimplantation development of blastomeres isolated from 4- and 8-cell mouse eggs”. en. In: *J. Embryol. Exp. Morphol.* 36.2 (Oct. 1976), pp. 283–290.

[91] A K Tarkowski and J Wróblewska. “Development of blastomeres of mouse eggs isolated at the 4- and 8-cell stage”. en. In: *J. Embryol. Exp. Morphol.* 18.1 (Aug. 1967), pp. 155–180.

[92] N Nishioka et al. “The Hippo signaling pathway components Lats and Yap pattern Tead4 activity to distinguish mouse trophectoderm from inner cell mass”. eng. In: *Dev. Cell* 16.3 (2009), pp. 398–410.

[93] Tristan Frum and Amy Ralston. “HIPPO signaling provides a fail-safe for resolving embryonic cell fate conflicts during establishment of pluripotency in vivo”. In: *bioRxiv* (2018).

[94] Tristan Frum, Jennifer L Watts, and Amy Ralston. “TEAD4, YAP1 and WWTR1 prevent the premature onset of pluripotency prior to the 16-cell stage”. In: *Development* 146.17 (Sept. 2019), dev179861.

[95] Eryn Wicklow et al. “HIPPO Pathway Members Restrict SOX2 to the Inner Cell Mass Where It Promotes ICM Fates in the Mouse Blastocyst”. In: *PLoS Genet.* 10.10 (2014).

[96] Yoshikazu Hirate et al. “Polarity-dependent distribution of angiomotin localizes Hippo signaling in preimplantation embryos”. en. In: *Curr. Biol.* 23.13 (July 2013), pp. 1181–1194.

[97] Claudia Gerri et al. “Initiation of a conserved trophectoderm program in human, cow and mouse embryos”. In: *Nature* 587.7834 (2020), pp. 443–447.

[98] Irene Aksoy et al. “Oct4 switches partnering from Sox2 to Sox17 to reinterpret the enhancer code and specify endoderm”. In: *EMBO J.* 32.7 (2013), pp. 938–953.

[99] Jérôme Artus, Anna Piliszek, and Anna Katerina Hadjantonakis. “The primitive endoderm lineage of the mouse blastocyst: Sequential transcription factor activation and regulation of differentiation by Sox17”. In: *Dev. Biol.* 350.2 (Feb. 2011), pp. 393–404.

[100] Tristan Frum et al. “Oct4 cell-autonomously promotes primitive endoderm development in the mouse blastocyst”. en. In: *Dev. Cell* 25.6 (June 2013), pp. 610–622.

[101] Stephen Frankenberg et al. “Primitive Endoderm Differentiates via a Three-Step Mechanism Involving Nanog and RTK Signaling”. In: *Dev. Cell* 21.6 (2011), pp. 1005–1013.

[102] Sarah J L Graham et al. “BMP signalling regulates the pre-implantation development of extra-embryonic cell lineages in the mouse embryo”. In: *Nat. Commun.* 5.May (2014).

[103] Dayana Krawchuk et al. “FGF4 is a limiting factor controlling the proportions of primitive endoderm and epiblast in the ICM of the mouse blastocyst”. In: *Dev. Biol.* 384.1 (2013), pp. 65–71.

[104] Jennifer Nichols and Qi-Long Ying. “Derivation and Propagation of Embryonic Stem Cells in Serum- and Feeder-Free Culture”. In: *Embryonic Stem Cell Protocols: Volume 1: Isolation and Characterization*. Ed. by Kursad Turksen. Totowa, NJ: Humana Press, 2006, pp. 91–98.

[105] A Nagy et al. “Derivation of completely cell culture-derived mice from early-passage embryonic stem cells”. en. In: *Proc. Natl. Acad. Sci. U. S. A.* 90.18 (Sept. 1993), pp. 8424–8428.

[106] G R Martin. “Isolation of a pluripotent cell line from early mouse embryos cultured in medium conditioned by teratocarcinoma stem cells”. en. In: *Proc. Natl. Acad. Sci. U. S. A.* 78.12 (Dec. 1981), pp. 7634–7638.

[107] Shang-Yi Chiu, Eri O Maruyama, and Wei Hsu. “Derivation of Mouse Trophoblast Stem Cells from Blastocysts”. In: *J. Vis. Exp.* 40 (2010).

[108] Satoshi Tanaka et al. “Promotion to trophoblast stem cell proliferation by FGF4”. In: *Science* 282.5396 (1998), pp. 2072–2075.

[109] Satoshi Tanaka. “Derivation and culture of mouse trophoblast stem cells in vitro”. In: *Methods Mol. Biol.* 329 (2006), pp. 35–44.

[110] Varvara B Zeldovich et al. “Placental syncytium forms a biophysical barrier against pathogen invasion”. In: *PLoS Pathog.* 9.12 (Dec. 2013), e1003821.

[111] Adrianne L Stefanski et al. “Murine trophoblast-derived and pregnancy-associated exosome-enriched extracellular vesicle {microRNAs}: Implications for placenta driven effects on maternal physiology”. In: *PLoS One* 14.2 (Feb. 2019), e0210675.

[112] Tilo Kunath et al. “Imprinted X-inactivation in extra-embryonic endoderm cell lines from mouse blastocysts”. en. In: *Development* 132.7 (Apr. 2005), pp. 1649–1661.

[113] Kathy K Niakan et al. “Derivation of extraembryonic endoderm stem (XEN) cells from mouse embryos and embryonic stem cells”. en. In: *Nat. Protoc.* 8.6 (June 2013), pp. 1028–1041.

[114] Asja T Moerkamp et al. *Extraembryonic Endoderm cells as a model of endoderm development*. 2013.

[115] Peter Rugg-Gunn. “Derivation and culture of extra-embryonic endoderm stem cell lines”. In: *Cold Spring Harb. Protoc.* 2017.1 (2017), pp. 33–37.

[116] Jérôme Artus et al. “BMP4 signaling directs primitive endoderm-derived XEN cells to an extraembryonic visceral endoderm identity”. In: *Dev. Biol.* 361.2 (2012), pp. 245–262.

[117] Agnieszka Paca et al. “BMP signaling induces visceral endoderm differentiation of XEN cells and parietal endoderm”. In: *Dev. Biol.* 361.1 (2012), pp. 90–102.

[118] Amy Ralston et al. “Gata3 regulates trophoblast development downstream of Tead4 and in parallel to Cdx2”. In: *Development* 137.3 (Feb. 2010), pp. 395–403.

[119] Dan Strumpf et al. “Cdx2 is required for correct cell fate specification and differentiation of trophectoderm in the mouse blastocyst”. In: *Development* 132.9 (May 2005), 2093 LP–2102.

[120] J Yan et al. “Retinoic acid promotes differentiation of trophoblast stem cells to a giant cell fate”. In: *Dev. Biol.* 235.2 (2001), pp. 422–432.

[121] Yojiro Yamanaka et al. *Cell and molecular regulation of the mouse blastocyst*. Sept. 2006.

[122] Anthony Parenti et al. “OSKM Induce Extraembryonic Endoderm Stem Cells in Parallel to Induced Pluripotent Stem Cells”. In: *Stem Cell Reports* (2016).

[123] Guy S Eakin and Anna-Katerina Hadjantonakis. “Production of chimeras by aggregation of embryonic stem cells with diploid or tetraploid mouse embryos”. en. In: *Nat. Protoc.* 1.3 (2006), pp. 1145–1153.

[124] Jennifer L Watts and Amy Ralston. *Universal assembly instructions for the placenta*. 2020.

[125] Yinli Yang et al. “Exosomes mediate hepatitis {B} virus ({HBV}) transmission and {NK-cell} dysfunction”. In: *Cell. Mol. Immunol.* 14.5 (May 2017), pp. 465–475.

[126] Hiroaki Okae et al. “Derivation of Human Trophoblast Stem Cells”. In: *Cell Stem Cell* 22.1 (2018), 50–63.e6.

[127] Amy Ralston. “XEN and the Art of Stem Cell Maintenance: Molecular Mechanisms Maintaining Cell Fate and Self-Renewal in Extraembryonic Endoderm Stem (XEN) Cell Lines”. In: *Chromatin Regulation of Early Embryonic Lineage Specification*. Ed. by Jason Knott and Keith Latham. Cham: Springer International Publishing, 2018, pp. 69–78.

[128] Annemiek A van der Eijk et al. “Miscarriage Associated with Zika Virus Infection”. In: *N. Engl. J. Med.* 375.10 (2016), pp. 1002–1004.

[129] Sophie Petropoulos et al. “Single-Cell RNA-Seq Reveals Lineage and X Chromosome Dynamics in Human Preimplantation Embryos”. en. In: *Cell* 167.1 (Sept. 2016), p. 285.

[130] Jennifer Watts et al. *Capturing and Interconverting Embryonic Cell Fates in a Dish*. 1st ed. Elsevier Inc., 2018, pp. 1–21.

[131] Lindsey N Block et al. “Embryotoxic impact of Zika virus in a rhesus macaque in vitro implantation model”. In: *Biol. Reprod.* 102.4 (Apr. 2020), pp. 806–816.

[132] Nisha K Duggal et al. “Sexual transmission of Zika virus enhances in utero transmission in a mouse model”. In: *Sci. Rep.* (2018).

[133] Erin M McDonald, Nisha K Duggal, and Aaron C Brault. “Pathogenesis and sexual transmission of Spondweni and Zika viruses”. In: *PLoS Negl. Trop. Dis.* 11.10 (2017).

[134] Laura J Yockey et al. “Vaginal Exposure to Zika Virus during Pregnancy Leads to Fetal Brain Infection”. en. In: *Cell* 166.5 (Aug. 2016), 1247–1256.e4.

[135] Omar Bagasra et al. “Cellular Targets and Receptor of Sexual Transmission of Zika Virus”. In: *Appl. Immunohistochem. Mol. Morphol.* (2017).

[136] Timothy Carroll et al. “Zika virus preferentially replicates in the female reproductive tract after vaginal inoculation of rhesus macaques”. In: *PLoS Pathog.* (2017).

[137] Liesel Stassen et al. “Zika Virus in the Male Reproductive Tract”. In: *Viruses* (2018).

[138] Ki Jun Yoon et al. “Zika-Virus-Encoded NS2A Disrupts Mammalian Cortical Neurogenesis by Degrading Adherens Junction Proteins”. In: *Cell Stem Cell* 21.3 (2017), 349–358.e6.

[139] Célia Basurko et al. “Maternal and foetal consequences of dengue fever during pregnancy”. In: *Eur. J. Obstet. Gynecol. Reprod. Biol.* 147.1 (2009), pp. 29–32.

[140] Helena Lucia Barroso Dos Reis et al. “Preterm birth and fetal growth restriction in HIV-infected Brazilian pregnant women”. In: *Rev. Inst. Med. Trop. Sao Paulo* (2015).

[141] Erica L Johnson et al. “Cytomegalovirus upregulates expression of CCR5 in central memory cord blood mononuclear cells, which may facilitate in utero HIV type 1 transmission”. In: *J. Infect. Dis.* (2015).

[142] Athena P Kourtis et al. *Understanding the timing of HIV transmission from mother to infant*. 2001.

[143] Claire Chazaud and Yojiro Yamanaka. *Lineage specification in the mouse preimplantation embryo*. 2016.

[144] Kaoru Mitsui et al. “The Homeoprotein Nanog Is Required for Maintenance of Pluripotency in Mouse Epiblast and ES Cells”. In: *Cell* 113.5 (May 2003), pp. 631–642.

[145] J Abramczuk et al. “Infection of mouse preimplantation embryos with simian virus 40 and polyoma virus”. In: *Proc. Natl. Acad. Sci. U. S. A.* 75.2 (1978), pp. 999–1003.

[146] Jan Abramczuk et al. “Interactions of preimplantation mouse embryos with reovirus serotypes 1 and 3”. In: *Infect. Immun.* 42.1 (1983), pp. 301–307.

[147] R B Gwatkin. “Passage of mengovirus through the zona pellucida of the mouse morula”. In: *J. Reprod. Fertil.* (1967).

[148] C Lavilla-Apelo et al. “the Infection of Mouse Preimplantation Virus (Parainfluenza”. In: *Theriogenology* 36.1 (1991), pp. 87–94.

[149] A M Hearne, M A O’Sullivan, and G J Atkins. “Infection of cultured early mouse embryos with Semliki Forest and rubella viruses”. In: *J. Gen. Virol.* 67.6 (1986), pp. 1091–1098.

[150] A V Makarevich et al. “Development and viability of bovine preimplantation embryos after the in vitro infection with bovine herpesvirus-1 (BHV-1): Immunocytochemical and ultrastructural studies”. In: *Zygote* 15.4 (2007), pp. 307–315.

[151] B Mateusen et al. “Receptor-determined susceptibility of preimplantation embryos to pseudorabies virus and porcine reproductive and respiratory syndrome virus”. In: *Biol. Reprod.* 76.3 (2007), pp. 415–423.

[152] Mauricio Montano et al. “Human Pre-Implantation Embryos Are Permissive to SARS-CoV-2 Entry”. In: *bioRxiv* (2021), pp. 1–30.

[153] Christopher M Goodwin, Shihao Xu, and Joshua Munger. *Stealing the Keys to the Kitchen: Viral Manipulation of the Host Cell Metabolic Network*. 2015.

[154] R Jaenisch, H Fan, and B Croker. “Infection of preimplantation mouse embryos and of newborn mice with leukemia virus: tissue distribution of viral DNA and RNA and leuke-

mogenesis in the adult animal". In: *Proc. Natl. Acad. Sci. U. S. A.* 72.10 (1975), pp. 4008–4012.

[155] Yasushi Odawara et al. "Zona Manipulation in an Assisted Reproductive Technologies (ART) Programme". In: *J. Obstet. Gynaecol.* (1995).

[156] A McLaren. "The fate of the zona pellucida in mice". In: *J. Embryol. Exp. Morphol.* (1970).

[157] Geert Vanroose et al. "Structural aspects of the zona pellucida of in vitro-produced bovine embryos: A scanning electron and confocal laser scanning microscopic study". In: *Biol. Reprod.* (2000).

[158] Abraham L Brass et al. "The IFITM proteins mediate cellular resistance to influenza A H1N1 virus, West Nile virus, and dengue virus". eng. In: *Cell* 139.7 (Dec. 2009), pp. 1243–1254.

[159] Mengxi Wu et al. "Isolation of exosomes from whole blood by integrating acoustics and microfluidics". In: *Proc. Natl. Acad. Sci. U. S. A.* 114.40 (Oct. 2017), pp. 10584–10589.

[160] Jennifer J Adibi et al. "Teratogenic effects of the Zika virus and the role of the placenta". eng. In: *Lancet* 387.10027 (Apr. 2016), pp. 1587–1590.

[161] Eric D'Ortenzio et al. "Evidence of Sexual Transmission of Zika Virus". In: *N. Engl. J. Med.* 374.22 (Apr. 2016), pp. 2195–2198.

[162] P J Rugg-Gunn et al. "Distinct histone modifications in stem cell lines and tissue lineages from the early mouse embryo". In: *Proceedings of the National Academy of Sciences* (2010).

[163] Nestor Saiz and Berenika Plusa. *Early cell fate decisions in the mouse embryo*. 2013.

[164] Yang Yang et al. "Derivation of Pluripotent Stem Cells with In Vivo Embryonic and Extraembryonic Potency". In: *Cell* 169.2 (2017), 243–257.e25.

[165] Dan Xie et al. "Rewirable gene regulatory networks in the preimplantation embryonic development of three mammalian species". en. In: *Genome Res.* 20.6 (June 2010), pp. 804–815.

[166] Sruti K Desai et al. "Zika Virus (ZIKV): a review of proposed mechanisms of transmission and associated congenital abnormalities". In: *Am. J. Stem Cells* 6.December 2016 (2017), pp. 13–22.

[167] Pietro Scaturro et al. "An orthogonal proteomic survey uncovers novel Zika virus host factors". en. In: *Nature* 561.7722 (Sept. 2018), pp. 253–257.

[168] Qi-Lin Xin et al. “Quantitative Proteomic Analysis of Mosquito C6/36 Cells Reveals Host Proteins Involved in Zika Virus Infection”. en. In: *J. Virol.* 91.12 (June 2017).

[169] Sergio P Alpuche-Lazcano et al. “Higher cytopathic effects of a zika virus brazilian isolate from bahia compared to a Canadian-imported thai strain”. In: *Viruses* (2018).

[170] Julu Bhatnagar et al. “Zika virus RNA replication and persistence in brain and placental tissue”. In: *Emerg. Infect. Dis.* 23.3 (2017), pp. 405–414.

[171] Darrell S Agbulos et al. “Zika virus: Quantification, propagation, detection, and storage”. In: *Curr. Protoc. Microbiol.* 2016.November (2016), pp. 15D.4.1–15D.4.16.

[172] Robert S Lanciotti et al. “Genetic and Serologic Properties of Zika Virus Associated with an Epidemic, Yap State, Micronesia, 2007”. In: *Emerging Infectious Disease journal* 14.8 (2008), p. 1232.

[173] V Haridas et al. “Bispidine-Amino Acid Conjugates Act as a Novel Scaffold for the Design of Antivirals That Block Japanese Encephalitis Virus Replication”. In: *PLoS Negl. Trop. Dis.* 7.1 (Jan. 2013), e2005.

[174] Shuhei Taguwa et al. “Zika Virus Dependence on Host Hsp70 Provides a Protective Strategy against Infection and Disease”. In: *Cell Rep.* 26.4 (2019), 906–920.e3.

[175] Kiyoshi Himmelsbach and Eberhard Hildt. “Identification of various cell culture models for the study of Zika virus”. In: *World Journal of Virology* (2018).

[176] G Misinzo, P L Delputte, and H J Nauwynck. “Inhibition of Endosome-Lysosome System Acidification Enhances Porcine Circovirus 2 Infection of Porcine Epithelial Cells”. In: *J. Virol.* (2008).

[177] Sam Salman et al. “Optimal antimalarial dose regimens for chloroquine in pregnancy based on population pharmacokinetic modelling”. In: *Int. J. Antimicrob. Agents* 50.4 (Oct. 2017), pp. 542–551.

[178] Cathrine Axfors et al. “Mortality outcomes with hydroxychloroquine and chloroquine in COVID-19 from an international collaborative meta-analysis of randomized trials”. In: *Nat. Commun.* 12.1 (2021), pp. 1–13.

[179] Olusola Olafuyi and Raj K S Badhan. “Dose Optimization of Chloroquine by Pharmacokinetic Modeling During Pregnancy for the Treatment of Zika Virus Infection”. In: *J. Pharm. Sci.* 108.1 (Jan. 2019), pp. 661–673.

[180] Hicham El Costa et al. *ZIKA virus reveals broad tissue and cell tropism during the first trimester of pregnancy*. 2016.

[181] Eduardo Esteves et al. “New Targets for Zika Virus Determined by Human-Viral Interactomic: A Bioinformatics Approach”. In: *Biomed Res. Int.* (2017).

[182] Lynn Eaton. “Preventing the next pandemic”. en. In: *Bull. World Health Organ.* 99.5 (May 2021), pp. 326–327.

[183] Patrcia Brasil et al. “Zika Virus Infection in Pregnant Women in Rio de Janeiro”. In: *N. Engl. J. Med.* 375.24 (2016), pp. 2321–2334.

[184] Kelli J Carroll et al. “A mouse model for adult cardiac-specific gene deletion with {CRISPR/Cas9}”. In: *Proc. Natl. Acad. Sci. U. S. A.* 113.2 (Jan. 2016), pp. 338–343.

[185] John T Brooks et al. *Update: Interim Guidance for Prevention of Sexual Transmission of Zika Virus — United States, July 2016*. 2016.

[186] José Moreira, Cristiane C Lamas, and Andr Siqueira. *Sexual transmission of zika virus: Implications for clinical care and public health policy*. 2016.

[187] Igor Toskin et al. “A combination approach of behavioural and biomedical interventions for prevention of sexually transmitted infections”. en. In: *Bull. World Health Organ.* 98.6 (June 2020), pp. 431–434.

[188] Michael F Wells et al. “Genetic Ablation of AXL Does Not Protect Human Neural Progenitor Cells and Cerebral Organoids from Zika Virus Infection”. en. In: *Cell Stem Cell* 19.6 (Dec. 2016), pp. 703–708.

[189] Paul Thomas and Rosa Beddington. “Anterior primitive endoderm may be responsible for patterning the anterior neural plate in the mouse embryo”. In: *Curr. Biol.* 6.11 (1996), pp. 1487–1496.

[190] Berenika Plusa et al. *Distinct sequential cell behaviours direct primitive endoderm formation in the mouse blastocyst*. 2008.

[191] Kathy K Niakan et al. “Sox17 promotes differentiation in mouse embryonic stem cells by directly regulating extraembryonic gene expression and indirectly antagonizing self-renewal”. In: *Genes and Development* 24.3 (Feb. 2010), pp. 312–326.

[192] Ariel A Avilion et al. “Multipotent cell lineages in early mouse development depend on SOX2 function”. In: *Genes and Development* (2003).

[193] M Nijs and A C Van Steirteghem. “Assessment of different isolation procedures for blastomeres from two-cell mouse embryos”. In: *Hum. Reprod.* 2.5 (1987), pp. 421–424.

[194] R B Gwatkin. “EFFECT OF VIRUSES ON EARLY MAMMALIAN DEVELOPMENT. I. ACTION OF MENGO ENCEPHALITIS VIRUS ON MOUSE OVA CULTIVATED IN VITRO”. en. In: *Proc. Natl. Acad. Sci. U. S. A.* 50 (Sept. 1963), pp. 576–581.

[195] Charles Romeo et al. “AAV diffuses across zona pellucida for effortless gene delivery to fertilized eggs: AAV diffuses across mouse ZP”. In: *Biochem. Biophys. Res. Commun.* 526.1 (May 2020), pp. 85–90.

[196] Fatih Anfasa et al. “Phenotypic Differences between Asian and African Lineage Zika Viruses in Human Neural Progenitor Cells”. In: *mSphere* (2017).

[197] J M Medlock et al. “An entomological review of invasive mosquitoes in Europe”. en. In: *Bull. Entomol. Res.* 105.6 (Dec. 2015), pp. 637–663.

[198] Sarah Cunze et al. “Niche conservatism of Aedes albopictus and Aedes aegypti - two mosquito species with different invasion histories”. en. In: *Sci. Rep.* 8.1 (May 2018), p. 7733.

[199] M Belaoussoff, S M Farrington, and M H Baron. “Hematopoietic induction and respecification of A-P identity by visceral endoderm signaling in the mouse embryo”. In: *Development* 125.24 (1998), pp. 5009–5018.

[200] Mary Madabhushi and Elizabeth Lacy. “Anterior visceral endoderm directs ventral morphogenesis and placement of head and heart via BMP2 expression”. en. In: *Dev. Cell* 21.5 (Nov. 2011), pp. 907–919.

[201] Susana M Chuva de Sousa Lopes et al. “BMP signaling mediated by ALK2 in the visceral endoderm is necessary for the generation of primordial germ cells in the mouse embryo”. en. In: *Genes Dev.* 18.15 (Aug. 2004), pp. 1838–1849.

[202] Jinzhe Mao et al. “The iron exporter ferroportin 1 is essential for development of the mouse embryo, forebrain patterning and neural tube closure”. en. In: *Development* 137.18 (Sept. 2010), pp. 3079–3088.

[203] Gloria S Kwon, Manuel Viotti, and Anna-Katerina Hadjantonakis. “The endoderm of the mouse embryo arises by dynamic widespread intercalation of embryonic and extraembryonic lineages”. en. In: *Dev. Cell* 15.4 (Oct. 2008), pp. 509–520.

[204] Janet Rossant. “Mouse and human blastocyst-derived stem cells: vive les differences”. en. In: *Development* 142.1 (Jan. 2015), pp. 9–12.

[205] Stephanie E Ander, Michael S Diamond, and Carolyn B Coyne. “Immune responses at the maternal-fetal interface”. In: *Sci Immunol* 4.31 (Jan. 2019).

[206] Anup K Talukder et al. “Oviduct epithelium induces interferon-tau in bovine Day-4 embryos, which generates an anti-inflammatory response in immune cells”. en. In: *Sci. Rep.* 8.1 (May 2018), p. 7850.

[207] Takahiro Shirozu et al. “Estrous cycle stage-dependent manner of type I interferon-stimulated genes induction in the bovine endometrium”. en. In: *J. Reprod. Dev.* 63.3 (June 2017), pp. 211–220.

[208] Anne Mclaren and Donald Michie. *Studies on the Transfer of Fertilized Mouse Eggs to Uterine Foster-Mothers*. 1959.

[209] Carolyn M Jenks, Stephen R Hoff, and Leena B Mithal. “Congenital Cytomegalovirus Infection: Epidemiology, Timely Diagnosis, and Management”. en. In: *Neoreviews* 22.9 (Sept. 2021), e606–e613.

[210] Lenore Pereira. “Have we overlooked congenital cytomegalovirus infection as a cause of stillbirth?” en. In: *J. Infect. Dis.* 203.11 (June 2011), pp. 1510–1512.

[211] Michael A Gaytant et al. “Congenital cytomegalovirus infection: review of the epidemiology and outcome”. en. In: *Obstet. Gynecol. Surv.* 57.4 (Apr. 2002), pp. 245–256.

[212] Yiska Weisblum et al. “Modeling of human cytomegalovirus maternal-fetal transmission in a novel decidual organ culture”. en. In: *J. Virol.* 85.24 (Dec. 2011), pp. 13204–13213.

[213] Guoqiang Sun et al. “Modeling Human Cytomegalovirus-Induced Microcephaly in Human iPSC-Derived Brain Organoids”. en. In: *Cell Rep Med* 1.1 (Apr. 2020), p. 100002.